ENGINEERING MACROPHAGES TO CONTROL THE FOREIGN BODY REACTION

Karen Eaton

A dissertation
submitted in partial fulfillment of the
requirements for the degree of

Doctor of Philosophy

University of Washington
2015

Reading Committee:
Marta Scatena, Chair
Cecilia Giachelli
James Bryers

Program Authorized to Offer Degree: Bioengineering

University of Washington

Abstract

ENGINEERING MACROPHAGES TO CONTROL THE FOREIGN BODY REACTION

Karen Eaton

Chair of the Supervisory Committee:
Research Associate Professor, Marta Scatena
Bioengineering

The foreign body reaction (FBR) is an inflammatory response driven by macrophages (MΦs). During the inflammatory response, MΦs influence fibrosis and angiogenesis by secreting certain cytokines. It is still unclear what roles the pro-inflammatory (M1) MΦ and pro-healing (M2) MΦ phenotypes play during these processes. However, given that the FBR leads to a non-vascularized fibrous capsule surrounding most medical devices, better device integration might be possible by controlling the MΦ phenotype at the implant site to lead to decreased fibrosis and increased vessel formation.

The research presented in this dissertation describes the development and characterization of engineered pro-inflammatory MΦs, MΦ-cTLR4 cells, which can be activated to a M1-like MΦ phenotype with a small molecule, the chemical inducer of dimerization (CID) drug. It is hypothesized that the engineered MΦ-cTLR4 cells in this study can functionally activate by

addition of CID drug and allow better integration of implanted medical devices, by inhibiting fibrosis and priming angiogenesis around implanted medical devices. The MΦ-cTLR4 cells when activated with the CID drug, express increased levels of M1 MΦ markers. Activated MΦ-cTLR4 cells stay stimulated for at least 48 hours; once the CID drug is withdrawn, the MΦ-cTLR4 cells return to baseline state within 18 hours. Further, *in vitro* CID-activated MΦ-cTLR4 cells induce upregulation of adhesion molecules on endothelial cells (ECs) in a TNFα-dependent manner. The MΦ-cTLR4 cells have also been shown to co-localize with pro-inflammatory regions following *in vivo* injection, which suggest these cells are still present and functionally active. Lastly, CID-treated mice with injected MΦ-cTLR4 cells within a Matrigel matrix exhibited less fibrosis overall in the Matrigel plugs. With the ability to specifically modulate the MΦ-cTLR4 cells with the presence or absence of a small molecule, a tool now exists to observe a primarily M1 MΦ response during inflammation. Using these engineered cells as a tool, this study has shown that pro-inflammatory MΦ-cTLR4 cells may be capable of inhibiting the fibrosis response, while also being able to prime the angiogenesis response. By controlling these two key processes that relate to the foreign body reaction, better medical device integration might be possible.

TABLE OF CONTENTS

List of Figures v

Chapter 1. Background 1

1.1 Significance and Innovation 1

1.1.1 Significance 1

1.1.2 Improvement 2

1.1.3 Innovation 2

1.2 Paradigm for Inflammation 2

1.3 Role of Macrophages in Inflammation 4

1.4 The Foreign Body Reaction 6

1.5 Macrophage Impact on Angiogenesis 7

1.6 Toll-like Receptor 4 Signaling 8

1.7 Chemically Induced Dimerization (CID) System 9

1.8 Rationale For Study 9

Chapter 2. Design and Construction of Engineered Pro-inflammatory Cells 13

2.1 Abstract 13

2.2 Introduction 13

2.2.1 TLR4 Receptor Structure 14

2.2.2 Selection of Monocyte-MΦ RAW264.7 Cell Line 14

2.3 Material and Methods 15

2.3.1 Reagents and Antibodies 15

2.3.2 Plasmid Construction of cTLR4 15

2.3.3 Cell Transduction of cTLR4 Lentiviral Constructs 16

2.3.4 Cell Culture 17

2.3.5 Western Blotting 17

2.3.6 Luciferase Assay 17

2.3.7 Cytokine Profile 18

2.3.8 Statistical Analysis 18

2.4 Results 18
2.4.1 Engineering Pro-inflammatory Macrophages 18
2.4.2 MyD88-dependent and MyD88-independent Signaling Pathway Activation in MΦ-cTLR4 Cells 19
2.4.3 Optimization of MΦ-cTLR4 Cell Line and CID Drug Dose 21
2.5 Discussion 21
2.6 Conclusions 24

Chapter 3. Phenotypic Properties of MΦ-cTLR4 Cells 33

3.1 Abstract 33
3.2 Introduction 33
3.2.1 M1 Macrophage Markers 34
3.2.2 Plasticity in Macrophages 34
3.3 Materials and Methods 35
3.3.1 Reagents and Antibodies 35
3.3.2 Cytokine Profile 35
3.3.3 Western Blotting 36
3.3.4 Statistical Analysis 36
3.4 Results 36
3.4.1 Pro-inflammatory Activation of MΦ-cTLR4 Cells 36
3.4.2 MΦ-cTLR4 Cells Response to Withdrawal and Length of Treatment 37
3.4.3 Plasticity of MΦ-cTLR4 Cells 37
3.5 Discussion 38
3.6 Conclusions 41

Chapter 4. Functional Properties of MΦ-CTLR4 Cells 49

4.1 Abstract 49
4.2 Introduction 49
4.2.1 Process of Angiogenesis During Inflammation 50
4.2.2 Macrophage Influence on Angiogenesis 50
4.2.3 Vascular Endothelial Growth Factor and Macrophages 51

4.3 Materials and Methods 52
4.3.1 Cell Culture 52
4.3.2 Endothelial Cell Activation 52
4.3.3 Wound Closure Assay 53
4.3.4 Tube Formation Assay 53
4.3.5 VEGF-A Level Measurement 54
4.3.6 Statistical Analysis 54
4.4 Results 54
4.4.1 MΦ-cTLR4 Endothelial Cell Activation 54
4.4.2 Wound Closure Assay with MΦ-cTLR4 MΦ-Conditioned Medium 55
4.4.3 Co-Culture of MΦ-cTLR4 Cells and Endothelial Cells in Tube Formation Assay .. 56
4.4.4 VEGF Expression in MΦ-cTLR4 Cells 56
4.5 Discussion 57
4.6 Conclusions 61

Chapter 5. The Role of MΦ-cTLR4 Cells In the Inflammatory Response In Vivo 71

5.1 Abstract 71
5.2 Introduction 72
5.2.1 In Vivo MΦ Characterization 72
5.2.2 M1 Macrophages During the FBR 73
5.3 Materials and Methods 74
5.3.1 Reagents and Antibodies 74
5.3.2 Animals 74
5.3.3 Histological Samples 75
5.3.4 Trichrome and H&E Staining 75
5.3.5 Immunofluorescence 76
5.4 Results 77
5.4.1 Morphology and Cell Survival of Implanted Matrigel Plugs 77
5.4.2 Collagen Deposition in Matrigel plugs 77
5.4.3 MΦ-cTLR4 Cells Co-localized with iNOS Inflammation Regions in Tissue 78
5.5 Discussion 78

5.6 Conclusions 81

Chapter 6. Conclusion and Future Studies 91

References 94

LIST OF FIGURES

Figure 1.1: TLR4 Pathway Diagram 11
Figure 1.2: Diagram of Engineered Receptor Expressed in RAW264.7 Cells 12
Figure 2.1: Chapter 2 Summary Diagram 25
Figure 2.2: Toll-like Receptor Diagram 26
Figure 2.3: Diagram of cTLR4 Construct and Engineered Receptor and Confirmation of cTLR4 Construct Expression 27
Figure 2.4: GFP+ Cell Comparison of MΦ-cTLR4 and Control Transduced Cells. 28
Figure 2.5: CID-treated MΦ-cTLR4 Cells Activate the MyD88-dependent Pathway 29
Figure 2.6: CID-treated MΦ-cTLR4 Cells Activate the MyD88-independent Pathway .. 30
Figure 2.7: Dose of 50 nM CID Drug Produces Maximum Activation of MΦ-cTLR4 Cells 31
Figure 2.8: MidLow MΦ-cTLR4 Cells Exhibit Highest Signal to Noise Ratio. 32
Figure 3.1: Chapter 3 Summary Diagram 42
Figure 3.2: CID-treated MΦ-cTLR4 Cells Exhibit Increased Expression of TNFα, IL-6, and iNOS 43
Figure 3.3: MΦ-cTLR4 Cells Return to Baseline Levels 18 Hours Following CID Drug Withdrawal 44
Figure 3.4: CID-treated MΦ-cTLR4 Cells Remain Activated for At Least 48 Hours 45
Figure 3.5: MΦ-cTLR4 Cells are Influenced by IL-4 Treatment. 46
Figure 3.6: MΦ-cTLR4 Cells are Influenced by IL-4 Treatment 47
Figure 3.7: Schemata of CID-activated Pathways and LPS-activated Pathways. 48
Figure 4.1: Chapter 4 Summary Diagram 63
Figure 4.2: Medium From CID-treated MΦ-cTLR4 Cells Upregulate VCAM-1 and ICAM-1 on Endothelial Cells 64
Figure 4.3: Wound Closure Assay 65
Figure 4.4: Rates of Wound Closure 66
Figure 4.5: Co-culture Angiogenesis Assay Results 67
Figure 4.6: Quantification of Co-culture Angiogenesis Assay 68

Figure 4.7: VEGF-A Expression in MΦ-cTLR4 Cells 69
Figure 4.8: VEGF-A Expression in MΦ-cTLR4 with IFN-γ Co-treatment 70
Figure 5.1: Chapter 5 Summary Diagram. 83
Figure 5.2: 14 Day Untreated Mice Matrigel Plug 84
Figure 5.3: 14 Day CID-treated Mice Matrigel Plug 85
Figure 5.4: Collagen Deposition in Untreated and CID-treated Mice 86
Figure 5.5: 14 Day Untreated Plugs with No GFP and iNOS Co-localization 87
Figure 5.6: 7 Day CID-treated Plugs with GFP and iNOS Positive Cells with Co-localization 88
Figure 5.7: Co-localization of GFP and iNOS in 14 day CID-treated Matrigel Plugs 89
Figure 5.8: 14 Day CID-treated Plugs with GFP and iNOS Positive Cells with Co-localization 90

ACKNOWLEDGEMENTS

Thank you to Melissa Jackson for helping me with everything from western blots and making buffers to designing animal studies. I also want to thank Hsueh Yang for mentoring me and helping me finish the cloning portion of my project. Thanks to Matt Coons for aiding in various BCA and ELISA experiments. Additionally, I would like to thank each of my committee members for their guidance in helping me develop into a scientist, especially Marta Scatena and Cecilia Giachelli. Lastly, I would like to thank my funding sources: the Royalty Research Fund, the Bioengineering Cardiovascular Training Grant, and the College of Engineering Fellowship.

DEDICATION

I dedicate this dissertation to my parents and brother, and most importantly to my husband Tim. I will never be able to adequately express my gratitude and thanks to each and every one of you. I am sure that I would not have made it this far without the love and support of my mother, father, and brother. To my parents, I thank you for supporting my journey through academia, even though it might have lasted longer than you could have imagined. Tim, I love you with all my tiny heart and I really appreciate all the encouragement you have given me along the way.

Chapter 1. BACKGROUND

1.1 SIGNIFICANCE AND INNOVATION

1.1.1 *Significance*

Implanted medical devices have been used for more than 40 years. There have been about 50 implantable medical devices approved per year by the FDA, since 2008; adding to the 80,000 worldwide total (1). Furthermore, it has been estimated that 20-25 million Americans currently have a medical device implant (2). The increase in implanted devices can be attributed to scientific advances in medical device development, which range from biosensors, heart valves and tissue engineering scaffolds to drug-eluting stents and implantable glucose monitoring systems (3). Oftentimes implantable medical devices lose functionality over time. Examples of certain devices that lose functionality over time include biosensors, pacemaker leads, as well as any other device that depends on direct interaction with the surrounding tissue. A critical barrier in medical device implantation is the activation of the foreign body reaction (FBR), which can be due to the lack of functional integration of the device. The FBR is an inflammatory/immune process, driven by MΦs and MΦ-derived foreign body giant cells, which are activated as a defense mechanism by the host. The FBR ultimately results in a physical and functional barrier between the host and the implanted device. The barrier or capsule is generally depleted of blood vessels and is characterized by extensive fibrosis, which prevents successful tissue integration and causes deleterious effects on biomedical device function (4). There have been strides to mitigate the FBR by creating devices with non-fouling coatings (5, 6) or using anti-inflammatory (7) or pro-angiogenic drugs (8). However, these techniques have only marginally affected the FBR (3). Being able to fully

understand and regulate the inflammation resolution response, and limit the FBR, could be the key to improving biocompatibility and integration of medical devices.

1.1.2 *Improvement*

An appealing new theoretical concept to tissue regenerative therapies and biomedical device implantation is the addition of engineered MΦs that allow manipulation of the host response, thus resulting in reduction and resolution of the foreign body reaction while also facilitating regeneration and integration. To improve clinical practice, these engineered MΦs that can be engineered from patient derived monocytes, could potentially be added or delivered to the surrounding of an implantable device via an encompassing natural scaffold, such as fibrin or collagen (9). Manipulation via the activation of engineered MΦs, could then be achieved by the addition of a small molecule drug that can activate specific pathways to polarize the MΦ into a distinct functional phenotype. Furthermore, development of this technology could be applied to a number of classic inflammatory diseases to promote a physiological and reparative response. None of these tasks have been reported to date.

1.1.3 *Innovation*

While the idea that macrophage polarization is well established, the new theoretical concept of controlled macrophage polarization modulation into distinct phenotypic states, by using a new cell therapy approach, is innovative and has not yet been investigated.

1.2 PARADIGM FOR INFLAMMATION

The physiological inflammatory response requires a highly orchestrated series of events characterized by four basic phases: reaction, regrowth, remodeling and resolution (10). There are two main types of inflammation: acute inflammation and chronic inflammation. Acute

inflammation has a faster reaction time, involves mostly neutrophil and macrophage cell types, exhibits prominent local and systemic signs, and culminates in resolution. Conversely, chronic inflammation has a much slower onset and if often characterized as persistent, involves mostly macrophage and lymphocyte cell types, exhibits less prominent and subtle systemic signs, and often ends with fibrosis of the tissue. Both acute and chronic inflammation responses are triggered by certain pro-inflammatory molecules of invading microbes. However, sterile stimuli such as mechanical trauma, ischemia, chemicals, and antigens also trigger inflammation (11). In the event of infection or sterile inflammation, cytokines and chemokines are released, which increase permeability of capillaries and attract wandering polymorphonuclear and mononuclear leukocytes. Neutrophils are the first cells to arrive, as they respond to chemokine attractants and directors, such as extracellular adenosine triphosphate and other damage-associated molecular patterns (12, 13). Neutrophils phagocytise debris, kill bacteria by releasing reactive oxygen species (ROS) and aid in the cleaning of the wound by secreting proteases that breakdown damaged tissue. Neutrophils are usually the most prevalent cell type during the first 48 hours of inflammation. Once neutrophils finish cleaning up the infection, they undergo controlled apoptosis and infiltrating MΦs will engulf and degrade the neutrophils in a safe and controlled manner. During the next 2-5 days, MΦs are the most prevalent cell type at the site of inflammation. MΦs mature from their circulating monocyte precursor cells at the site of inflammation and respond to key cytokine signals such as IL-4 and IFN-γ. There are two main types of MΦs that exist: pro-inflammatory (M1 MΦ) and pro-healing (M2 MΦ). However, any polarized MΦ can be viewed as a single state in the continuum of diverse polarization states. Pro-inflammatory MΦs are the first MΦ sub-type to appear and aid in the natural debriding of the wound with neutrophils. Around three days post-infection, the pro-healing MΦ sub-type becomes the prominent player at the site

of infection by secreting anti-inflammatory cytokines, such as IL-10, and performing efferocytosis of apoptotic pro-inflammatory MΦs and neutrophils (14). Pro-healing MΦs also release factors, like TGFβ, which recruit endothelial cells, epithelial cells and fibroblasts; all key players in the next regrowth phase of healing. The regrowth phase can start as early as day three post-infection and last until day ten post-infection (15). During this phase, new cells grow into the wound and these cells begin to lay down collagen and other extracellular fibers. At this same time, new blood vessels are formed and begin to grow into the wounded areas. This tissue is called the granulation tissue. The remodeling and resolution phases take place concurrently, in that the resolution phase decreases the number of fibroblasts and pro-healing MΦs, as well as thins the dense capillary network. This occurs while the remodeling phase contracts the scar tissue and allows the scar to adjust to the tensions applied during everyday life. Inflammatory resolution can take up to 21 days to complete; however, the remodeling phase can take up to 6-12 months to adjust for physical movements, depending on the tissue. In some cases, the resolution phase fails to resolve inflammation, which can ultimately lead to a chronic inflammatory state or constant fibrotic remodeling in the affected tissues (16). The dysregulation of the innate immune response has been implicated as a key player contributing to these defective mechanisms (16). Therefore, the ability to regulate the intricate processes in innate inflammation could potentially elucidate culpable dysregulated mechanisms, which could possibly lead to remedies and an overall better understanding of inflammatory reactions and deadly inflammatory diseases.

1.3 Role of Macrophages in Inflammation

Monocytes are the precursor cells to macrophages (MΦs), which are a main inflammatory cell type that are known to be key players in the inflammatory response. When activated, they exist in two major phenotypes that can be broadly defined as: pro-inflammatory MΦs and pro-healing MΦs.

Pro-inflammatory MΦs are the first to arise at the site of injury and propagate the initial response by releasing pro-inflammatory cytokines as well as producing reactive oxygen species (ROS) in order to destroy foreign material at the injury site. Thus, pro-inflammatory MΦs are absolutely necessary in cleaning the injured and inflamed site, before any healing can begin. On the other side of the spectrum, pro-healing MΦs promote growth and regeneration and are present following the pro-inflammatory MΦ decline. These type of MΦs are present toward the end of the inflammatory response and mainly function to end and resolve inflammation, stimulate healing and restore tissue homeostasis characterized by proper vascularization and little to no fibrosis (17). In chronic inflammation patients, pro-inflammatory MΦs are the most prominent MΦ sub-type in the tissue with little pro-healing MΦ cells. This elevated pro-inflammatory MΦ level stays increased and tissues show no signs of resolution. The pro-inflammatory/pro-healing MΦ ratio can be helpful in determining the phase of the immune response. It has been hypothesized that a high pro-inflammatory/pro-healing MΦ ratio can lead to chronic inflammation from pro-inflammatory MΦ efferocytosis failure, due to the small numbers of efferocytic pro-healing MΦs available (18). If the pro-inflammatory MΦs are not efferocytized by pro-healing MΦs before they undergo necrosis, then the pro-inflammatory MΦ cytotoxic contents released into the tissue can cause further inflammation and recruitment of inflammatory cells. Left untreated, this condition is thought to be caught in an infinite loop of necrosis and further inflammation. Conversely, it is hypothesized that fibrosis is the result of a low pro-inflammatory/pro-healing MΦ ratio in which there is an excess of TGFβ-producing pro-healing MΦs (19). Due to high levels of TGFβ, there is a constant influx of collagen depositing fibroblasts and inflammation is never completely resolved. These notions strengthen the argument that it is necessary to have a balance of both pro-healing

and pro-inflammatory MΦs and any skewing of this balance could potentially lead to chronic inflammation or fibrosis of the tissue.

1.4 The Foreign Body Reaction

The foreign body reaction (FBR) to implanted biomedical devices begins almost immediately following implantation. The reaction starts with the non-specific adsorption of proteins to the device surface (20) and inflammatory cell infiltration. Neutrophils are the predominant cell type during the first few days, however, these cells are short lived and MΦs eventually predominate the inflammatory response (21). The recruitment of macrophages to the implant site promotes the production of additional chemoattractants, which amplifies the response. Up until this step, the FBR correlates closely with that of the natural inflammatory reaction to invading microbes and sterile stimuli. The next divergent steps involve the unsuccessful attempt of MΦs to phagocytose the implant. These MΦs then fuse to form multinucleated foreign body giant cells. In the final stage of the foreign body reaction a fibrotic response occurs in which fibroblasts proliferate and deposit collagen, which leads to the formation of a foreign body capsule isolating the implant from the surrounding tissue. During this response, the MΦ phenotype also becomes a mixed population, which is characterized by both M1 and M2 MΦ markers. This mixed population or intermediate phenotype of MΦ contrasts with the acute inflammatory response, which is characterized by distinct phases of M1 and M2 MΦ populations in a temporal manner. Previous studies have tried to mitigate the FBR by methods involving: steroid-releasing polymers, non-fouling techniques, regulating key matricellular proteins, anti-sense RNA and siRNA approaches, as well as porous biomaterials (22). Cellular approaches mainly focus on pre-treating the device surface with stem cells (23) or modulating lymphocyte and MΦ cell-cell interactions (24). Currently in literature, there have been no cellular engineering approaches to control or modulate MΦ polarization to

lessen the FBR. Having the ability to control MΦ polarization during and after implantation could potentially allow for the manipulation of the host response and the successful integration of biomedical devices.

1.5 Macrophage Impact on Angiogenesis

Angiogenesis or neovascularization, the formation of new blood vessels from pre-existing capillaries or de novo, is a physiologic and pathologic process that has been associated in cancer, chronic inflammation and ischemic diseases. Although normal tissue remodeling and repair during ontogenesis and adult life is characterized by new vessel formation for supply of oxygen and nutrients, there is also a large range of different and unrelated diseases linked to neovascularization (25). While some diseases might benefit from an inhibition of angiogenesis, like cancer, atherosclerosis and fibrosis, there are some diseases or conditions that could benefit from a pro-angiogenic response, such as cardiac failure, ischemia or the FBR. Several studies in the field strongly suggest that macrophages (MΦs) can affect the pro- and anti-angiogenic balances that encompass many of these disease pathologies (26, 27). It has been shown that pro-inflammatory MΦs have inhibited tube formation in an *in vitro* co-culture angiogenesis assay (28). On the other hand, pro-healing MΦs have been reported to express increased levels of vascular endothelial growth factor (VEGF) receptor 1 and 2, which is activated by the potent angiogenic factor VEGF (25). This VEGF production from MΦs is thought to aid in the survival and growth of endothelial cells, thus enhancing angiogenesis. Furthermore, during *in vivo* Matrigel plug experiments and *in vitro* angiogenesis assays, pro-healing MΦs have been shown to enhance angiogenic potential (28). Increasing angiogenesis around an implantable biomedical device, via MΦ phenotype modulation, could be a solution to better device integration. Accordingly, angiogenesis makes for an appealing

application in order to investigate the potential for engineered macrophages to influence endothelial neovessel formation and morphogenesis via polarization into different phenotypes.

1.6 TOLL-LIKE RECEPTOR 4 SIGNALING

Toll-like receptor 4 (TLR4) belongs to a family of toll-like receptors (TLRs) that recognize pathogen-associated molecular patterns (PAMPs) that are expressed on foreign agents. Following recognition of a PAMP, a TLR will mediate specific cytokine production necessary to combat the foreign agent. TLR4 specifically detects lipopolysaccharides (LPS) and Lipid A from Gram-negative bacteria and activates the innate immune system accordingly. When LPS binds to TLR4, the receptor homodimerizes and subsequently activates few downstream pathways. It was once believed that TLR4 only signaled via the adaptor proteins MyD88 and TIRAP, which lead directly to NF-κB activation (MyD88-dependent pathway). However, a second MyD88-independent pathway was discovered in which TRIF and TRAM adaptor proteins were involved (Figure 1.1). This MyD88-indpendent pathway initiates the type 1 IFN response as well as late NF-κB activation (29-33). Most importantly, TLR4 activation is associated with pro-inflammatory MΦ polarization (34). Exposure to LPS and INF-γ are commonly known to drive *in vitro* classical pro-inflammatory MΦ polarization (34). Knockout studies of TLR4 have shown MΦs to be hyporesponsive to the strong pro-inflammatory immune elicitation of LPS. Moreover, overexpression rescue experiments revealed activation of NF-κB, which indicates that TLR4 is necessary for pro-inflammatory LPS signaling (35). Overall, these studies strengthen the argument that TLR4 is a key receptor in controlling pathways during the innate pro-inflammatory response and should definitely be considered in experiments aiming to engineer polarization of pro-inflammatory MΦs.

1.7 Chemically Induced Dimerization (CID) System

For the endogenous TLR4 membrane-spanning receptor, it is necessary for this receptor to dimerize in order to activate its pathways. Receptor dimerization causes activation of the intracellular signaling cascade at the cytoplasmic side of the receptor. Physiologically, dimerization is achieved by a specific ligand binding to the receptor. Techniques in protein engineering utilizing the chemically induced dimerization (CID) system can activate pathways in the absence of a receptor's specific ligand (36) (Figure 1.2). This system works by fusing the intracellular domain of the receptor to a protein engineered dimerization domain, which binds to a diffusible synthetic ligand (AP20187) that is a chemical inducer of dimerization (CID). The F36V engineered dimerization domain is derived from a mutated version of the endogenous FKBP12 protein (phenylalanine to valine point mutation) and the FRB engineered domain is derived from FKBP rapamycin-associated protein with a threonine to leucine point mutation (37). The diffusible synthetic ligand is a redesigned version of the naturally occurring FK506 molecule. The Blau group has used this CID technology to engineer red blood cells with a chemically-induced myeloproliferative leukemia virus oncogene (mpl) that can stimulate red blood cell expansion following cell transplantation (38). The significance of this implemented technology is CID-regulated erythropoiesis independent of the mpl-ligand erythropoietin (Epo), which is a pathway that has been implicated in many types of cancer (39). The successful application of this system to the mpl receptor, and various other receptor domains (40-44), has given incentive to attempt this methodology with TLR4 to develop engineered pro-inflammatory MΦs.

1.8 Rationale For Study

There have been various attempts at mitigating the FBR. Firstly, steroid releasing polymers surrounding the implant have been used since the 1980's (45). The most common steroid is

dexamethasone. However, even though this steroid decreases the inflammation response, the mechanism of action is still unknown. Other groups have attempted using non-fouling techniques, which involved creating implant materials that decrease protein adsorption and immune cell adhesion, however these materials are very unstable and degrade quite fast (46). Groups have also attempted regulating key matricellular proteins involved in vessel formation to increase angiogenesis or attempted regulating specific genes with siRNA, such as *RAC1* which is involved in cytoskeleton rearrangement and fusion of foreign body giant cells (47, 48). However, these techniques are heavily dependent on the delivery of the molecules used to regulate these targets and the efficiency of these methods. Lastly, groups have attempted to surround devices in porous biomaterials, such as sphere-templated scaffolds that recruit specific immune cells to allow the better integration of implanted devices, however the mechanism of action of these biomaterials is still not completely understood (49). With none of these current treatment strategies being ideal, my solution is to use a cell therapy approach, in which an encompassing scaffold is added to the device during the implant procedure that contains engineered M1-like pro-inflammatory cells (MΦ-cTLR4 cells). Since the FBR is thought to be a dysregulated state that displays both M1 and M2 MΦ markers at the same time, as opposed to the acute inflammation response that exhibits distinct M1 and M2 MΦ phases, I hypothesize that an initial distinct M1 pro-inflammatory response, with no M2 MΦ phase present, can decrease fibrosis and increase angiogenesis for better device integration. In fact, there have been reports that scaffolds containing exclusively M1 MΦs have been associated with more vessel formation (50). These results indicate that M1 MΦs might play a key role in regulating this process. The addition and activation of the engineered MΦ-cTLR4 cells around device implants might be the necessary tool to regulate the adverse effects of the FBR.

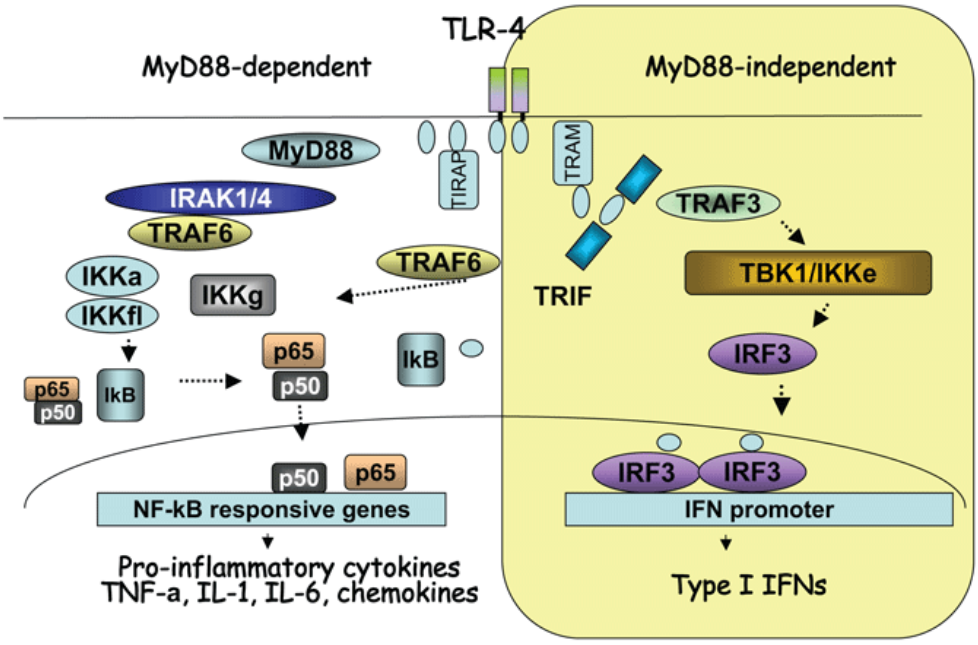

Figure 1.1: TLR4 Pathway Diagram including both MyD88 dependent and independent pathways. Figure from Szabo, et al. (2011)(51)

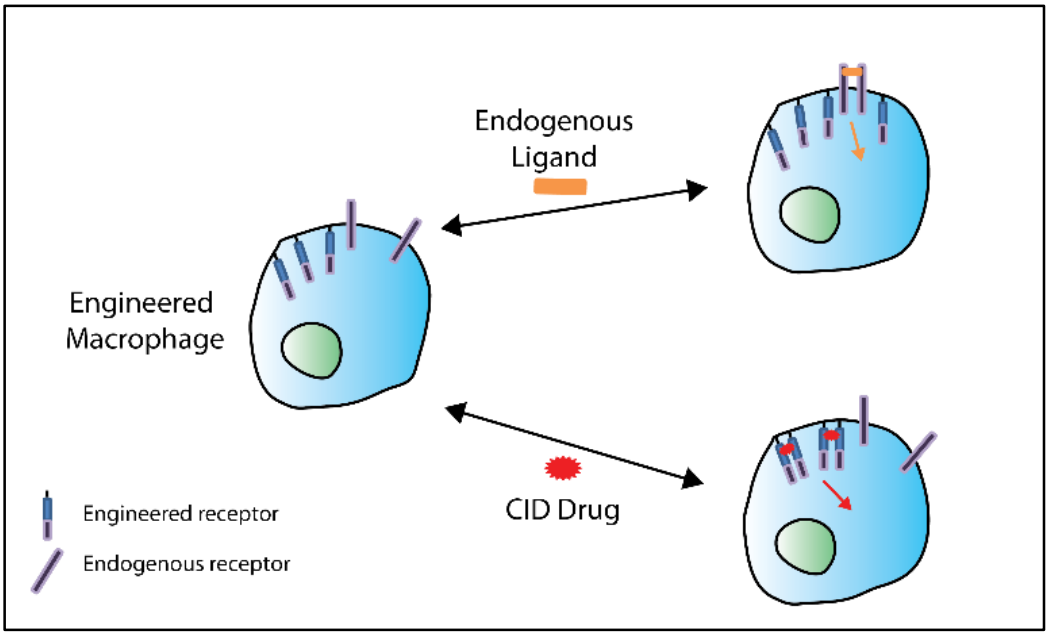

Figure 1.2: Diagram of Engineered Receptor Expressed in RAW264.7 Cells. Comparison of CID drug and endogenous ligand treatments.

Chapter 2. DESIGN AND CONSTRUCTION OF ENGINEERED PRO-INFLAMMATORY CELLS

2.1 ABSTRACT

In this chapter, I have outlined the design of the cTLR4 pro-inflammatory MΦ construct and explored the pathway activation of the MΦ-cTLR4 cells, following transduction of the cTLR4 construct into the monocyte-like RAW264.7 cell line. I validated the presence of the construct by probing for the FKBP12/F36V protein via western blot analysis and optimized the engineered cell line by sorting for >90% transduction efficiency. As the TLR4 receptor is known to be activated during M1 MΦ responses, I hypothesized that the engineered CID-induced cTLR4 construct would dimerize and activate TLR4-specific pathways following addition of CID drug. To this end, I tested for both MyD88-dependent and MyD88-independent pathway activation, which included ERK1/2, NF-κB, and IRF-3 activation. All three proteins exhibited activation in CID-treated MΦ-cTLR4 cells. Lastly, optimization of the engineered cell line was accomplished by sorting for different GFP intensity populations, in which GFP was the tag in the engineered MΦ-cTLR4 cells, and subsequently performing a CID-drug titration on the MΦ-cTLR4 cells. A "midlow" GFP intensity population, as well as a CID drug concentration of 50 nM, was selected for all future experiments.

2.2 INTRODUCTION

M1 MΦs are the first MΦ population to arrive at the injury site following an innate inflammatory response. In comparison, a distinct M1 MΦ response does not occur during the FBR, which is thought to reflect a dysregulated inflammation state. Instead the MΦ population present around the implanted device usually has both M1 and M2 MΦ characteristics. I have hypothesized that a distinct M1 MΦ response at the onset of the FBR can lead to better integration of implanted

devices, as well as better healing outcomes. In this chapter, I will summarize the design and validation of the engineered pro-inflammatory MΦs with the plan to use these engineered MΦs to control the innate inflammatory response to display a distinct primary M1 MΦ burst in order to prime the reaction for subsequent M2 MΦ events (Figure 2.1).

2.2.1 *TLR4 Receptor Structure*

All toll-like receptors evolved from a common structural framework. This common structural framework is comprised of Leucine-Rich Repeat (LRR) structures, which allows for various modes of molecular recognition (52). LRRs are repeated units of about 25 conserved hydrophobic amino acids in the protein structure. Each LRR secondary structure contains a short parallel β-sheet, a turn, and then a variable region. When repeated one after another, the blocks form a solenoidal structure (53). It is the inner concave surface of the solenoid that mediates the specific molecular recognition, by interactions with the ligands and the protruding side chains that extend off of the short parallel β-strands. Moreover, similar to other type I receptors, TLR4 is connected to the cytoplasmic toll-interleukin receptor domain by a single transmembrane helix. Even though there is no sequence homology in these segments between different TLRs, the transmembrane sequences likely play a significant role in receptor activation. For this reason, I chose to include this key transmembrane helix in the engineered construct. A representative toll-like receptor can be seen in Figure 2.2.

2.2.2 *Selection of Monocyte-MΦ RAW264.7 Cell Line*

Bone marrow derived MΦs (BMDMs) are the gold standard for *in vitro* MΦ experimentation. However, adequate amounts of BMDMs are difficult to obtain and achieving high transduction efficiencies are even more challenging. Therefore, for the *in vitro* studies, I used a cell line that could be stably transduced. Three potential monocyte-MΦ cell lines were available to choose from:

IC-21, J774A.1, and RAW264.7 cells. All cell lines have been compared to BMDMs for cell morphology, surface antigen expression, and cytokine production (54). Literature searches revealed that IC-21 cells display similar morphology as BMDMs, but generally have significantly higher levels of most surface antigens and cytokines. The J774A.1 cell line do not share morphological similarities with BMDMs and these cells are also missing the presence of key mRNAs, such as GM-CSF. The RAW264.7 cell line do not have morphological similarities to BMDMs, however, this cell line shares similar levels of surface antigen expression, as well as similar levels of key cytokines, such as TNFα and IL-6. For the purposes of the studies, I selected RAW264.7 cells, as this cell line is most functionally similar to the BMDMs.

2.3 Material and Methods

2.3.1 *Reagents and Antibodies*

The monoclonal anti-human/mouse/rat FKBP12 antibody was purchased from Thermo Scientific. The following antibodies were purchased from Cell Signaling: p44/42 MAPK, Phospho -p44/42 MAPK, IRF3 and Phospho-IRF3. The anti-iNOS/NOS type II antibody was purchased from BD Biosciences. The HRP-conjugated goat-anti-rabbit antibody was obtained from Jackson ImmunoResearch Laboratories, Inc. and the HRP-conjugated goat-anti-mouse antibody was obtained from Life Technologies. LPS was purchased from Sigma. AP20187 (CID drug) was purchased from Clontech. Lipofectamine 2000 was purchased from Invitrogen. The Dual-Luciferase ® reporter assay system was obtained from Promega Corporation.

2.3.2 *Plasmid Construction of cTLR4*

The mouse Sport6-TLR4 vector was purchased from Open Biosystems. The cytoplasmic portion of TLR4 (cTLR4) was amplified (mRNA base pairs 2207-2748) and inserted into a pBluescript II KS+ vector with an existing myristolation domain and engineered F36V domain (pBluescript-

Myr-F36V) (55) following BamHI and EcoRV restriction enzyme (RE) cuts. PCR products were gel purified using a QIAEX II gel extraction kit (Qiagen) before ligations were performed. This resulted in a pBluescript-Myr-F36V-cTLR4 construct. The pCDH-EF1α-MCS-T2A-copGFP lentiviral cDNA and expression vector was purchased from System Biosciences. This vector was cut in the MCS with both NheI and EcoRI, and a PCR amplified portion of the Myr-F36V-cTLR4 sequence was ligated into this site within the pCDH-EF1α-MCS-T2A-copGFP vector (7.26 kb). This resulted in the final cTLR4 lentiviral plasmid: pCDH-EF1α-Myr-F36V-cTLR4-T2A-copGFP (8.18 kb).

2.3.3 *Cell Transduction of cTLR4 Lentiviral Constructs*

We utilized a 3rd generation lentiviral vector, pCDH (System Biosciences), carrying the cTLR4 gene under the control of the EF-1α promoter. For stable lentiviral transductions, $5x10^6$ HEK293T packaging cells were seeded in 10-cm cell culture dishes that were previously coated with 50 ug/mL poly-D-lysine hydrobromide (Sigma). Culture medium was changed just prior to transduction. In total, 12 µg plasmid DNA was used for each 10-cm dish (2.8 µg transfer vector (cTLR4), 0.9 µg pSL3 (vesicular stomatitis virus G envelope), 5.4 µg pSL4 (HIV-1 gag/pol packing genes), and 2.8 µg pSL5 (rev gene required for HIV-1 envelope protein expression). DNA and Lipofectamine 2000™ (Life Technologies) were diluted in Opti-MEM® medium (Gibco) separately. After a 5 minute incubation, DNA and lipofectamine were combined and incubated for 20 minutes at room temperature. The complexes were then added, drop-wise, to cell dishes with 8 mL growth medium and medium was replaced after 14-16 hours. Virus supernatant was collected following an additional 48 hours by filtering through a 0.45 µm filter. Filtered virus supernatant was then added either directly or in concentrated form to previously plated RAW264.7 cells ($5x10^5$ cells per well) in 6-well plates. Following initial transduction, only 40% of cells were positive for

GFP expression. Cells were then sorted for GFP expression to acquire a greater than 90% GFP positive MΦ-cTLR4 cell line.

2.3.4 *Cell Culture*

RAW264.7 were obtained from ATCC. RAW264.7 cells were cultured in DMEM medium from Invitrogen containing 10% (v/v) heat-inactivated FBS and 100 U/ml pen/strep (Invitrogen) and incubated at 37°C with 5% CO_2.

2.3.5 *Western Blotting*

Protein from RAW264.7, MΦ-T2A (vector control cells), and MΦ-cTLR4 cell monolayers were extracted by lysis in Laemmli buffer containing 1x Halt Protease Inhibitor cocktail (Thermo Scientific). Following lysis, samples were boiled and protein concentration was determined by performing a BCA assay from Thermo Scientific. Samples (10-30 µg of lysates) were run on 4-20% Mini-PROTEAN® TGX precast polyacrylamide gels (Bio-Rad). Protein from gels were transferred onto PVDF membranes and probed with the appropriate primary antibody overnight. Membranes were washed between each antibody incubation and subsequently probed with the appropriate HRP-conjugated secondary antibody (Life Technologies). The Clarity Western ECL Substrate (Bio-Rad) was used to detect bands.

2.3.6 *Luciferase Assay*

Two hundred thousand cells/well were seeded in 24-well plates. The following day each well was transfected with a total of 0.8 µg plasmid DNA, which consisted of a 20:1 ratio of pBIIX-LUC (NFκB reporter construct):pRL (Renilla luciferase construct). The pBIIX-LUC reporter construct driving the luciferase gene was a kind gift from D. Baltimore (Massachusetts Institute of Technology, Boston, MA) to Drs Scatena and Giachelli (55). The promoterless pGL4.10 vector was also transfected in a 20:1 ratio of pGL4.10:pRL, as a control. Transfections of each well were

performed with 2 µL Lipofectamine 2000 (Invitrogen). The following morning transfection reagents were replaced with fresh serum-free medium and treated with either vehicle (100% EtOH) or CID drug (50 nM) for 4 hours. Cell lysate was harvested and luciferase activity was measured using a Dual-Luciferase ® reporter assay kit (Promega) according to manufacturer's instructions. All groups were normalized to Renilla luciferase.

2.3.7 *Cytokine Profile*

We tested IL-6 concentrations in supernatants of transduced RAW264.7 cells *in vitro*. Briefly, MΦ-cTLR4 cells (1×10^6) were plated in each well of a 6-well plate and treated with vehicle (100% EtOH), LPS (100 ng/mL), CID drug (50 nM), or left untreated in DMEM without serum. Supernatants were collected after 24 hours and tested using the mouse IL-6 ELISA Ready-SET-Go! Kit (eBioscience) according to the manufacturer's instructions. Plates were read at 450 nM with a 570 nM wavelength subtraction, normalized to standard solutions, and concentrations (pg/mL) were calculated.

2.3.8 *Statistical Analysis*

Results are expressed as mean ± SE unless otherwise specified. Significance between groups was determined by one-way ANOVA and p-values less than 0.05 were considered significant.

2.4 RESULTS

2.4.1 *Engineering Pro-inflammatory Macrophages*

With the goal of developing inducible M1 MΦ cells, I have engineered the murine monocytic cell line RAW264.7 to express a fusion protein comprising the intracellular TLR4 signaling domain and F36V-dimerization domain that binds to a cell permeable CID drug (Figure 2.3A). The cTLR4 construct is in a pCDH expression system. The 5' end of the construct starts with a myristoylation

domain (Myr), which allows targeting to the membrane to mirror the spatial localization of the endogenous full length TLR4 domain. The Myr domain is followed by the engineered F36V dimerization domain, which has a binding site for the CID drug. This domain is linked to the cTLR4 domain, which is only the cytoplasmic portion and the entire transmembrane domain of the receptor that is necessary for proper signal transduction. This design allows dimerization via a F36V-F36V interaction with the homodimerization CID drug (AP20187). Lastly, there is a T2A ribosome skipping sequence that allows the separate expression of GFP at the 3' end of the construct. The GFP expression allows the transcriptional verification of transduced cells.

Delivery of the cTLR4 engineered constructs to RAW264.7 cells was achieved via lentiviral methods. Control MΦ cells were also generated. These cells were transfected with constructs lacking the cytoplasmic and engineered domain (MΦ-T2A). Confirmation that the whole engineered construct was being transcribed was validated by the expression of the GFP reporter marker in the MΦ-cTLR4 cell line (Figure 2.4). Protein expression of the cTLR4 construct in the MΦ-cTLR4 engineered cells was verified by western blot analysis for the FKBP12/F36V domain. A corresponding 35.5 kDa band can be seen in Figure 2.3B.

2.4.2 *MyD88-dependent and MyD88-independent Signaling Pathway Activation in MΦ-cTLR4 Cells*

Following LPS stimulation, the TLR4 pathway leads to activation of NF-κB and the three MAPK pathways through the MyD88-dependent pathway. Both NF-κB and MAPK pathways directly control the transcription of the TNFα, IL-6 and iNOS inflammatory genes, as well as control the mRNA stability of those transcripts. For the activated MΦ-cTLR4 cells, ERK1/2 phosphorylation is expected if the MyD88 dependent pathway and subsequent downstream TRAF6 activation has

occurred. Therefore, I performed a western blot to probe for phosphorylated-ERK (p-ERK) and total ERK and compare the p-ERK/total ERK ratio relative to the zero timepoint (Figure 2.5A). As time increases from 0 minutes to 60 minutes, the CID-treated MΦ-cTLR4 cells exhibit an upregulation of ERK1/2 phosphorylation at the 5 minute timepoint, a subsequent decrease for the 15 minute timepoint, and then a significant increase for the last two 30 minute and 60 minute timepoints. The LPS-treated MΦ-cTLR4 cells exhibited a similar ERK1/2 phosphorylation pattern but with lower maximum phosphorylation. The NF-κB transcription factor has also been shown to be activated following TLR4 dimerization. Thus, MΦ-cTLR4 cells were tested for NF-κB promoter activation via a Dual-Luciferase reporter assay. Cells were transduced with a NF-κB responsive promoter element driving the luciferase gene. Measurement of the luciferase activity following CID treatments (Figure 2.5B) shows that CID-treated MΦ-cTLR4 cells have increased NF-κB promoter activation when compared to the vehicle. These results suggest that the CID-treated cells signal through the MyD88 dependent pathway.

To determine if the MΦ-cTLR4 cells were signaling through the MyD88-independent pathway, I tested for phosphorylated IRF3. This protein is downstream of the MyD88-independent pathway and has been shown to translocate into the nucleus and regulate type I interferon responses (56). Western blot analysis of the p-IRF3/total IRF3 ratio relative to the zero timepoint (Figure 2.6) shows a pronounced activation peak at 2 hours for both CID- and LPS-treated MΦ-cTLR4 cells when compared to vehicle. The IRF3 phosphorylation of the CID- and LPS-treated MΦ-cTLR4 cells starts to decrease following the 2 hour timepoint and subsequently reaches similar levels as vehicle at the 6 and 12 hour timepoints.

2.4.3 *Optimization of MΦ-cTLR4 Cell Line and CID Drug Dose*

For MΦ-cTLR4 cells, IL-6 levels are elevated in CID-treated cells when compared to controls. In order to find the optimal *in vitro* dosage, an IL-6 ELISA was performed to test for the maximum signal of this cytokine in a CID drug titration experiment. The optimal dose of CID drug corresponds to the lowest dose that induces the highest level of IL-6 expression. The IL-6 ELISA results are seen in (Figure 2.7). These results suggest that a dose of at least 50 nM, produces the maximum activation of MΦ-cTLR4 cells in the range from 50 nM - 250 nM.

The MΦ-cTLR4 cells were also optimized for maximal signal to baseline activation by sorting four different GFP intensity populations: dim, midlow, midhigh, and high. An IL-6 ELISA was performed to determine activation of these populations compared to unsorted MΦ and MΦ-T2A populations (Figure 2.8). As signal intensity increased, the baseline activation of MΦ-cTLR4 cells also increased. A potential explanation for the high baseline activation as GFP intensity increases might be that some cells have more cTLR4 construct copies integrated into their genome, thus resulting in higher GFP intensity. This higher number of copies will yield a greater concentration of the engineered cTLR4 construct on the cell surface and might result in self-dimerization, if the constructs are in close enough proximity. Ultimately, I determined that the "midlow" MΦ-cTLR4 population had similar CID and LPS activation, as well as the highest signal to noise ratio, so I used this sorted population for future experiments.

2.5 DISCUSSION

The CID system has been successfully used in literature to trigger a variety of signal transduction cascades. *In vitro* immunology studies using this system have been mostly focused on downstream effects of a specific engineered receptor's signaling pathway (57-59). For instance, Kuenzel et al.

transfected HeLaS3 cells with a nucleotide-binding oligomerization domain-like receptor 5 (NLRC5)-FKBP fusion protein and determined that induced oligomerization of this receptor activated certain IFN signaling pathways that contributed to an antiviral defense mechanism (58). In another study, Fooksman et al. transiently transfected T2 cell lines with a dimerizable mouse class I H2-K^b H chain-FKBP fusion protein and determined that induced dimerization, and thus clustering of this class I MHC construct, enhanced lymphoblast recognition by T cells (59). In contrast to using the CID system to examine cause and effect relationships within a specific pathway, this study is the first to use this system to regulate the phenotype of a cell by polarizing RAW264.7 cells into a specific pro-inflammatory MΦ. Further, my lab has previously demonstrated that this system can be used to engineer inducible bone resorbing osteoclasts from the monocyte-macrophage RAW264.7 cell line, in which it is important to note that monocytes are a common precursor to both macrophages and osteoclasts (60).

Other groups have attempted to engineer macrophages to control the inflammatory response. For example, Wu et al. transduced MΦs *in vitro* with the IFN-γ gene and delivered them intratracheally to immunodeficient mice (61). These MΦs restored immune function in the lungs of the immunodeficient mice. However, these constitutively active IFNγ-expressing pro-inflammatory MΦs probably have limited applications, since the cells were not engineered to be tunable. Additionally, Oxford BioMedica has engineered human MΦs to express cytochrome P450, which can convert a cancer prodrug into its active form during hypoxic tumor conditions. When delivered into an avascular spheroid model, the human engineered P450 MΦs were able to induce tumor cell death following the addition of the prodrug (62). The success of this study was dependent on the hypoxia-driven expression of cytochrome P450 in MΦs. The engineered MΦ-cTLR4 in this study,

on the other hand, can be controlled temporally and specifically with the addition or withdrawal of the CID drug and activation is independent of the local environment. The ability to tune the engineered MΦs with respect to selective activation provides a large added benefit, since the engineered MΦ-cTLR4 cells could be turned on or off when and if necessary.

Even with the successful generation of the pro-inflammatory MΦs, there were some complications with the transduction and activation that may be of concern when and if this technology is translated into clinical use. First, there were issues with high levels of transduction. The GFP expression was very dim and only about 2-5% positive, following lentiviral transduction. The low transduction efficiency required sorting the cells to acquire a higher GFP positive population. This suggests that another method of DNA integration is necessary, if this technique were to be used in primary cells, as these cells are even more difficult to transduce. Secondly, once the cells were sorted, there was a high baseline of self-activation. The self-activation required sorting different populations and testing each population for the highest signal to noise ratio. This technique worked well for the cell line, however, this would probably not be an option for primary cells, since the technique utilizes a significant amount of cells. Lastly, the MΦ-cTLR4 cells did not respond differentially in the CID drug titration experiment. This suggests that there is a uniform activation that may or may not allow fine-tuning in the MΦ-cTLR4 cells. Although it would be beneficial to control the level of activation of MΦ-cTLR4 cells by the concentration of CID drug treatment, this is not necessary and the engineered cells could still be turned on and off by addition or withdrawal of the drug. Ultimately, while the optimization of the cTLR4 transduction would be beneficial for primary cells and subsequent translational work, this chapter illustrates a proof-of-principle cell

line engineering study that is equally useful, as a tool to understand inflammation and the healing process in various diseases at a higher level.

2.6 CONCLUSIONS

In this section, I designed and optimized the engineered pro-inflammatory MΦ cell line (MΦ-cTLR4). I confirmed that the engineered cTLR4 receptor was being expressed in the stably transduced RAW264.7 cell line via western blot analysis. Additionally, I determined that both MyD88-dependent and MyD88-independent pathways were activated by CID drug treatment in MΦ-cTLR4 cells, by testing for NF-κB, ERK1/2, and IRF3 activation. Further, the cell line was optimized for CID dose and for highest signal to noise ratio via cell population sorting. This optimization resulted in selecting the "midlow" population for the highest signal to noise ratio and choosing a CID drug dose of 50 nM as the lowest dose to fully activate the MΦc-TLR4 cells. With the creation and optimization of the MΦ-cTLR4 cells, subsequent steps involve utilizing these cells in *in vitro* experiments to test for further M1 MΦ characteristics.

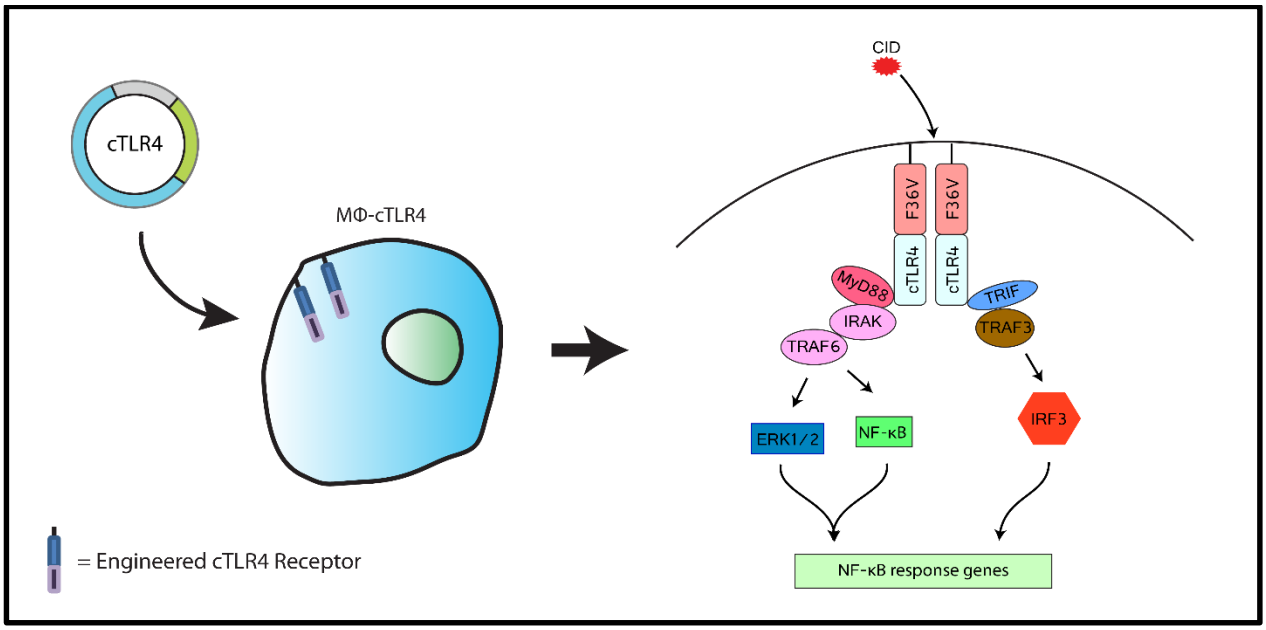

Figure 2.1: Chapter 2 Summary Diagram. The cTLR4 construct was designed and then transduced into RAW264.7 cells using lentiviral methods. After optimization, MΦ-cTLR4 cells were tested for TLR4-specific pathway activation, by testing for phosphorylated ERK1/2 levels and NF-κB promoter activation for the MyD88-dependent pathway and testing for phosphorylated IRF3 levels for the MyD88-independent pathway.

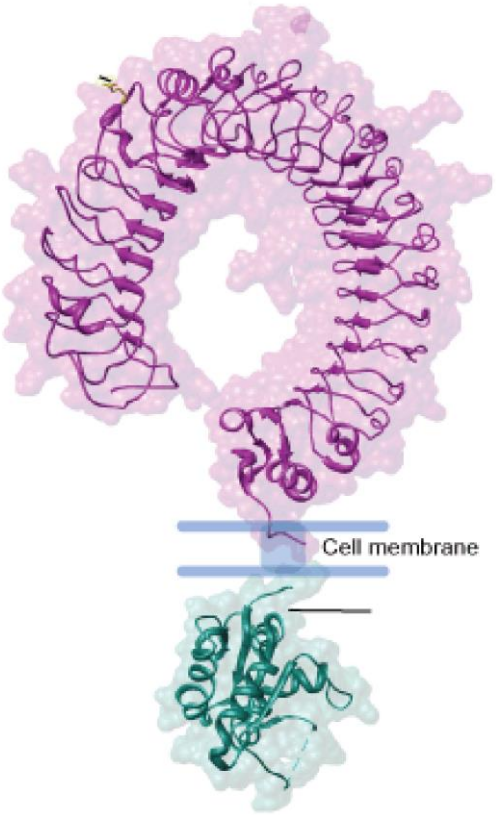

Figure 2.2: Toll-like Receptor Diagram. Bottom green domain is the cytoplasmic toll-interleukin receptor (TIR) domain which is connected through the membrane by the transmembrane domain. The top purple domain is the LRR portion in the shape of a solenoid that interacts with the ligand.

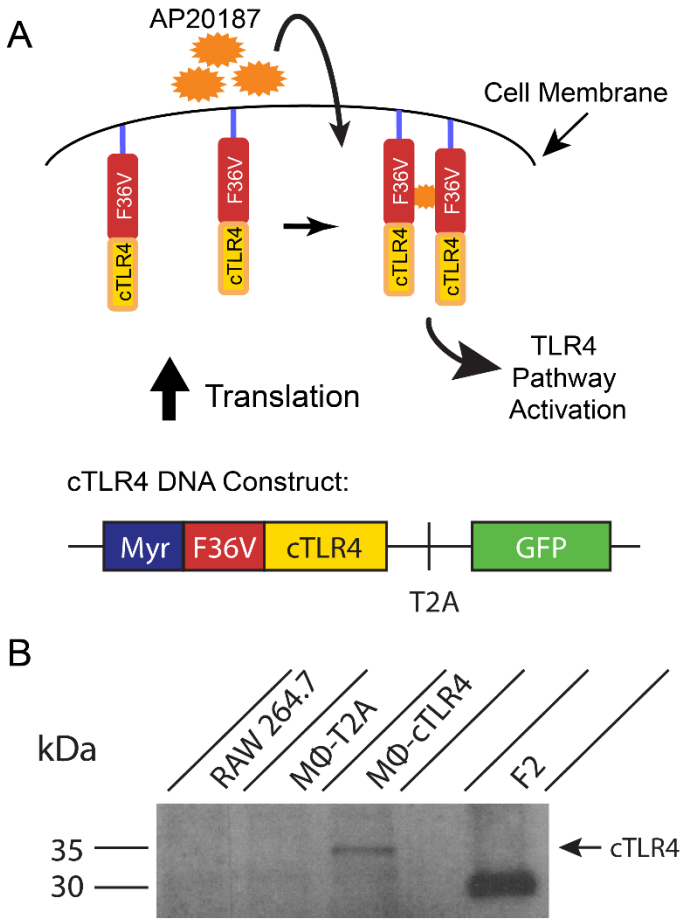

Figure 2.3: Diagram of cTLR4 Construct and Engineered Receptor and Confirmation of cTLR4 Construct Expression. (A) The cTLR4 construct. (B) Western blot probing for the FKBP12/F36V domain (35.5 kDa) containing lysates from RAW264.7 cells, MΦ-T2A negative control cells, MΦ-cTLR4 cells, and F2 positive control cells. MΦ-T2A cells have been transduced with a construct that contains only the T2A ribosome skipping sequence with the GFP tag. F2 cells have been transduced with just two adjacent F36V domains.

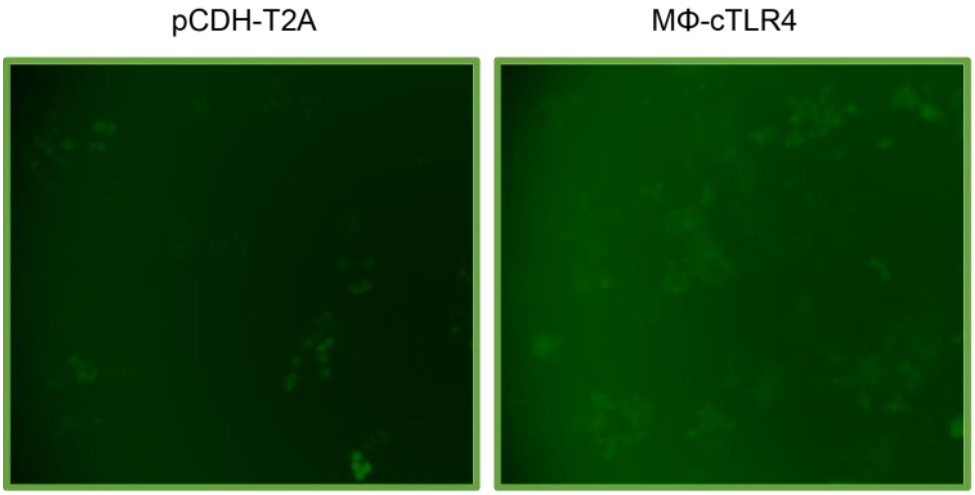

Figure 2.4: GFP+ Cell Comparison of MΦ-cTLR4 and Control (pCDH-T2A) Transduced Cells.

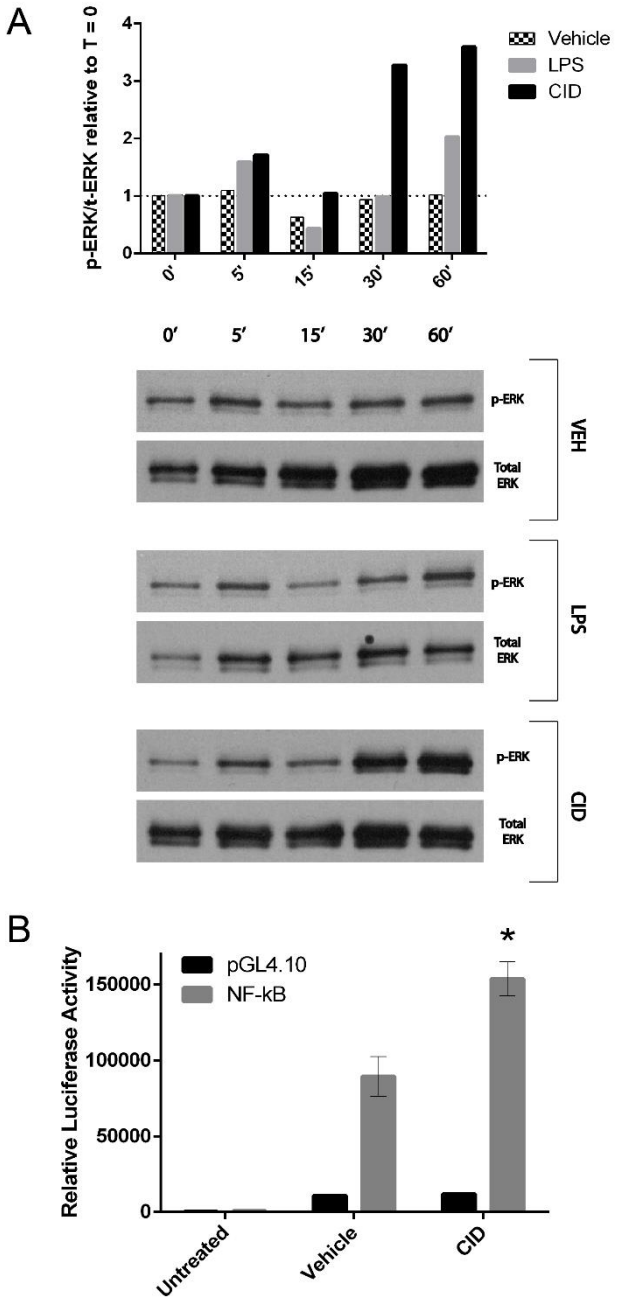

Figure 2.5: CID-treated MΦ-cTLR4 Cells Activate the MyD88-dependent Pathway. (A) Western blot probing for p-ERK and total ERK. Top panel shows phosphorylated over total ERK ratio relative to the zero timepoint for each subsequent timepont. Bottom panel shows corresponding blots (B) A Dual-luciferase® assay was used to determine NF-κB activity in MΦ-cTLR4 cells.

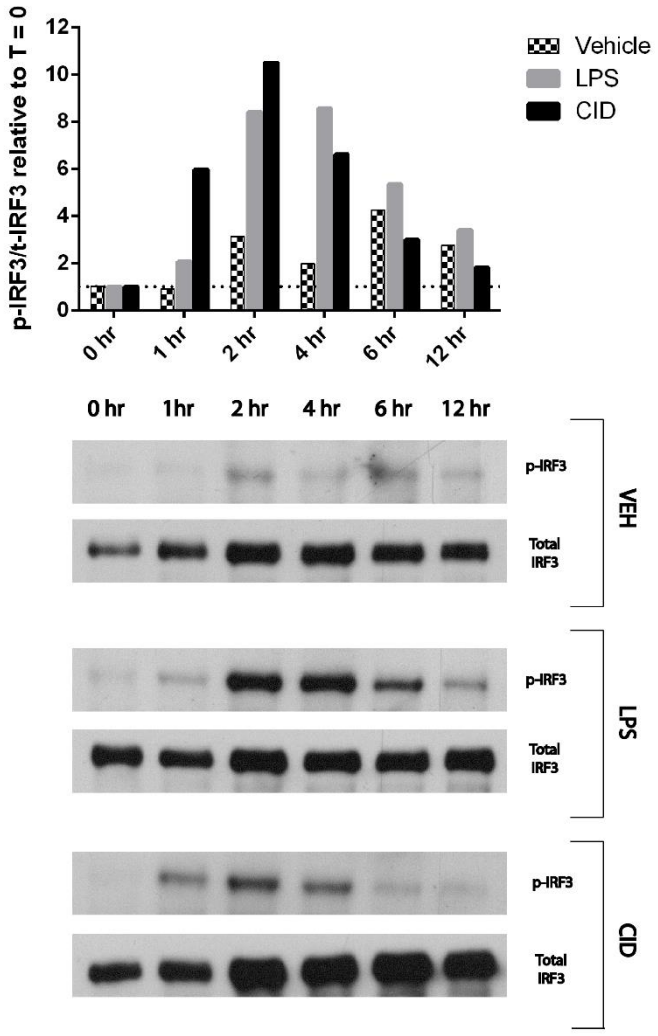

Figure 2.6: CID-treated MΦ-cTLR4 Cells Activate the MyD88-independent Pathway. Western Blot for p-IRF3 and total IRF3. Top panel shows phosphorylated over total IRF3 ratio relative to the zero timepoint for each subsequent timepoint. Bottom panel shows corresponding blots.

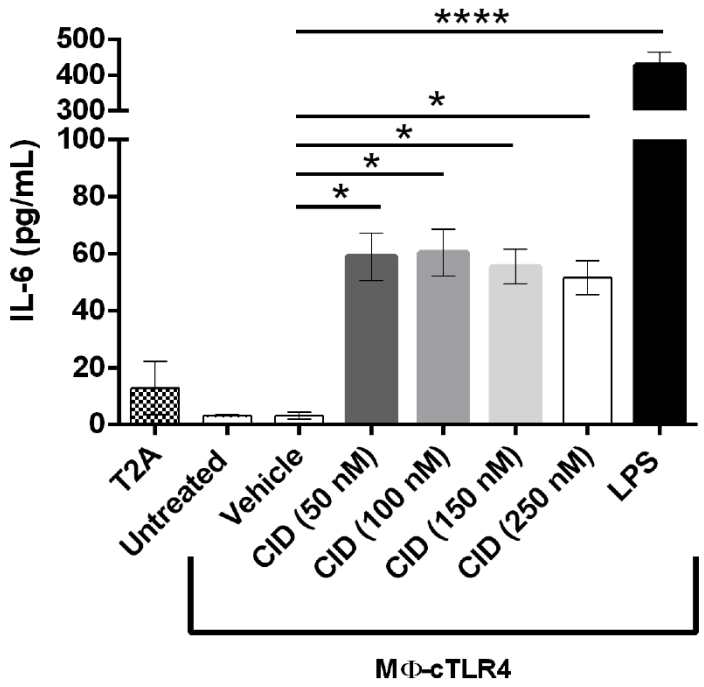

Figure 2.7: Dose of 50 nM CID Drug Produces Maximum Activation of MΦ-cTLR4 Cells. CID drug dosage optimization for MΦ-cTLR4 cells, determined by IL-6 expression. An IL-6 ELISA was performed to test for the maximum signal of this cytokine in a CID drug titration experiment. CID drug doses ranged from 50 nM to 250 nM CID-treated MΦ-cTLR4 cells were compared to vehicle and the LPS positive control. Cell medium was collected following 24 hour treatment.

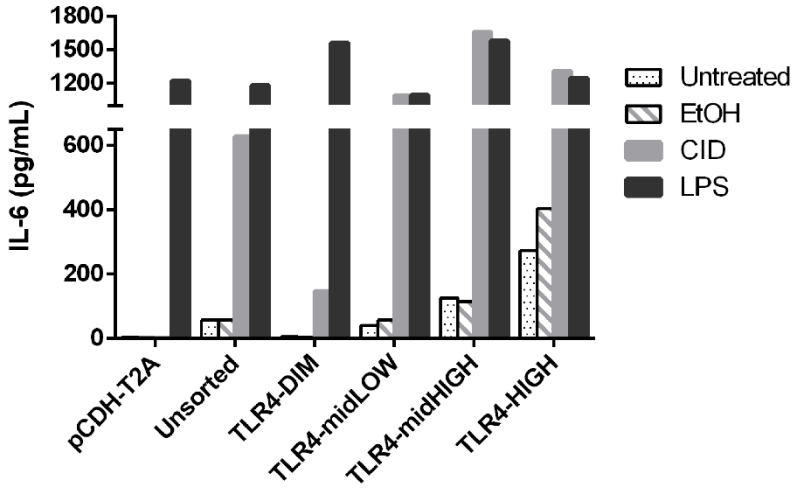

Figure 2.8: MidLow MΦ-cTLR4 Cells Exhibit Highest Signal to Noise Ratio. An IL-6 ELISA was performed on unsorted cells and four groups of sorted cells from the lowest to the most intense GFP intensity of MΦ-cTLR4 cells.

Chapter 3. PHENOTYPIC PROPERTIES OF MΦ-CTLR4 CELLS

3.1 ABSTRACT

In this chapter, I have investigated the MΦ-cTLR4 cells for M1 MΦ-like behavior. Since M1 MΦs express classical inflammation markers, such as TNFα, IL-6, and reactive oxygen species (ROS), I hypothesized that the CID-treated MΦ-cTLR4 cells would express these M1 markers. Indeed, the CID-treated MΦ-cTLR4 cells did express all of these M1 MΦ markers. Additionally, the engineered cells were tested for longevity of activation and length of time for cells to reach baseline levels after withdrawal of CID drug. The MΦ-cTLR4 cells stayed activated for at least 48 hours with constant CID drug treatment and cells converged to their baseline state at approximately 18 hours. Lastly, engineered cells were tested for plasticity propensity and the MΦ-cTLR4 cells showed signs of plasticity when exposed to cocktail treatments of CID/IL-4. MΦ-cTLR4 cells treated with CID/IL-4 exhibited about half the expression of IL-6 and iNOS, but TNFα expression was not affected.

3.2 INTRODUCTION

In the following sections, I will investigate the phenotypic properties of the MΦ-cTLR4 cells and how these engineered cells compare to the M1-activated MΦ (Figure 3.1). The phenotype of the M1 MΦ has been described extensively in literature (34, 63). M1 MΦs differ from the M2 MΦ subsets by the expression of different key membrane receptors, cytokines, and chemokines. Unlike M2 MΦs that can polarize into multiple phenotypes (M2a, M2b, and M2c), M1 MΦ activators induce polarization of a single analogous pro-inflammatory MΦ phenotype. This phenotype is naturally induced by INF-γ and LPS. Additionally, plasticity has been described as the hallmark of the monocyte-macrophage lineage. Mononuclear leukocytes are subjected to a combination of signals *in vivo* with different temporal patterns. Consequently, MΦ polarization can be viewed as

a single MΦ state at a given time, which exists in the continuum of diverse polarization states (64). In this study, I will be specifically examining the M1 MΦ phenotype following 24 hours of activation.

3.2.1 *M1 Macrophage Markers*

The pro-inflammatory phenotype is characterized by the promotion of the Th1 response, the expression of pro-inflammatory cytokines, and the high production of reactive nitrogen and oxygen intermediates. The M1 MΦ phenotype is typically IL-12^{high} and IL-10^{low} and cytokine expression also includes IL-1, TNFα, and IL-6. M1 polarization signals and subsequent NF-κB activation leads to transcription of inflammatory factors, such as various CXCL and CCL chemokine ligands. M1 MΦs also produce ROS, which originate primarily from the induced nitric oxide synthase (iNOS) enzyme. The production of NO by iNOS acts as an immune defense, as NO is a free radical with an unpaired electron that can react with superoxide and form peroxynitrate, which is a potent bactericidal agent (65). Following M1 MΦ activation, the main inhibitory molecule for pro-inflammatory genes is IL-10. This interleukin activates STAT6 pathways, which sequester coactivator molecules required for the LPS pathway activation and prime the cell for a M2 MΦ phenotype transition (66). Ultimately, it is the balance of these cytokines, chemokines, and ROS that dictate the polarization state of a MΦ.

3.2.2 *Plasticity in Macrophages*

The phenotypes of M1 and M2 MΦs *in vivo* and *in vitro* can be reversed to some extent. The pathology of the tissue has a large influence on the polarization state and influences whether the MΦ displays a more inflammatory M1 phenotype or a more resolving and reparative M2 phenotype (67). However, it still remains unclear whether the recruitment of circulating monocytes or the reprogramming of cells is the main mechanism for this phenotype switch. Nevertheless, it

has been shown *in vivo* that M2 MΦs can be skewed to a M1 MΦ phenotype by certain stimuli or genetic mutations. Guiducci et al. reported that gene therapy of CCL16 chemokine used to accumulate macrophages and dendritic cells, combined with TLR9 ligand and anti-IL-10 antibody, was potent enough to redirect macrophages towards a tumor rejection phenotype (68). In another study, the genetic deletion of p50 NF-κB allowed for tumor-associated M2 MΦs to express M1 markers in sufficient amounts to reduce tumor growth (69). Lastly, in an *in vitro* study, Boehler et al. showed that delivery of IL-10 promotes an anti-inflammatory M2 MΦ phenotype, even after polarizing the MΦs to a M1 phenotype (70). Thus, MΦs can be influenced to transition from a M2 to M1 phenotype, as well as be induced to transition from a M1 to M2 phenotype.

3.3 Materials and Methods

3.3.1 *Reagents and Antibodies*

The anti-iNOS/NOS type II antibody was purchased from BD Biosciences. The HRP-conjugated goat-anti-rabbit antibody was obtained from Jackson ImmunoResearch Laboratories, Inc. and the HRP-conjugated goat-anti-mouse antibody was obtained from Life Technologies. Recombinant mouse IL-4 was purchased from eBioscience.

3.3.2 *Cytokine Profile*

We tested IL-6, TNFα, and IL-10 concentrations in supernatants of transduced RAW264.7 cells *in vitro*. Briefly, MΦ-cTLR4 cells (1×10^6) were plated in each well of a 6-well plate and treated with vehicle (100% EtOH), IL-4 (60ng/mL), LPS (100 ng/mL), CID drug (50 nM), or left untreated in DMEM without serum. Supernatants were collected and tested using the mouse IL-6 ELISA Ready-SET-Go!, mouse IL-10 ELISA Ready-SET-Go!, and the mouse TNFα ELISA Ready-SET-Go! Kits (eBioscience) according to the manufacturer's instructions. Plates were read at 450 nM

with a 570 nM wavelength subtraction, normalized to standard solutions, and concentrations (pg/mL) were calculated.

3.3.3 *Western Blotting*

Protein from MΦ-T2A (vector control cells) and MΦ-cTLR4 cell monolayers were extracted by lysis in Laemmli buffer containing 1x Halt Protease Inhibitor cocktail (Thermo Scientific). Following lysis, samples were boiled and protein concentration was determined by performing a BCA assay from Thermo Scientific. Samples (30-50 µg of lysates) were run on 4-20% Mini-PROTEAN® TGX precast polyacrylamide gels (Bio-Rad). Protein from gels were transferred onto PVDF membranes and probed with the appropriate primary antibody overnight. Membranes were washed between each antibody incubation and subsequently probed with the appropriate HRP-conjugated secondary antibody (Life Technologies). The Clarity Western ECL Substrate (Bio-Rad) was used to detect bands.

3.3.4 *Statistical Analysis*

Results are expressed as mean ± SE unless otherwise specified. Significance between groups was determined by one-way ANOVA and p-values less than 0.05 were considered significant.

3.4 RESULTS

3.4.1 *Pro-inflammatory Activation of MΦ-cTLR4 Cells*

Polarized classical inflammatory MΦs are known to have increased levels of TNFα, IL-6, and iNOS (34). Therefore the MΦ-cTLR4 cells were tested for the presence and levels of these markers. Engineered MΦ-cTLR4 cells were seeded in 6-well culture plates overnight and then treated for 24 hours with CID drug, vehicle, or LPS as a positive control. Polarization was confirmed by ELISA and western blot analyses. CID-treated MΦ-cTLR4 cells expressed increased

TNFα and IL-6 levels when compared to uninduced controls (Figure 3.2A & 3.2B). However, the CID-treated MΦ-cTLR4 cell levels were not as high as the LPS-treated cells. I also tested for iNOS via a western blot and observed similar results with this marker. The positive control LPS-treated cells had a substantial increase in iNOS expression and there is a band evident at 130 kDa in the CID-treated lane, however, it has much lower intensity than the LPS-treated cells (Figure 3.2C).

3.4.2 *MΦ-cTLR4 Cells Response to Withdrawal and Length of Treatment*

A withdrawal experiment was performed to determine the time in which the cells would revert to a baseline state following CID drug withdrawal. MΦ-cTLR4 cells were seeded in a 6-well culture plate ($1x10^6$ cells/well). Cells were treated with vehicle, CID drug, or LPS for 24 hours. Timepoints were collected after complete CID drug withdrawal and IL-6 levels were measured at each timepoint to determine activation intensity. Results showed that cells converged to their baseline state at approximately 18 hours (Figure 3.3).

In order to determine how long the engineered MΦ-cTLR4 cells would stay "on" or activated, I performed a longevity study for TNFα, IL-6, and iNOS. With constant CID drug presence in the medium, I found that the MΦ-cTLR4 cells maintain considerable elevated levels of all three pro-inflammatory markers for at least 48 hours (Figure 3.4A-3.4C). The IL-6 levels stayed activated the longest for 72 hours.

3.4.3 *Plasticity of MΦ-cTLR4 Cells*

Diversity and plasticity are hallmarks of cells from the MΦ lineage and they can change phenotype depending on the surrounding microenvironment (67). Thus, I tested how the expression of classical MΦ markers in the MΦ-cTLR4 cells were influenced by a M2 MΦ activator. Engineered cells were treated with a cocktail of either vehicle/IL-4, CID/IL-4, or LPS/IL-4, as well as the

appropriate controls. The degree of polarization was assessed by ELISA and western blot analyses for IL-6, TNFα, and iNOS (Figure 3.5). Both CID- and LPS-treated groups responded similarly to the IL-4 cocktail treatment and exhibited about half the expression of IL-6 and iNOS when compared to treatment groups without IL-4. However, TNFα levels for both CID drug and LPS with and without IL-4 were not significantly different. Similar results to iNOS and IL-6 were observed with IL-10 cytokine expression (Figure 3.6), which is a canonical pro-healing M2 MΦ marker. Cocktail treatment of CID/IL-4 and LPS/IL-4 displayed increased levels of IL-10, when compared to controls without IL-4 present.

3.5 DISCUSSION

We have shown that MΦ polarization induced by LPS has different effects than that of the CID-treated MΦ-cTLR4 cells. Short-term activation results in LPS exhibiting a higher expression of key pro-inflammatory cytokines, however pathway activation of MyD88-dependent and MyD88-independent pathways is either similar or lower for LPS, when compared to CID-treated MΦ-cTLR4 cells. This suggests that LPS activates M1-like processes through other parallel pathways, such as CD14 or MΦ scavenger receptor co-activation. These other receptors or co-receptors might enhance the existing pathways or activate through other pathways, leading to greater NF-κB downstream effects. Thus, there is potentially more input signal from LPS than the CID drug, which only activates through TLR4 (Figure 3.7). In fact, it has been shown that the LPS/CD14 complex can lead to robust NF-κB activation (71), which might support the idea that existing enhanced pathway activation could be the main driver, since this complex also signals through the MyD88-dependent and MyD88-independent pathways. CD14 could be a co-activator that has higher affinity for recruiting MyD88 or TRIF in these pathways when compared to CID drug, which does not utilize this co-receptor.

A common occurrence with LPS exposure, is a phenomenon called LPS tolerance. This tolerance is described as the reduced response to LPS following the initial MΦ or monocyte endotoxin exposure (72). The molecular mechanism of this tolerance leads to downregulation of IL-1 and NF-κB in tolerant MΦs. More importantly, TLR4 mRNA levels stay stable, however, TLR4 protein expression gradually decreases after 1 hour of activation and returns to baseline levels at about 24 hours. An advantage of the engineered MΦ-cTLR4 cells might be the protection against LPS tolerance, as the CID drug works mechanistically different with the overexpressed engineered cTLR4 construct. With the MΦ-cTLR4 cells, downregulation of the cell surface cTLR4 construct is not likely, since it is driven by a constitutive EF-1α promoter. This could be a large advantage when the cells are injected and treated *in vivo*, as the MΦ-cTLR4 cells could potentially continue to display a pro-inflammatory M1-like MΦ polarized state for longer than endogenous MΦs, which have inherent LPS tolerance mechanisms.

During the natural innate inflammation response, the M1 MΦ phase lasts for about 48 hours (73). Similarly, the MΦ-cTLR4 cells exhibit activation as early as 6 hours and activation lasts for about 48 hours with constant CID treatment, at least with cytokine expression and iNOS production. This timeline of activated M1 MΦs has been described in both sterile and non-sterile innate inflammatory responses. Thus, it might be an inherent property of MΦs/monocytes to naturally depolarize or convert to a M2 MΦ following M1 MΦ polarization. Additionally, the withdrawal of CID drug yielded an 18 hour deactivation timeline for MΦ-cTLR4 cells. As previously stated, LPS tolerance leads to deactivation within 24 hours (35). Both of these deactivation timelines are similar and suggest that the same mechanism might be used, which could simply stem from the

inactivity of TLR4 dimerization driving the pathway activation. Both the activation and deactivation of the MΦ-cTLR4 cells is optimal for *in vivo* applications, as the cells can be turned "on" very quickly, stay activated for a robust M1 MΦ response, and then be turned "off" to represent a natural initial phase of the innate inflammatory response.

Even though MΦ-cTLR4 cells can be regulated *in vitro* by the CID drug in a relatively controlled manner, the same regulation might not translate to *in vivo* applications. Endogenous signals will be present upon the introduction of the cells, as well as during MΦ-cTLR4 activation. Thus, it is unknown what will occur *in vivo* with the addition or withdrawal of CID drug. The IL-4 cocktail results showed that the MΦ-cTLR4 cells had decreased IL-6 and iNOS levels when compared to CID drug or LPS treatment alone, however, IL-4 did not seem to affect TNFα levels. The IL-4 cocktail experiments also show increased levels of IL-10 when compared to controls. The IL-10 cytokine has been known to not only directly block inflammatory responses in M1 MΦs, but also promote the transition from a M1 phenotype to a M2 phenotype and enhance efferocytosis. The increase in efferocytosis propensity further promotes IL-10 production (74). This suggests that the engineered cells are influenced by competing M2-like MΦ signals. These competing signals may be changing the phenotype of the engineered MΦ-cTLR4 cells into an intermediate phenotype or even skewing the cells toward a M2-like MΦ phenotype. These results are not completely surprising, as MΦs are known to be very plastic cells and can change phenotypes depending on the surrounding microenvironment. Future *in vivo* studies will be necessary to determine if elevated TNFα levels, or other increased pro-inflammatory MΦ markers, are adequate enough to maintain a pro-inflammatory surrounding environment with M2 MΦ competing signals present. In a physiological setting, the CID-treated and subsequently CID-withdrawn engineered MΦs

could potentially: 1) be primed to polarize into M2 pro-healing MΦs, 2) remain in a pro-inflammatory MΦ phenotype state due to the surrounding environment, 3) develop into an intermediate phenotype state due to M2 MΦ competing signals, 4) undergo apoptosis or, 5) migrate out of the inflammation site. Future studies will determine the degree of plasticity of the engineered cells, as well as how precise these cells can be controlled *in vivo*.

3.6 CONCLUSIONS

In this chapter, I showed that CID-treated MΦ-cTLR4 cells displayed M1-like MΦ characteristics, such as increased IL-6, TNFα, and iNOS expression. Additionally, the MΦ-cTLR4 cells remained polarized in response to CID drug for at least 48 hours and CID drug withdrawal experiments suggest that the engineered cells became deactivated 18 hours after drug withdrawal.

In the plasticity studies, MΦ-cTLR4 cells were influenced by IL-4 cocktail treatment, however, the engineered cells still displayed M1 MΦ characteristics, albeit at lower expression levels. Lastly, the MΦ-cTLR4 cells were able to transition from a M1 to a M2 MΦ phenotype evidenced by levels of M1 markers and IL-10 (M2 marker), but a M2 to M1 MΦ transition was not observed.

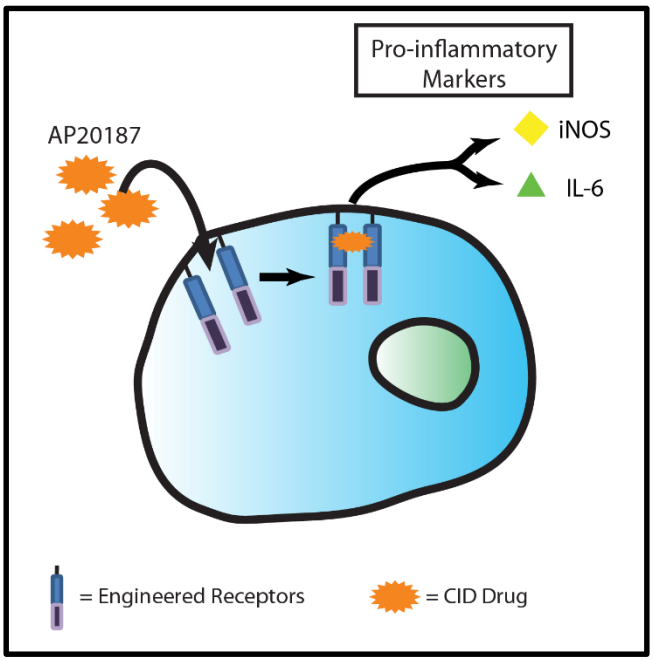

Figure 3.1: Chapter 3 Summary Diagram. MΦ-cTLR4 cells were tested for classical inflammatory MΦ markers, such as iNOS, IL-6, and TNFα. Using these markers as a polarization indicator for MΦ-cTLR4 cells, withdrawal of CID drug and length of CID drug treatment was also tested. Lastly, the plasticity of the MΦ-cTLR4 cells was tested by using IL-4 and CID in a cocktail treatment.

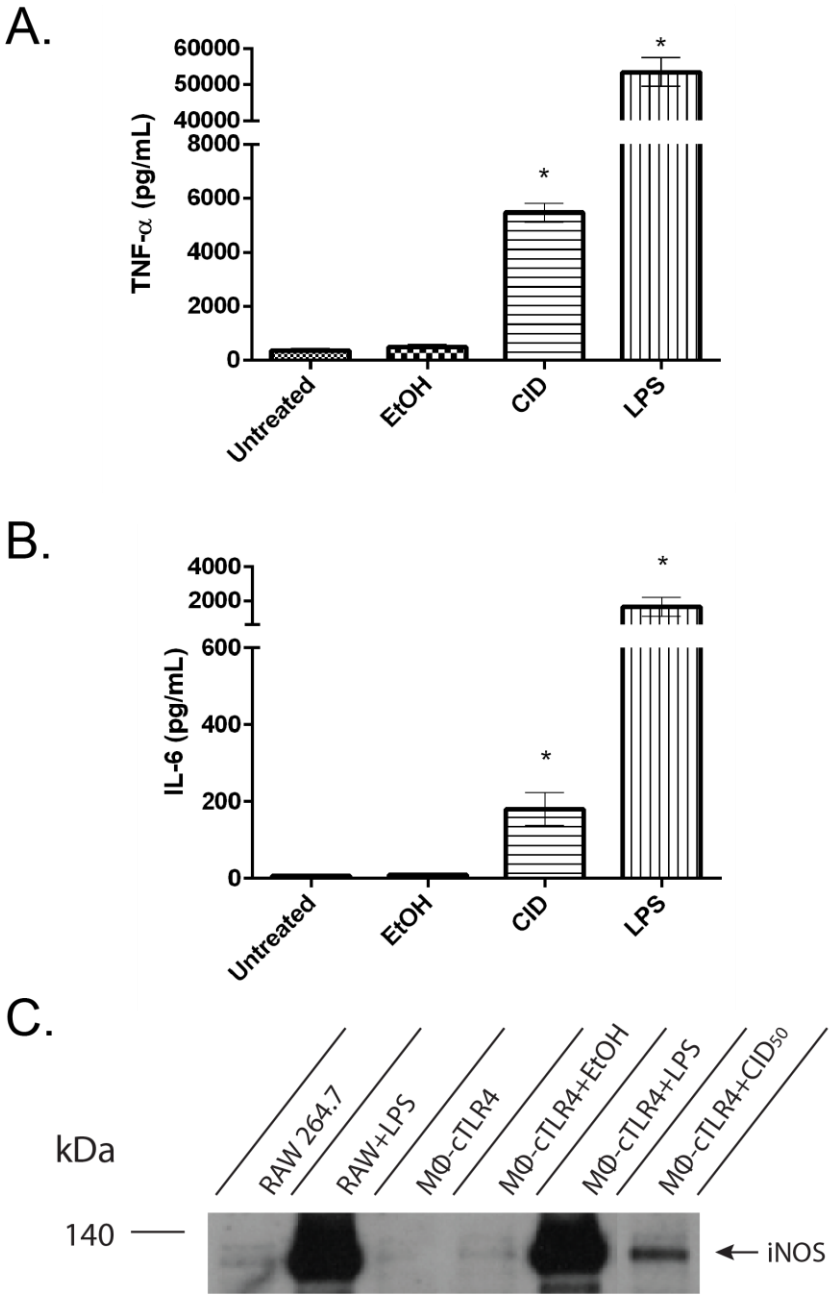

Figure 3.2: CID-treated MΦ-cTLR4 Cells Exhibit Increased Expression of TNFα, IL-6, and iNOS. Expression of classical inflammatory MΦ phenotype markers, determined by sandwich ELISA assay. Bar graphs show the levels of (A) TNFα and (B) IL-6 of CID-treated (50 nM) MΦ-cTLR4 cells compared to untreated, vehicle (100% EtOH), and LPS-treated cells (100 ng/mL). (C) Western blot shows intensity of iNOS expression (130 kDa) for CID and LPS-treated MΦ-cTLR4 cells when compared to controls.

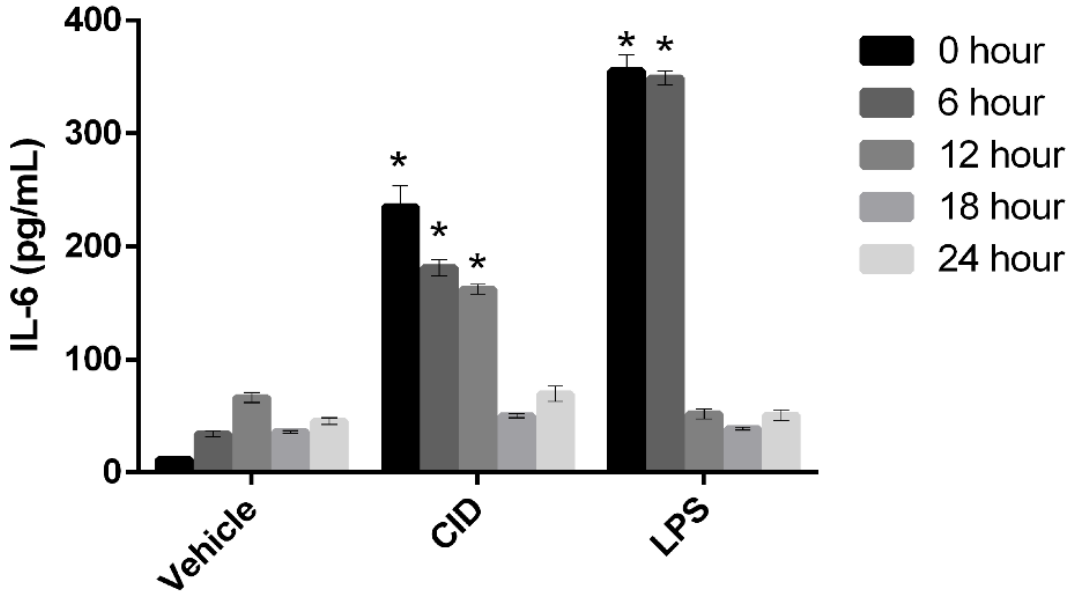

Figure 3.3: MΦ-cTLR4 Cells Return to Baseline Levels 18 Hours Following CID Drug Withdrawal. CID drug withdrawal experiment, determined by IL-6 expression. Cells were treated with CID drug (50 nM), LPS (100 ng/mL), or vehicle for 24 hours and then left untreated after each medium change for up to 24 hours.

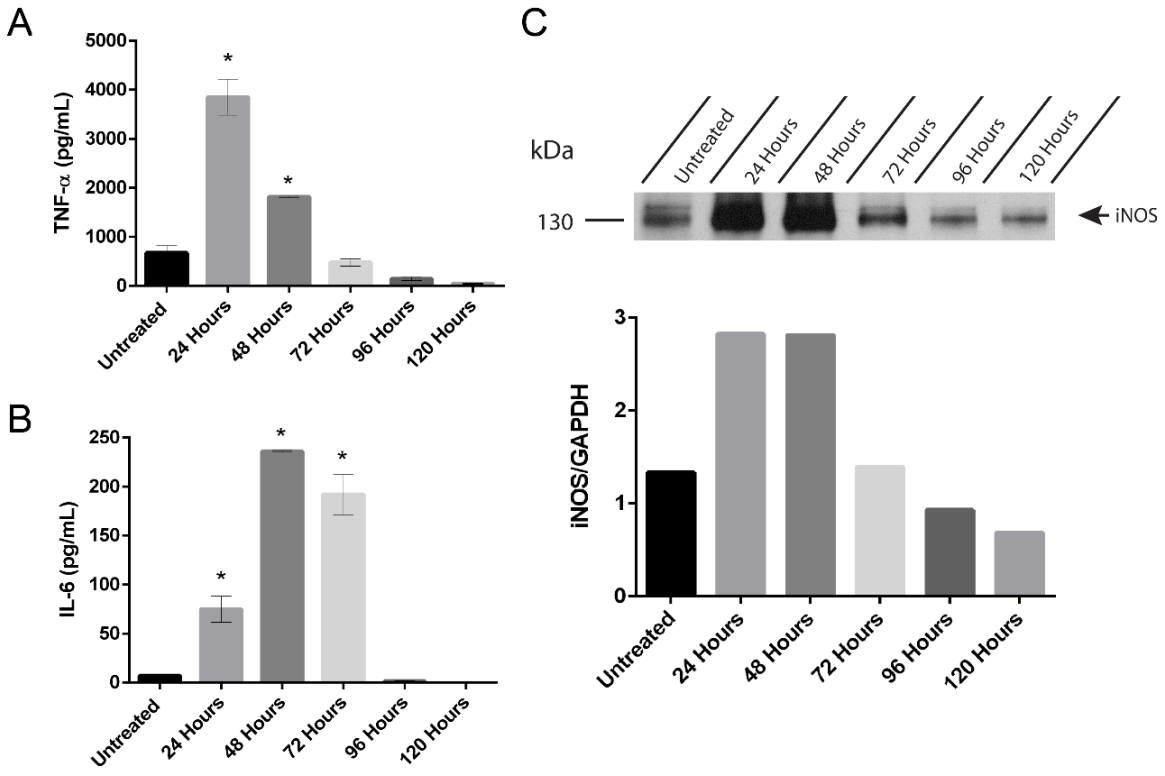

Figure 3.4: CID-treated MΦ-cTLR4 Cells Remain Activated for At Least 48 Hours. Longevity study determined by expression of (A) TNFα, (B) IL-6, and (C) iNOS in MΦ-cTLR4 cells. Medium containing CID drug (50 nM) was changed every 24 hours.

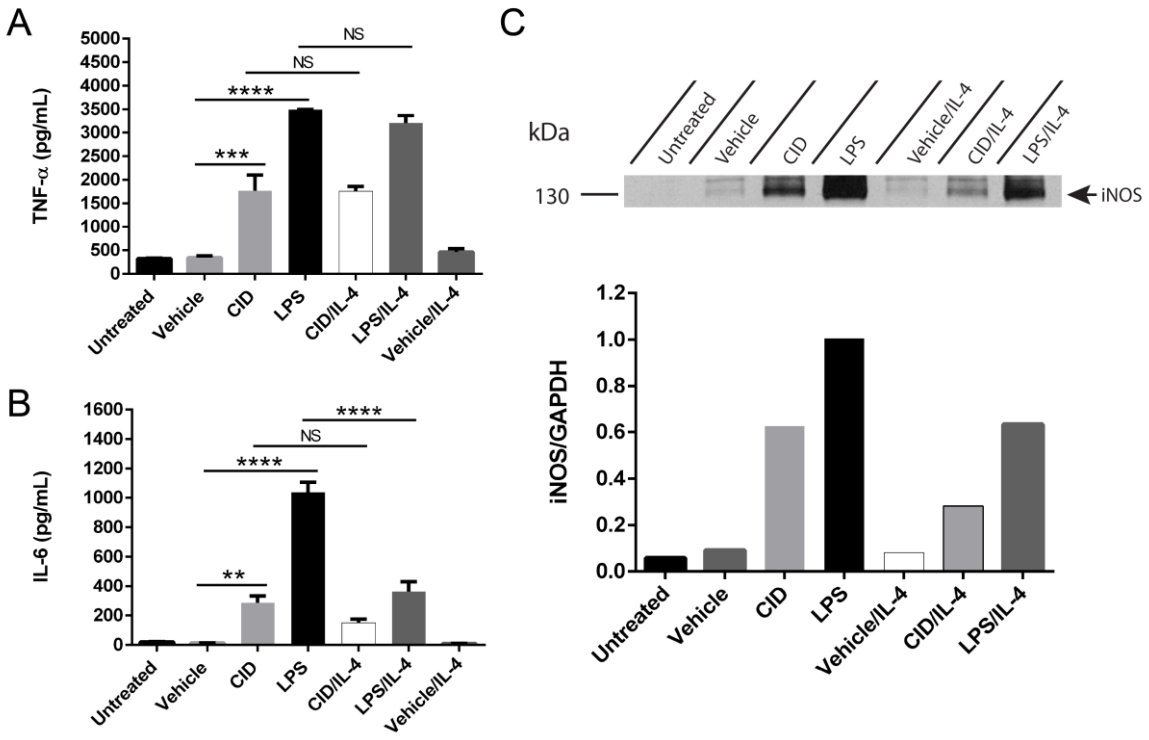

Figure 3.5: MΦ-cTLR4 Cells are Influenced by IL-4 Treatment. Expression of classical inflammatory MΦ phenotype markers following cocktail treatment of IL-4 (60 ng/mL) and CID drug (50 nM), LPS (100 ng/mL) or vehicle. Bar graphs show the levels of (A) TNFα and (B) IL-6 of cocktail-treated cells compared to controls. Cell medium was collected following 24 hour treatment. (C) Western blot shows intensity of iNOS expression (130 kDa) for cocktail-treated MΦ-cTLR4 cells when compared to controls. Cells were lysed following 24 hour treatment.

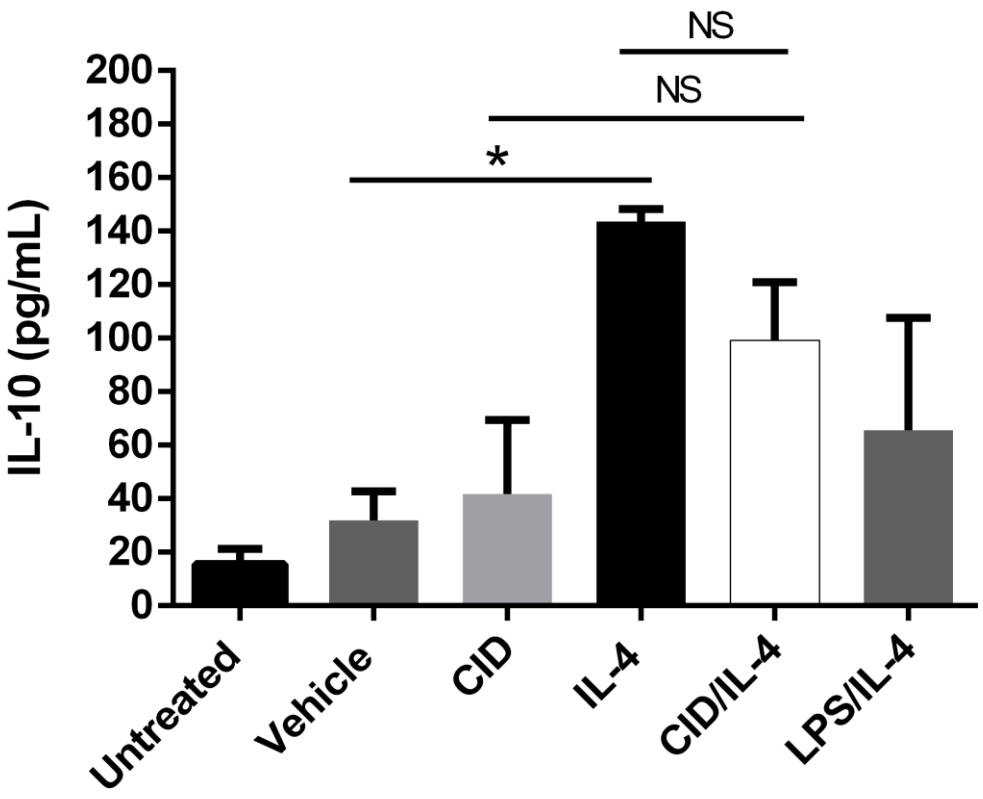

Figure 3.6: MΦ-cTLR4 Cells are Influenced by IL-4 Treatment. Expression of the IL-10 cytokine (M2 marker) following cocktail treatment of IL-4 (60 ng/mL) and CID drug (50 nM), LPS (100 ng/mL), or vehicle. Bar graph shows the levels of IL-10 for cocktail-treated cells compared to controls. Cell medium was collected following 48 hour treatment.

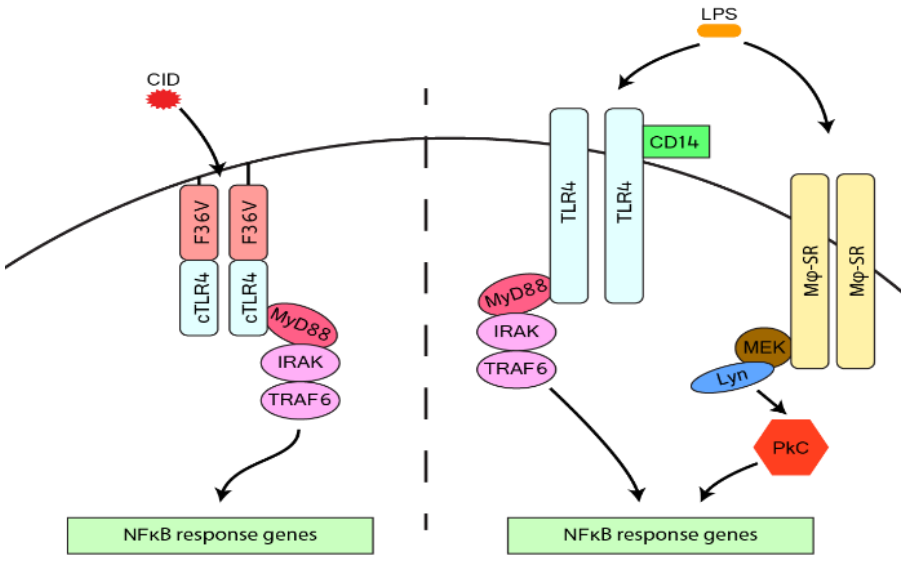

Figure 3.7: Schemata of CID-activated Pathways and LPS-activated Pathways. CID drug only activates through the MyD88-dependent and MyD88–independent pathway to lead to NF-κB responses. LPS has more NF-κB response input due to other receptor and co-receptor activation with CD14 and MΦ scavenger receptor.

Chapter 4. FUNCTIONAL PROPERTIES OF MΦ-CTLR4 CELLS

4.1 ABSTRACT

This chapter reports on the influence of MΦ-cTLR4 cells on angiogenic processes. Although the relative role of MΦs in angiogenesis is still not completely understood, it is currently well appreciated that MΦs can affect pro- and anti-angiogenic processes. I hypothesized that MΦ-cTLR4 cells would have the ability to prime the angiogenesis response. Thus, I have quantified the ability of MΦ-cTLR4 cells to activate endothelial cells (ECs) by testing for VCAM-1 and ICAM-1 adhesion molecules and CID-activated MΦ-cTLR4 cells induced upregulation of VCAM-1 and ICAM-1 on ECs in a TNFα-dependent manner. Further, MΦ-cTLR4 conditioned medium influence on a wound closure assay with ECs was quantified. The wound closure assay indicated that CID-treated MΦ-cTLR4 conditioned medium inhibited proliferation and migration of ECs when compared to vehicle-treated MΦ-cTLR4 conditioned medium, which showed the highest closure rate. Since recent data suggests that direct contact of MΦs and ECs is necessary to modulate the angiogenesis process, a co-culture tube formation assay was performed to quantify cell-cell interactions between ECs and the MΦ-cTLR4 cells. The co-culture tube formation assay suggested that CID-treated MΦ-cTLR4 cells brought about behavior similar to that created by LPS-treated MΦ-TLR4 cells and inhibited tube formation from occurring. Lastly, VEGF-A expression in the MΦ-cTLR4 cells was determined when treated with CID, LPS, CID/IFN-γ, or LPS/IFN-γ. VEGF-A levels were significantly decreased in MΦ-cTLR4 cells in all treatment groups.

4.2 INTRODUCTION

In the following sections, MΦ-cTLR4 cells will be tested for their influence on *in vitro* angiogenic processes (Figure 4.1). M1 MΦs have been associated with inflammation and subsequent

angiogenesis behavior, as they can activate ECs to enhance proliferation, migration, and survival. The main factor associated with activation of endothelial cells by MΦs is VEGF. Thus the induction of VEGF receptor (VEGFR) on the EC surface is responsible for increasing matrix metallopeptidase 9 (MMP-9) and other vascular-bed specific growth factors for ECM invasion. The other growth factors consist of TGF, FGF, as well as insulin-like growth factor-1, which help ECs proliferate and grow into the granulation tissue. The tube formation of ECs that follows is hypothesized to be driven by secreted angiogenic factors, as well as cell-cell interactions between ECs and various leukocytes.

4.2.1 *Process of Angiogenesis During Inflammation*

In the first step of acute inflammation, functional changes occur in the vasculature, in which the vasculature exhibits dilation, an increase in permeability, and EC activation. During this stage, MΦs provide a continuous source of cytokines that stimulate fibroblasts and ECs (75). In the later phases, ECs display increased mitotic activity and capillaries and venules start remodeling and forming new tubes (25). Fibroblast cells are very important in this phase, as they construct the new extracellular matrix (ECM) necessary to support cell ingrowth. New blood vessel formation contains ECs that digest and penetrate the underlying vascular basement membrane. The ECs then invade into the stroma and form branching tube-like structures which are directed by proliferating ECs from the sprout region, as well as chemotaxis, which guides the leading edge. All these steps require a dynamic environment of ECs, angiogenic factors, and surrounding ECM proteins that are interacting both spatially and temporally.

4.2.2 *Macrophage Influence on Angiogenesis*

In animals, wounds generally activate an inflammatory response with an ensuing repair process. The influx of MΦs are part of this response and MΦs have been found to be mandatory for final

tissue resolution to occur (76). There are multiple observations that point to MΦs as a key influential cell type in angiogenesis. For example, MΦs extracted from wounds can induce neovascularization in a variety of angiogenesis assays, such as in the mouse cornea, the rabbit ear chamber, and in *in vitro* tube formation assays (77-79). Some report that secretory products alone of MΦs can influence the many stages of the angiogenic process (80). One of these processes includes altering the ECM for favorable angiogenesis, by producing metalloproteases and serine proteases that degrade ECM molecules. MΦs can also secrete G-CSF and bFGF that enhance EC secretion of proteases, as well as TGFβ that has an inhibitory effect on secretion of these EC proteases (26). Another process that MΦs influence is the activation of ECs. The TNFα secreted by M1 MΦs has the ability to increase the expression of adhesion molecules and integrins on ECs, which include VCAM-1, ICAM-1, PECAM-1, $\alpha_v\beta_3$, and $\alpha_v\beta_5$. These adhesion molecules and integrins have been implicated in EC survival and proliferation, as well as integrin-dependent angiogenesis (25). Even though secretory products seem to activate ECs, recent data suggests that direct contact of MΦs and ECs is necessary to modulate the physiological angiogenesis process (28, 81, 82). Furthermore, co-culture assays of MΦs and various other cell types have generally given better functional results (83, 84). Collectively, these data suggest that MΦs have both a secretory role, as well as a cell-cell interaction role during the process of angiogenesis.

4.2.3 *Vascular Endothelial Growth Factor and Macrophages*

During inflammation, oxygen levels decrease and generate hypoxic stress within the tissue. TLR4 has been reported to be associated with hypoxic conditions and its expression is upregulated in the tissues of patients with ischemia-based injuries. The hypoxia-inducible transcription factor (HIF-1) is activated during hypoxia and plays a critical role in downstream activation of angiogenesis. This transcription factor controls the VEGF gene, which suggests an early contribution of VEGF

in the angiogenic process. Moreover, the VEGF receptor (VEGFR) is upregulated under ischemic conditions as well. MΦs have been known to express VEGF and this signal protein is directly responsible for vasodilation, increasing vascular permeability, as well as inducing expression of proteases and receptors on ECs that are important for survival, invasion, and proliferation (25). Monocytes and MΦs also express VEGFRs and when activated, the subsequent signal transduction events lead to an increase in migration potential. Specifically, M1 MΦs have been shown to express high levels of VEGF with IFN-γ treatment in humans (85), however, this has not been repeated in mice and most studies suggest that only M2 MΦs express VEGF (86). The mechanism of VEGFR and VEGF production in MΦs is still not completely understood, but MΦs could be playing a larger role than previously thought in the angiogenesis process. Nonetheless, angiogenesis is not completely dependent on VEGF production; indeed many other mediators stimulate new vessel formation (87). Thus, MΦ-derived VEGF expression likely represents a small portion of the complicated and dynamic process of angiogenesis and inflammation.

4.3 Materials and Methods

4.3.1 *Cell Culture*

bEnd.3 cells were obtained from ATCC and were cultured in DMEM medium from Invitrogen containing 10% (v/v) heat-inactivated FBS and 100 U/ml pen/strep (Invitrogen) and incubated at 37°C with 5% CO_2. RAECs were a gift from Dr. Giachelli's lab and cultured in EBM medium (Lonza) containing 10% (v/v) heat-inactivated FBS and 100 U/ml pen/strep (Invitrogen) and incubated at 37°C with 5% CO_2.

4.3.2 *Endothelial Cell Activation*

MΦ-cTLR4 conditioned medium, following a 6 hour treatment in 6-well plates ($1x10^6$ cells/well), was transferred to plated bEnd.3 cells in a 12-well plate ($0.2x10^6$ cells/well). Before medium

transfer, TNFα neutralizing and IgG isotype antibody (1 μg/mL) were incubated in medium for 15 minutes. Medium was then added to bEnd.3 cells for 12 hours. Following incubation, bEnd.3 cells were trypsinized and stained for directly PE-conjugated ICAM-1 and VCAM-1. Cell cytometry was performed on a FACSCanto II Cell Analyzer (BD Biosciences) equipped with 488 nm and 647 nm lasers. Typically, 10,000 cells were analyzed per sample. Experiments were repeated at least three times. Non-specific staining was evaluated using a monoclonal antibody for directly PE-conjugated IgG2b and IgG2a (eBioscience).

4.3.3 *Wound Closure Assay*

MΦ-cTLR4 conditioned medium, following a 24 hour treatment in 6-well plates ($1x10^6$ cells/well), was transferred to plated bEnd.3 cells in a 6-well plate (90-95% confluent). Before medium addition, three separate scratches were made in each well with a p200 pipet and subsequently washed with PBS to remove any cell debris. Images of the same region of interest were taken at 6 hour intervals up to 24 hours. Images were analyzed using the ImageJ "Wound Healing Tool" macro.

4.3.4 *Tube Formation Assay*

MΦ-cTLR4 cells and rat aortic endothelial cells (RAEC) were seeded together in 6-well plates ($1x10^6$ cells per well) with 3 wells of MΦ-T2A cells and 9 wells of MΦ-TLR4 cells. MΦs were pre-treated with either vehicle, CID (50nM), LPS (100 ng/mL) or left untreated. The thin gel method was used to coat the bottom of a 24-well plate with 100 μL of Matrigel. Plates were left to solidify in a 37°C incubator for 1 hour. Mixed suspensions of both RAECs and MΦ-cTLR4 cells were seeded on top of solidified Matrigel ($1x10^5$ REACs and $2x10^5$ pre-treated MΦ-cTLR4 cells). At the start of co-cultures, wells were treated again with vehicle, CID, or LPS to keep cells

polarized. Wells were imaged for tube formation at 6, 9, 12, and 24 hours. No more than $4x10^5$ total cells were used in a maximum of 500 μL medium for optimization experiments.

4.3.5 *VEGF-A Level Measurement*

We tested vascular endothelial growth factor concentrations in supernatants of transduced RAW264.7 cells *in vitro*. Briefly, MΦ-cTLR4 cells (1×10^6) were plated in each well of a 6-well plate and treated with vehicle (100% EtOH), LPS (100 ng/mL), CID drug (50 nM), IFN-γ (20 ng/mL), or left untreated in DMEM without serum. Supernatants were collected and tested using the mouse VEGF-A Platinum ELISA kit (eBioscience) according to the manufacturer's instructions. Plates were read at 450 nM with a 620 nM wavelength subtraction, normalized to standard solutions, and concentrations (pg/mL) were calculated.

4.3.6 *Statistical Analysis*

VEGF-A ELISA and tube formation quantification results are expressed as mean ± SE unless otherwise specified. Significance between groups was determined by one-way ANOVA and p-values less than 0.05 were considered significant. For wound closure assay, two-way ANOVA was used with p-values less than 0.05 considered significant.

4.4 RESULTS

4.4.1 *MΦ-cTLR4 Endothelial Cell Activation*

Better wound healing outcomes have been correlated with increased angiogenesis (88). Furthermore, areas containing almost entirely pro-inflammatory MΦ have been shown to correlate with angiogenesis, in specific cases (50, 88). Thus, I tested whether engineered MΦ-cTLR4 cells-derived factors were able to induce EC activation by measuring the expression of the VCAM-1 and ICAM-1 adhesion molecules. ECs incubated with medium from MΦ-cTLR4 treated with

TNFα and CID drug both had increased expression of VCAM-1 and ICAM-1 (Figure 4.2A & 4.2B) when compared to vehicle alone. For the TNFα-treatment group, 93.5% of EC were positive for VCAM-1 and 57.2% of EC were positive for ICAM-1. The CID drug-treatment group was very similar, with 93.7% of the EC being positive for VCAM-1 and 64.4% of the EC being positive for ICAM-1. The vehicle group had a baseline VCAM-1 and ICAM-1 expression when compared to the isotype control.

To determine if the TNFα was the main driver of the EC activation, I repeated the experiment with a neutralizing antibody for TNFα (Figure 4.2C & 4.2D). Before adding the MΦ-cTLR4 conditioned medium to the EC, a TNFα neutralizing antibody was incubated in the medium for 15 minutes. The CID and the TNFα groups with the neutralizing antibody had severely decreased levels of both VCAM-1 and ICAM-1 when compared to the IgG control. The VCAM-1 expression was decreased by a factor of three and the ICAM-1 expression was decreased by a factor of two and fell below vehicle/baseline treatment, thus indicating that some of the activity at baseline is TNFα-dependent.

4.4.2 *Wound Closure Assay with MΦ-cTLR4 MΦ-Conditioned Medium*

In order to determine how fast ECs would migrate into a "wounded" area of a bEnd.3 cell monolayer, I performed a wound closure assay (Figure 4.3). Following the initial scratches, vehicle-treated MΦ-cTLR4 conditioned medium exhibited the most complete closure of the "wound," followed by the untreated MΦ-cTLR4 conditioned medium. TNFα-treated and CID-treated MΦ-cTLR4 conditioned medium groups had less "wound" closure than that of the untreated or vehicle-treated medium. The rates at which closure occurred were not significantly different (Figure 4.4A). However, the amount of closure at the last timepoint (48 hours) was

significantly different between vehicle-treated and untreated groups, when compared to the TNFα-treated group, but not that of the CID-treated group (Figure 4.4B).

4.4.3 *Co-Culture of MΦ-cTLR4 Cells and Endothelial Cells in Tube Formation Assay*

Since cell-cell interactions have been shown to be important for ECs and MΦs, a co-culture tube formation assay was performed (Figure 4.5). Untreated MΦ-cTLR4 cells co-cultured with RAECs, with no added factors to the medium, had the least amount of isolated segments, the least amount of branches, and the most amount of branching interval. CID-treated and LPS-treated MΦ-cTLR4 cells co-cultured with RAECs, with CID or LPS added to the medium, had much more braches than untreated co-cultures with a smaller branching interval. The CID-treated group differed from the LPS-treated group in isolated segment analysis, as LPS-treated MΦc-TLR4 cells co-cultured with RAECs had the highest number of isolated segments and CID-treated MΦc-TLR4 cells co-cultured with RAECs had slightly more isolated segments than the untreated group. The number of branches and the branching interval for the CID- and LPS-treated groups were significantly different than the control. However, the number of master segments and isolated segments for the CID- and LPS-treated groups were not significantly different, when compared to the control (Figure 4.6).

4.4.4 *VEGF Expression in MΦ-cTLR4 Cells*

In order to determine if the MΦ-cTLR4 cells were expressing the key angiogenic molecule VEGF-A, I performed an ELISA to test for VEGF-A levels in MΦ-cTLR4 medium following various treatments (Figure 4.7). CID-treated and LPS-treated MΦ-cTLR4 cells expressed significantly decreased amounts of VEGF, when compared to controls. Since studies have shown human and rat MΦs express increased VEGF with IFN-γ treatment, I also tested the response with this factor.

Figure 4.8 shows cocktail treatment of IFN-γ treatment with CID or LPS, or IFN-γ alone. All groups also show a significant decrease in VEGF when compared to the control.

4.5 DISCUSSION

The EC and MΦ-cTLR4-conditioned medium wound closure experiment did not yield any significant results in relation to CID-treated MΦ-cTLR4 conditioned medium. However, there was a distinct grouping of 48 hour endpoint quantification, in which the CID and TNFα MΦ-cTLR4 conditioned medium wounds closed similarly and the untreated and vehicle MΦ-cTLR4 conditioned medium wounds closed similarly. This distinct grouping might suggest that the high levels of TNFα in the medium were actually inhibiting the EC proliferation and migration, as continuous TNFα presence has been shown to inhibit angiogenesis by unknown mechanisms (89). Furthermore, there were differences between quantifications of vehicle and CID- or LPS-treated MΦ-cTLR4 co-culture experiments, in which there were significant differences in the branching quantification. Other groups have shown that conditioned medium from M1 polarized MΦs has an enhancing effect on EC tube formation, however, these studies were done with primary cells (28). Conversely, when this same group used co-cultures instead of conditioned medium, the M1 MΦs had an inhibitory effect of EC tube formation.

Other groups have suggested that direct contact is necessary to mirror the physiological environment of angiogenesis, as MΦs are known to bridge endothelial tip cells and to be located at vascular junctions (81). The presence of MΦs at these specific locations help close tip cell apposition for fusion and aid in joining vessel segments. Even though MΦs were found at key "joining" regions during vessel formation, the MΦs were not tested for polarization markers, thus it is unknown whether the MΦs in this study were skewed to the M1 or M2 MΦ phenotype. The

MΦ-cTLR4 data in this chapter suggests that cell-cell interactions are absolutely necessary for EC functional influence, at least for M1 MΦs. Furthermore, secreted growth factors from MΦ-cTLR4 cells were not enough to significantly influence EC wound closure. Nevertheless, the possibility of exosome or microvesicle release has not been excluded in this study. Recent studies have shown that MΦs produce abundant amounts of exosomes and microvesicles *in vitro* that contain microRNAs and other factors (82). Although transfer of these cargo from MΦs to ECs needs further investigation, these exosomes could potentially be modulating the gene expression and function of ECs engaged in angiogenesis. In the case of the MΦ-cTLR4 cells, these cells might be secreting exosomes which are inhibiting EC function during the tube formation and wound closure *in vitro* assays.

The expression of certain cytokines and surface receptors can differ from cell lines to primary cells. Specifically, RAW264.7 cells are useful to use for *in vitro* experiments, however, these cells express significantly less GM-CSF than primary cells and might have difficulty enhancing EC secretion of proteases for activation to occur (54). There have been no reports of decreased VEGF expression in RAW264.7 cells. However, there have also been reports of increased VEGF in RAW264.7 cells after treatment with advanced glycation end products (AGEs), which coincided with ROS levels (90). These results suggest that VEGF levels are not inherently low in this cell line and can be activated, although certain pathway activation may differ. Regardless, I observed a significant decrease in VEGF expression when MΦ-cTLR4 cells were treated with either CID, LPS, IFN-γ, or a combination of the treatments when compared to controls. This is consistent with the co-culture tube assay, in which LPS- and CID-treated MΦ-cTLR4 cells inhibited tube formation. The down-regulation of VEGF could be maintaining the angiogenesis process at the

first stage, which is the destabilization step. The second and third step involve sprouting and branching, respectively, which necessitates increases in VEGF expression. Since MΦ-cTLR4 cells are actively down-regulating this factor, I believe that this might play a large role in the anti-angiogenic behavior of the activated engineered cells.

In chapter 3, it was found that MΦ-cTLR4 cells express TNFα, which is known to be a key angiogenic cytokine. Several studies have elucidated that temporal expression of key angiogenic cytokines, such as TNFα, is necessary for tip formation in ECs (89). Sainson et al. showed that 2- to 3-day pulses of TNFα *in vitro* and *in vivo* stimulates angiogenesis, as opposed to the inhibition of angiogenesis with continuous administration. I observe robust TNFα expression in the engineered pro-inflammatory MΦ-cTLR4 cells, which may possibly be utilized to promote angiogenesis, if controlled in a time-based manner. Indeed, the MΦ-cTLR4 engineered cells may be tailored to exhibit pulse behavior with the simple addition and withdrawal of CID drug at certain timepoints. In addition, I do observe that the MΦ-cTLR4-conditioned medium stimulates EC activation by increasing VCAM-1 and ICAM-1 adhesion molecule expression in an *in vitro* setting and in a TNFα-dependent manner, which suggests that the engineered MΦs may be able to promote angiogenesis. Further, iNOS levels directly correlate with VCAM-1 expression (91). I do see similar activation patterns with both TNFα and iNOS in the MΦ-cTLR4 cells, so both of these factors could be working in concert to upregulate adhesion molecule expression. Activation of VCAM-1 and ICAM-1 has been shown to destabilize endothelial junctions resulting in leaky vessels, a first step in the angiogenesis process. It has been suggested that a subsequent M2 MΦ phase may be necessary for the process of angiogenesis to continue and come to completion, as the M2 MΦ phenotype has been hypothesized to bridge and stabilize newly formed vessels (92).

Thus, CID drug activated MΦ-cTLR4 cells may provide the required priming step for angiogenesis to initiate.

In addition to iNOS and TNFα, the CID-treated MΦ-cTLR4 cells were found to produce increased levels of IL-6 in chapter 3. The IL-6 cytokine has been closely associated with promotion of angiogenesis. Increased IL-6 mRNA levels correlated with the development of ovarian follicles and the uterine lining, which are two independent physiological angiogenic processes (93). Moreover, IL-6 treatment has been shown to promote tubule formation in brain microvessel EC in an *in vitro* setting. This correlated with increased IL-6 and VEGF mRNA expression in the healing adult murine brain tissue following injury (94). These studies suggest that IL-6 may play a role in normal physiological angiogenesis as well as angiogenesis related to inflammatory remodeling of tissue. Studies in IL-6 KO mice showed that the IL-6 deletion resulted in delayed wound healing, accompanied with both delayed angiogenesis and collagen deposition (95). The direct mechanism of IL-6 and its influence on pro-angiogenic behavior is still not completely understood, however, IL-6 seems to be a key player in this process. The engineered MΦ-cTLR4 cells produce IL-6, along with two other factors implicated with pro-angiogenic behavior. This strongly suggests that the MΦ-cTLR4 cells may have the ability to aid in the priming of the endothelium for early stage angiogenesis.

Despite the possible use of the MΦ-cTLR4 cells as angiogenesis priming agents, in which a following M2 MΦ response might need to be necessary, these cells could also be used in certain diseases to skew the balance of a M2 MΦ-abundant process. For example, diseases characterized by excessive fibrosis could benefit from this technology, as there is often a local abundance of M2

MΦs present during fibrotic events. Fibrosis occurs due to the abundance of these M2 MΦs over-producing TGFβ, which in turn recruits fibroblasts. The recruitment of fibroblasts then leads to the overproduction of collagen, thus leading to a fibrotic state. This dysregulated process is often associated with the dense collagen fibrous capsule that surrounds an implanted material, as well as with cardiac fibrosis that plagues congestive heart failure patients (96). A few studies have suggested that a proper balance of M1 and M2 MΦs is necessary to achieve a reduction in the extent of fibrosis (97, 98). Thus, CID-activated MΦ-cTLR4 cells may provide a tool to reestablish the proper M1 vs M2 MΦ equilibrium and decrease the excessive collagen deposition. Another possible application of the MΦ-cTLR4 cells could be tumor inhibition. Tumor-induced angiogenesis is essential for cancer cell survival, tumor growth and metastasis propagation. An abundance of pro-angiogenic, anti-inflammatory M2 MΦs, known as tumor-associated MΦs (TAMs), is normally present in the tumor environment thus aiding tumor progression. In contrast, very few M1 MΦs able to activate NK cells and T_H1 responses are present in and around the growing tumor mass (99). Thus, the delivery of tunable MΦ-cTLR4 cells to the tumor may halt progression by activating a more pro-inflammatory immune response.

4.6 CONCLUSIONS

In this chapter, I investigated the influence of MΦ-cTLR4 cells on ECs. I showed that the engineered cells have functional properties by performing a MΦ-cTLR4 conditioned medium experiment to test for EC activation potential. CID-polarized MΦ-cTLR4 conditioned medium had the ability to activate ECs by upregulating both VCAM-1 and ICAM-1 expression on the cell surface, which are two cell adhesion molecules associated with angiogenic processes (100, 101). Further, the activation of ECs by CID-treated MΦ-cTLR4 cells was determined to be dependent on TNFα. Furthermore, I found that secretory factors alone from MΦ-cTLR4 cells do not

significantly influence EC proliferation and migration in the wound closure assay, but that there were distinct groupings of endpoint quantification, in which the CID and TNFα MΦ-cTLR4 conditioned medium wounds closed similarly and the untreated and vehicle MΦ-cTLR4 conditioned medium wounds closed similarly. Additionally, I found that MΦ-cTLR4 cell and EC cell-cell interactions were sufficient and necessary for EC influence on tube formation. CID-treated MΦ-cTLR4 co-cultures were similar to LPS-treated MΦ-cTLR4 co-cultures in that they both inhibited tube formation from occurring, when compared to the vehicle. Lastly, I showed that VEGF was significantly decreased in activated MΦ-cTLR4 M1-like cells, which might play a large factor in the destabilization and inhibitory role that MΦ-cTLR4 cells displayed in the EC assays. Overall, it was suggested that the engineered M1 MΦs might be a suitable priming agent to stimulate angiogenesis, however, persistent M1 polarization does not seem permissive for angiogenesis or vessel growth.

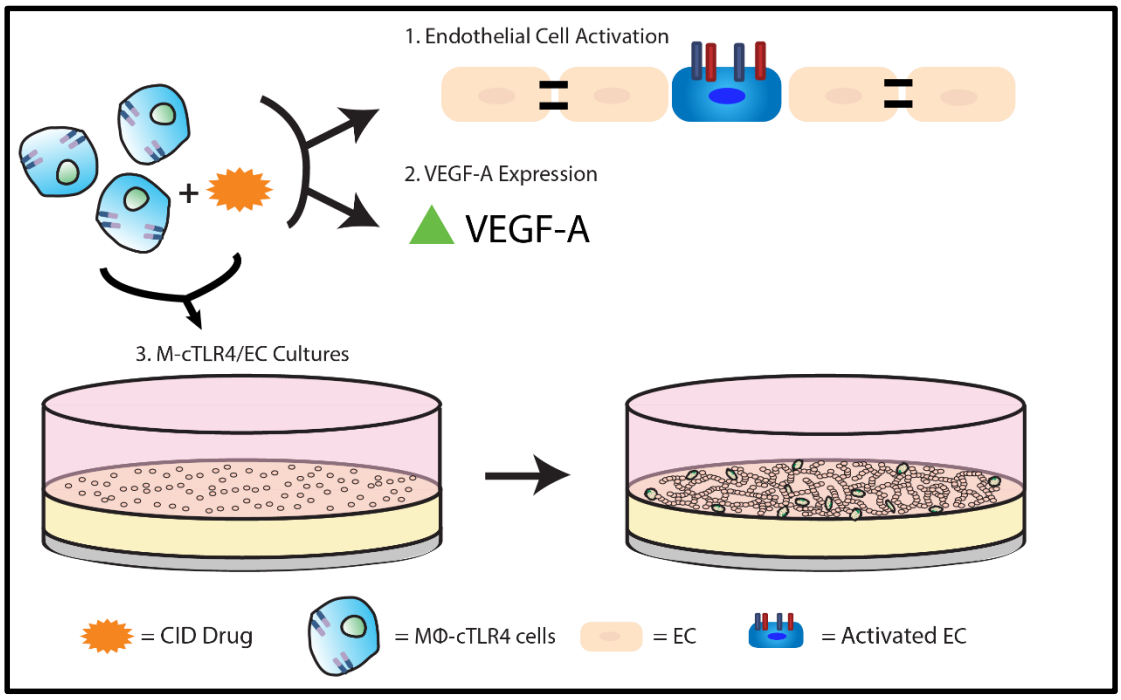

Figure 4.1: Chapter 4 Summary Diagram. MΦ-cTLR4 cells were first tested for EC activation by looking for VCAM-1 and ICAM-1 upregulation on ECs. Next, MΦ-cTLR4 conditioned medium was tested in a wound closure assay to look for secreted factor influence on ECs. MΦ-cTLR4 cells were then tested in a co-culture tube formation assay with ECs to investigate cell-cell interactions. Lastly, MΦ-cTLR4 cells were tested for VEGF-A expression.

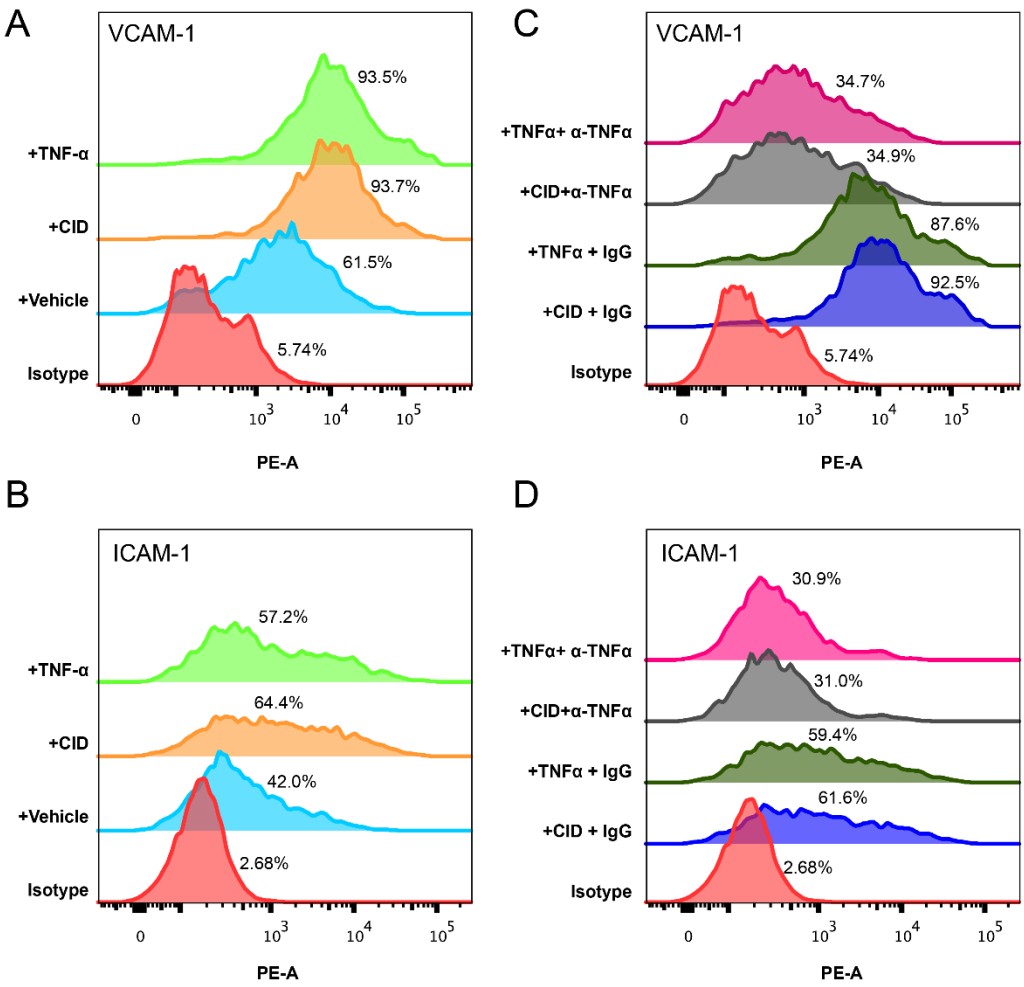

Figure 4.2: Medium From CID-treated MΦ-cTLR4 Cells Upregulate VCAM-1 and ICAM-1 on Endothelial Cells. Endothelial activation, determined by flow cytometry. Conditioned medium from MΦ-cTLR4 cells treated for 6 hours with TNFα, CID, and vehicle was transferred to plated bEnd.3 endothelial cells and left to incubate for 12 hours. Following the 12 hour incubation, bEnd.3 cells were then trypsinized and stained for both VCAM-1 and ICAM-1. (A & B) Histograms showing intensity of VCAM-1 and ICAM-1 expression on bEnd.3 cells incubated with MΦ-TLR4 conditioned medium treated with TNFα (20 ng/mL), CID (50 nM), or vehicle (C & D) Histograms showing intensity of VCAM-1 and ICAM-1 expression on bEnd.3 cells incubated with MΦ-TLR4 conditioned medium treated with TNFα (20 ng/mL), CID (50nM), or vehicle, as well as with or without TNFα neutralizing antibody (α-TNFα).

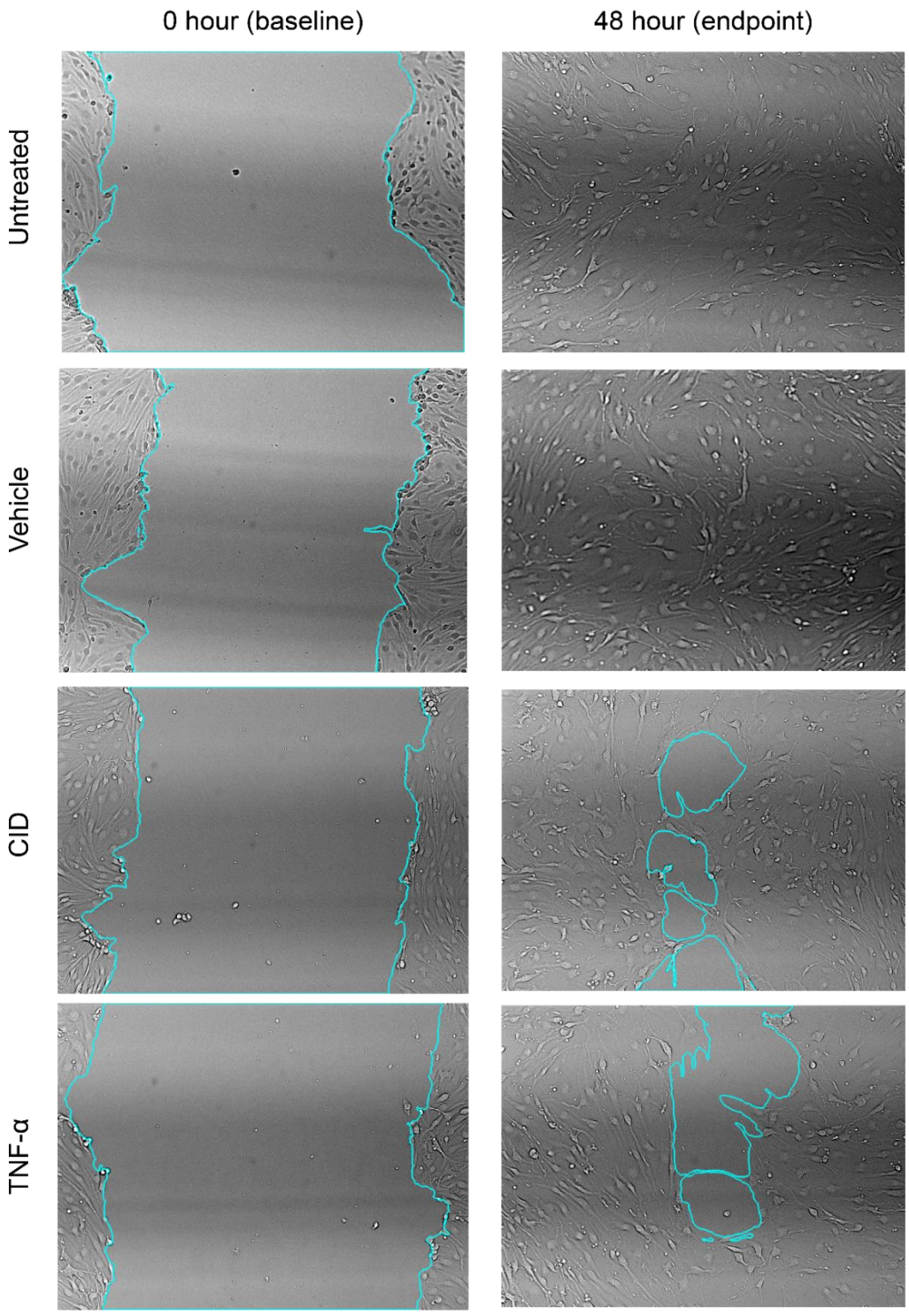

Figure 4.3: Wound Closure Assay. MΦ-cTLR4 conditioned medium was used in a wound closure assay to determine EC proliferation and migration potential depending on MΦ-cTLR4 treatments. Left panels show initial baseline scratch, while right panels show the endpoint EC proliferation and migration into the scratch at 48 hours for untreated, vehicle-treated, CID-treated (50 nM), and TNFα-treated (30 ng/mL) MΦ-cTLR4 cell conditioned medium.

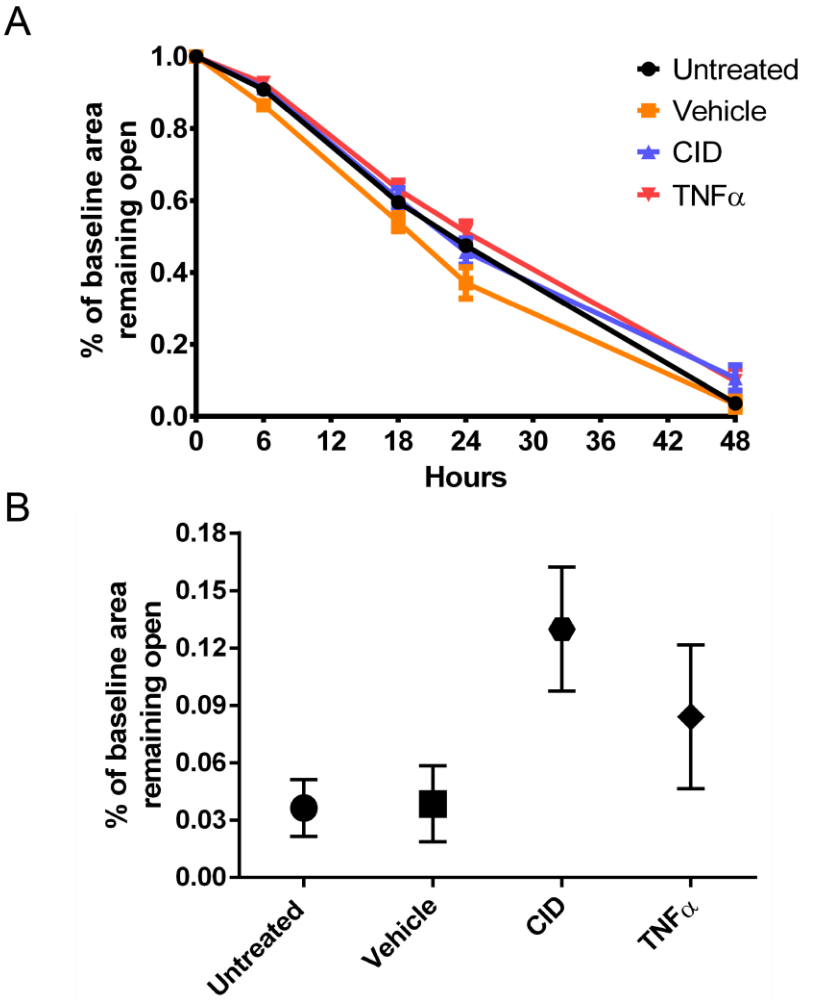

Figure 4.4: Rates of Wound Closure. (A) Rate of closure for untreated, vehicle-treated, CID-treated (50 nM), and TNFα-treated (30 ng/mL) wound closure assays. (B) The 48 hour endpoint of each group, showing two distinct groupings and error bars.

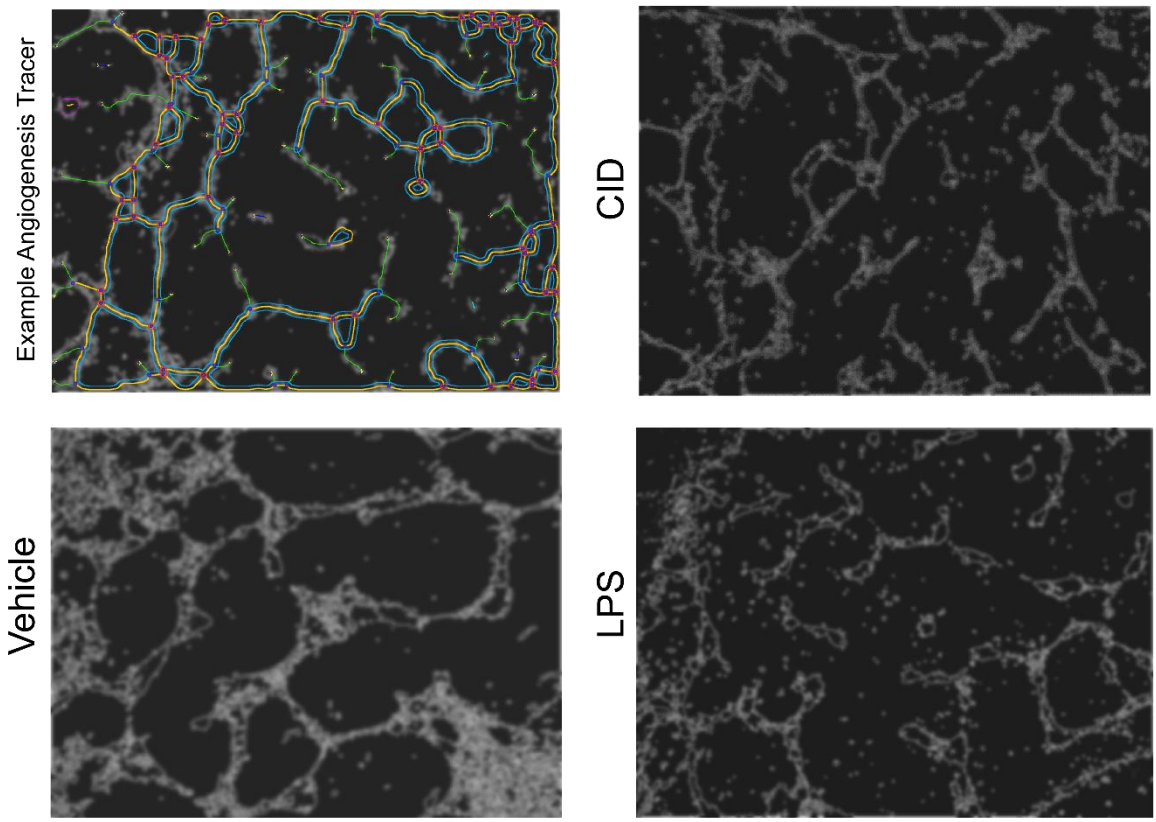

Figure 4.5: Co-culture Angiogenesis Assay Results. Top right panel shows example of the angiogenesis analyzer, where: green = branches; cyan = twigs; magenta = segments; orange = master segments; blue sky = meshes; red surrounded by blue = nodes surrounded by junctions symbol; junctions surrounded by red = master junctions; blue = isolated elements; cyan = small isolated elements; red surrounded by yellow = extremities. Bottom left panel shows network formation for vehicle-treated MΦ-cTLR4 cells co-cultured with RAECs. Top right panel shows network formation for CID-treated (50 nM) MΦ-cTLR4 cells co-cultured with RAECs. Bottom right panel shows network formation for LPS-treated (100 ng/mL) MΦ-cTLR4 cells co-cultured with RAECs.

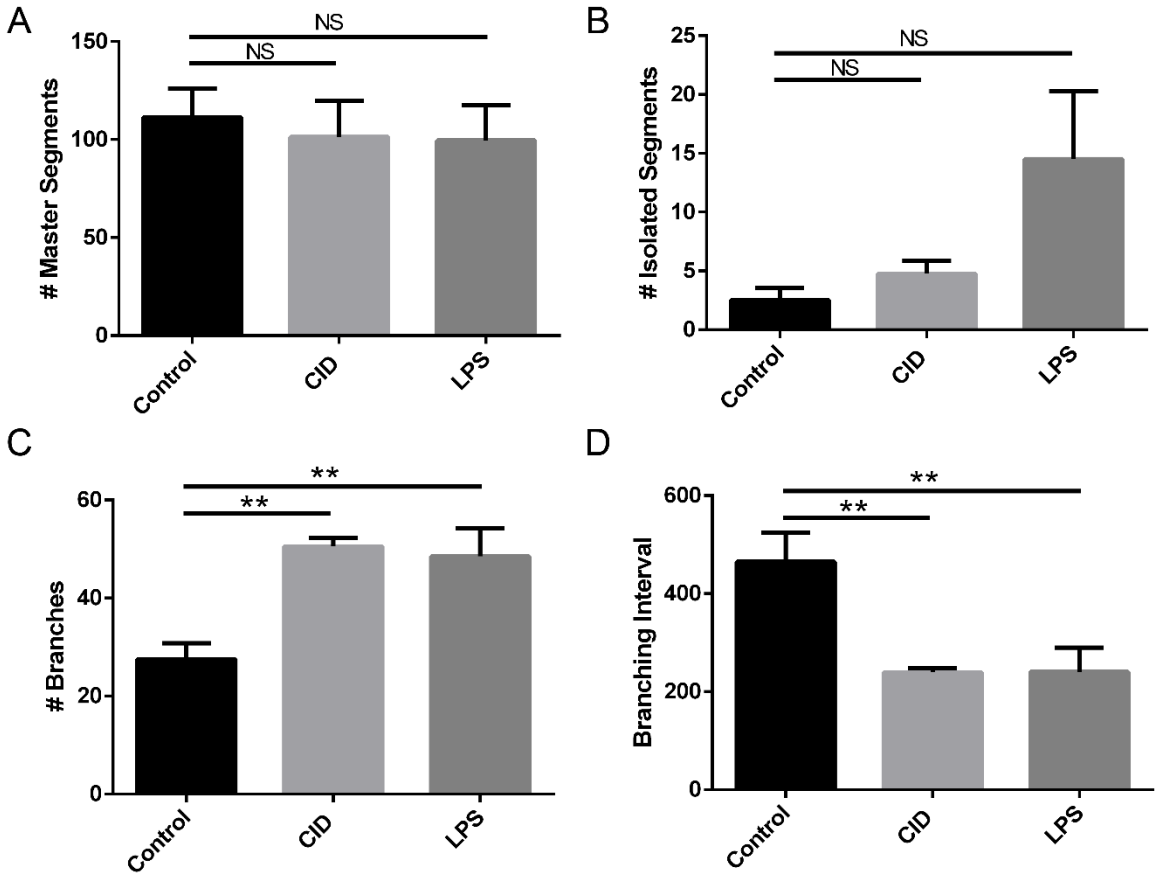

Figure 4.6: Quantification of Co-culture Angiogenesis Assay. (A) Bar graph of quantification of master segments. (B) Bar graph of quantification of isolated segments. (C) Bar graph of quantification of branch number. (D) Bar graph of quantification of branching interval.

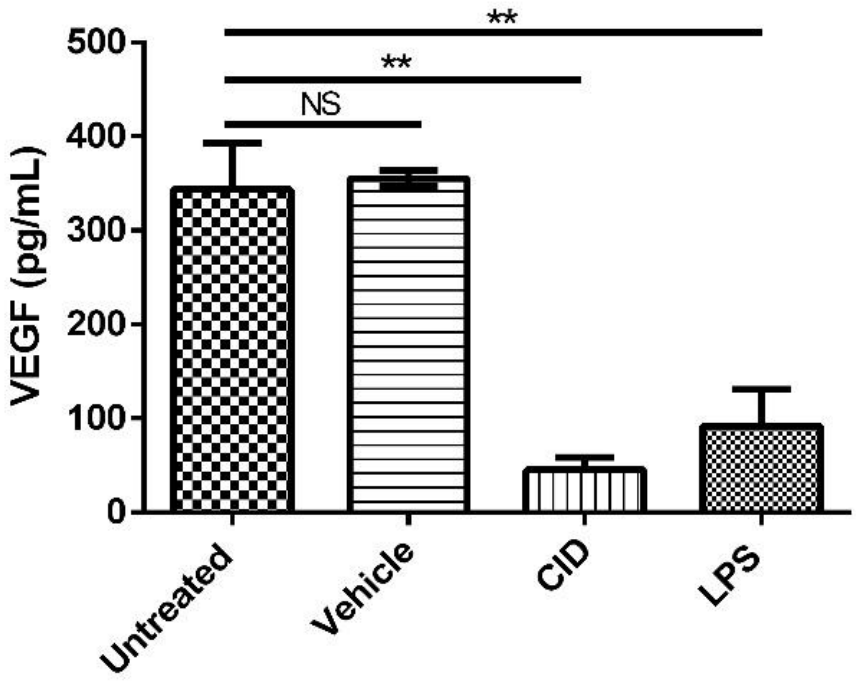

Figure 4.7: VEGF-A Expression in MΦ-cTLR4 Cells. Bar graph shows levels of VEGF for cells treated with vehicle, CID drug (50 nM), LPS (100 ng/mL), or left untreated. Cell medium was collected following 24 hour treatment.

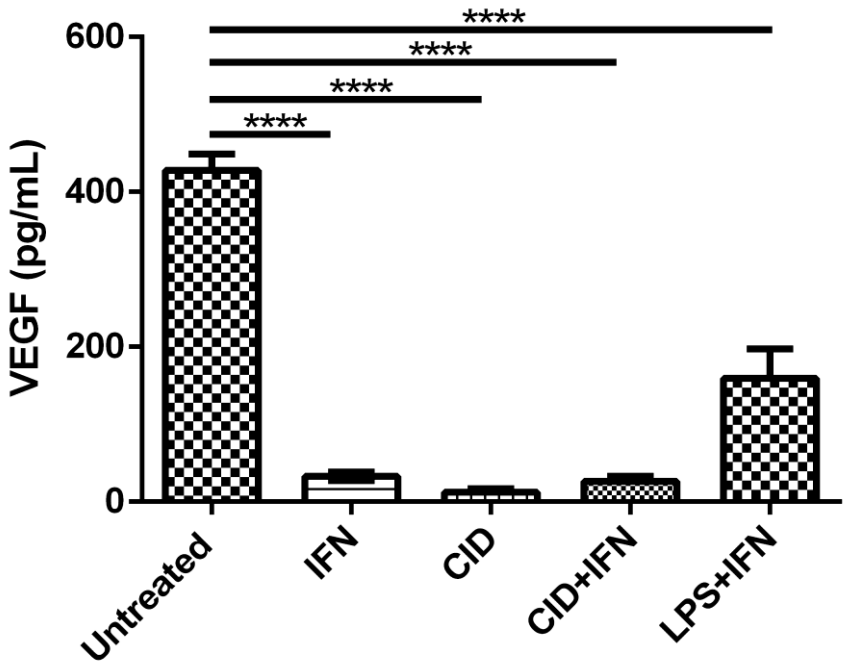

Figure 4.8: VEGF-A Expression in MΦ-cTLR4 with IFN-γ Co-treatment. Bar graph shows levels of VEGF for cells treated with IFN-γ (20ng/mL) and CID drug (50 nM) or LPS (100 ng/mL), or left untreated. Groups were compared to corresponding controls. Cell medium was collected following 24 hour treatment.

Chapter 5. THE ROLE OF MΦ-CTLR4 CELLS IN THE INFLAMMATORY RESPONSE IN VIVO

5.1 ABSTRACT

In this chapter, the MΦ-cTLR4 cells were tested in a mouse model injected with a Matrigel plug containing engineered cells. Both 7 day and 14 day timepoints for injected Matrigel plugs were performed and two groups existed for each experiment: untreated mice and CID-treated mice. I hypothesized that Matrigel plugs containing MΦ-cTLR4 cells would still be present following the duration of the experiments and that the MΦ-cTLR4 cells would be functionally active in CID-treated mice, but not for untreated mice. This would suggest that pro-inflammatory regions would be present surrounding the MΦ-cTLR4 cells after plug retrieval from CID-treated mice. Plug morphology was analyzed using H&E and trichrome staining. Cell infiltration was greatly increased for the CID-treated mice in the 14 day experiment, when compared to the untreated mice. Furthermore, MΦ-cTLR4 cells in the Matrigel plug pockets appeared dead in the untreated mice from lack of nuclei staining, however, CID-treated mice had MΦ-cTLR4 cells in plug pockets that had clear nuclei staining. Matrigel plugs were additionally analyzed using trichrome staining, which can detect collagen deposition. Collagen fibril formation was detected in regions surrounding the plug, as well as in the Matrigel plug, which might suggest the presence of fibrosis. Lastly, plugs were analyzed via immunofluorescence to test for co-localized regions of GFP positive MΦ-cTLR4 cells and iNOS inflammatory regions, which would suggest that MΦ-cTLR4 cells were present and functionally active. MΦ-cTLR4 cells were still present in the 7 day experiments, however, MΦ-cTLR4 cells either died or migrated out of the plug for the 14 day experiment, as there were very few GFP positive cells observed. Nonetheless, even with very few

GFP positive cells present, there were some MΦ-cTLR4 cells detected in the 14 day experiment that co-localized with iNOS inflammatory regions.

5.2 INTRODUCTION

In the following sections, I will investigate the functional properties of MΦ-cTLR4 cells in an *in vivo* environment (Figure 5.1). It has been shown that mice injected with Matrigel plugs containing pre-polarized MΦs can influence inflammatory properties (28). However, while a pre-polarized MΦ approach may be helpful in determining *in vitro* inflammatory outcomes, this technique is not suitable for examining long-term *in vivo* inflammation resolution outcomes. This is attributable to the competing local inflammatory environment, in which these pre-polarized cells are being introduced. These competing signals could potentially change the phenotype of the injected cells, depending on the influence of different chemokines, cytokines, and other factors. To overcome this limitation, I have used MΦ-cTLR4 cells, which can be injected and subsequently polarized into a pro-inflammatory phenotype. I have tested these cells in an *in vitro* plasticity assay and even though MΦ-cTLR4 cells are influenced by IL-4 cocktail treatment, the cells still display M1 MΦ characteristics, albeit at lower levels. Injection of these cells and subsequent treatment with CID drug will allow me to hypothetically maintain desired phenotype characteristics of the cells via numerous CID drug intraperitoneal injections.

5.2.1 *In Vivo MΦ Characterization*

For *in vivo* MΦ characterization, phenotype determination is more complicated than *in vitro* studies. While the *in vitro* M1 MΦ and M2 MΦ extremes described in literature are a nice concept, unfortunately these extremes are a continuum of intermediate MΦ cell phenotypes. This becomes clear when looking at MΦ phenotypes *in vivo* instead of cells cultured *in vitro* with only LPS or IL-4 (102). The question is not whether extreme pro-inflammatory MΦs or extreme pro-healing

MΦs are present, but rather whether the present MΦs are more or less skewed toward the pro-inflammatory or pro-healing phenotype. For this reason, upregulation of pro-inflammatory markers does not mean that pro-healing markers are downregulated, or vice versa. Therefore, for *in vivo* experiments, it is often necessary to look at M1/M2 marker ratios, such as the iNOS/Arginase I ratio or the IL-12/IL-10 ratio to determine how the MΦ phenotypes have been skewed (103). This study is merely attempting to co-localize the MΦ-cTLR4 cells with inflammatory regions, however, it is helpful to keep in mind that absolute levels of inflammatory regions in this study might differ from sample to sample, as ratios could be similar, but levels could differ.

5.2.2 *M1 Macrophages During the FBR*

During the FBR, MΦ phenotypes do not fit into the conventional M1/M2 MΦ dichotomy. Instead MΦs exhibit a mixed M1/M2 MΦ phenotype that could contribute to a dysregulated state of the inflammatory process during this reaction. In many investigations of the FBR, the most abundant MΦ phenotype present is a M2-skewed MΦ and the M1-skewed MΦs are generally found at much lower numbers around the implanted device (104, 105). As M2 MΦs are known to recruit fibroblasts, cells that lay down collagen, these overly abundant cells without a strong M1 MΦ response could be contributing heavily to the undesirable capsule formation. M1 MΦs or MΦ-cTLR4 cells could theoretically be used correct this balance or reinitiate the innate inflammatory response. Furthermore, M1-skewed MΦs have been associated with angiogenic regions closely surrounding the implanted material or device (50). Therefore, M1 MΦs could be used as a tool to both reactivate inflammation, as there a very few of these M1-skewed MΦs, and increase angiogenesis in close proximity to the device or implanted material for better integration.

5.3 MATERIALS AND METHODS

5.3.1 *Reagents and Antibodies*

The anti-iNOS/NOS type II antibody was purchased from Abcam. The anti-TurboGFP(d) antibody was purchased from Evrogen. Normal goat and rabbit serum was purchased from Jackson Laboratories. Goat and rabbit IgG control was purchased from BD Pharmingen.

5.3.2 *Animals*

Four groups of 4 week old female BALB/c mice (total of 16 mice) were used in this *in vivo* study. The four groups consisted of: 7 day non-treated mice, 7 day CID-treated mice, 14 day non-treated mice, and 14 day CID-treated mice. The day before Matrigel injections, needles, 200 μL pipets tips, and syringes were chilled at 4°C. At day of injection, pre-plated MΦ-cTLR4 cells were lifted off T75 flasks with trypsin, spun down, and resuspended in 3-5 mLs of DMEM. Cells were counted and $0.5x10^6$ cells were placed in 8 separate Eppendorf tubes with at most 100 μL medium. In procedure room, tubes containing cells were placed on ice to cool, so that Matrigel did not solidify when mixed with cells in tubes. Matrigel was added to medium/cells in pre-chilled tubes (400 μL of Matrigel with no dilution). Tubes were flicked to mix contents. The Matrigel and cell suspension was then immediately loaded into chilled 1 mL syringes with a chilled 23 gauge needle. The isoflurane chamber was set up (2% O_2, 1.5% isoflurane for chamber, and 0.5% isoflurane for nose cone) and anesthetized mice were s.c. injected with the Matrigel and MΦ-cTLR4 cell suspension into the right back dorsal area (after shaving mouse). Before placing mouse back in cage, mice were injected with the first intraperitoneal CID drug dose (2 mg/kg mouse weight). Treatment groups were given CID drug injections every other day during the course of the experiment.

5.3.3 *Histological Samples*

Mice were euthanized using CO_2, as per IACUC protocol. Following dissection, tissues containing Matrigel plug, skin, and muscle were placed in 10% formalin for 24 hours to fix tissue. Samples were then transferred to 70% EtOH for 24 hours. For cryo freezing, samples were then transferred to 20% sucrose (W/V in PBS) for 24 hours and then embedded in Tissue-tek molds with optimum cutting temperature (O.C.T.) compound. Molds were placed in freezing isopentane to freeze the samples rapidly and then blocks were sectioned at 5 μM for analysis. For paraffin embedded samples, tissues were processed using a Thermo Shandon Citadel 2000. Tissues were embedded in paraffin and blocks were sectioned at 5 μM for analysis.

5.3.4 *Trichrome and H&E Staining*

Trichrome staining was performed using the Accustain Trichrome Stains from Sigma. Briefly, slides were deparaffinized and hydrated with deionized water. Slides were then placed in Bouin's solution at room temperature overnight. The next day, the slides were rinsed in tap water and washed to remove any yellow color remaining from Bouin's solution. Slides were stained in Weigert's Iron Hematoxylin Solution for 10 minutes and subsequently washed in running tap water for 5 minutes and rinsed in deionized water. Next, the slides were stained in Biebrich Scarlet-acid Fucshin for 7 minutes and then rinsed in deionized water. Following this step, phosphotungstic/phosphomolybdic acid solution was placed on the slides for 5 minutes and then immediately placed in Aniline Blue solution for 5 minutes without washing between steps. Lastly, the slides were placed in Acetic Acid (1%) for 2 minutes, dehydrated through alcohol, and cleared in xylene to be cover slipped. For Hematoxylin and Eosin staining, slides were deparaffinized and hydrated with deionized water. Slides were then placed in Hematoxylin solution for 2 minutes and rinsed in water several times. Clearing solution (95% EtOH & 1% HCl) was then placed in the

sections for 5 seconds. Slides were rinsed in water and subsequently placed in Eosin solution for 40 seconds. Slides were rinsed in water again, dehydrated, and cover slipped.

5.3.5 *Immunofluorescence*

For immunofluorescence, slides were deparaffinized and hydrated with TN basic solution (100 mM Tris base, 150 mM NaCL, pH 7.5). Antigen retrieval was performed by placing slides in Coplin jar with citrate buffer and boiling citrate solution for 5 minutes. Once temperature reached 90-95°C, Coplin jar containing heated citrate solution was placed in a heated water bath and allowed to cool for 30-35 minutes. Slides were rinsed with TN basic solution for 5 minutes and sections were divided by "Ruby" red nail polish. Once nail polish was dried, slides were placed in an incubation chamber and TN working solution (TN basic solution with 0.3% Tween-20, 1% BSA, and 1% appropriate serum) was applied to sections to block for 1 hour at room temperature. After blocking step, the appropriate amount of primary antibody was diluted in TN working solution and placed on slides to be incubated overnight at 4°C. The next day, slides were rinsed with TN basic solution 3 times for 15 minutes each. Following washes, the sections were covered with secondary antibody diluted in TN working solution for 1 hour at room temperature. Slides were then rinsed 3 times for 10 minutes each and placed in sudan black solution (0.3% sudan black and 95% EtOH) for 5 minutes to dampen background signal. Slides were rinsed in water and dipped in 70% EtOH to remove any preceipitates from sudan black. Lastly, slides were dipped in TN basic solution with 0.3% Tween and cover slipped with Prolong® Diamond Antifade Mountant with DAPI (Life Technologies).

5.4 RESULTS

5.4.1 *Morphology and Cell Survival of Implanted Matrigel Plugs*

Cell survival is important for the MΦ-cTLR4 cells, as cells need to remain in the vicinity of the delivery site for the full duration of inflammatory resolution to be used as a tool for *in vivo* applications. Cell survival in both 7 day and 14 day experiments were analyzed by H&E staining. The Matrigel plugs for the untreated 14 day group were mostly dead and contained no nuclei staining (Figure 5.2). However, the CID-treated 7 day, as well as CID-treated 14 day plugs still contained pockets of alive cells (Figure 5.3 & 5.6). Cell infiltration is also important for Matrigel plugs, as MΦ-cTLR4 cells need to interact with the endogenous inflammatory cells to influence the overall inflammatory environment. As for cell infiltration, 14 day CID-treated Matrigel plugs had much more endogenous cell infiltration, when compared to 14 day untreated Matrigel plugs (Figure 5.2 & 5.3). Both cell survival and endogenous cell infiltration were qualitative analyses.

5.4.2 *Collagen Deposition in Matrigel plugs*

The presence of collagen in or around the MΦ-cTLR4 Matrigel plug exists in one of two forms: 1) dense collagen formation surrounding the outside of the plug or 2) sparse collagen formation interspersed throughout the plug. The region of collagen deposition is also an indication of whether there is a healing or a fibrosis response occurring. During the FBR, the fibrosis response often creates a fibrotic capsule or collagen layer around the object to isolate it from the surrounding environment. However, during the normal healing response, collagen is used for the formation of granulation tissue in a less dense and delocalized manner. With this in mind, it can be proposed that collagen fibrils seen within the Matrigel plug are indicative of a healing response, but dense collagen formation on the perimeter of the plug may indicate the start of the fibrosis process. Collagen formation was increased in the 14 day untreated Matrigel plugs, when compared to the

14 day CID-treated plugs (Figure 5.4). When present, collagen formation was mostly observed on the perimeter of the Matrigel plug in both untreated and CID-treated Matrigel plugs. However, there was a higher degree of collagen formation around plugs in untreated plugs, as opposed to CID-treated plugs, where collagen was mostly observed within the plug, if observed at all. Figure 5.4 shows the only CID-treated mouse that displayed collagen staining, however, this mouse did not contain any GFP positive MΦ-cTLR4 cells at the 14 day timepoint. The collagen fibril formation for untreated mice was also much denser and more abundant, unlike CID-treated plugs, which contained less dense and sparser collagen formation.

5.4.3 *MΦ-cTLR4 Cells Co-localized with iNOS Inflammation Regions in Tissue*

The existence of GFP positive MΦ-cTLR4 cells and iNOS co-localization indicates that the MΦ-cTLR4 cells remain functional within the Matrigel plug and also indicates the potential influence of the MΦ-cTLR4 cells on the local environment. As most cells were dead in the 14 day untreated Matrigel plugs, there were no regions of co-localization of GFP MΦ-cTLR4 cells and iNOS regions (Figure 5.5). However, the 14 day CID-treated plugs had some occurrences of GFP/iNOS co-localization (Figure 5.7 and 5.8).

5.5 DISCUSSION

To perform the Matrigel plug experiments, BALB/c mice were chosen, since RAW 264.7 cells originate from this specific mouse strain and had the least chance of rejection. Matrigel was also chosen as a delivery vehicle, due to the fact that this is a murine ECM, which is well-characterized and yields reliability and reproducibility. Furthermore, it was necessary to keep the ECM consistent with Chapter 4 *in vitro* studies. Lastly, both 7 and 14 day timepoints for Matrigel plugs were chosen to coincide with Matrigel plug experiments performed in literature (28, 106). Even though BALB/c mice might exhibit the least amount of rejection, future experiments should use

nude mice, as these mice lack T-cells and thus cannot mount an antibody response. Nude mice might allow the cells to survive longer and for Matrigel plugs to contain larger amounts of MΦ-cTLR4 cells at the endpoints.

In order for *in vivo* applications to be possible with MΦ-cTLR4 cells, cell survival is necessary for the duration of the innate inflammation response, which is at least 10 days, depending on the degree of injury. The fact that cells did not look alive in the pockets of Matrigel plugs from the 14 day untreated mice, suggests that these cells might have died, due to lack of activation signal. CID-treated mice had a dose of CID that could theoretically activate the MΦ-cTLR4 cells in the injected Matrigel plugs. These plugs experienced much more activity, such as increased cell infiltration, as well as more degraded Matrigel, suggesting that the MΦ-cTLR4 cells might have been communicating with the endogenous environment. In this scenario, MΦ-cTLR4 would secrete signals that recruit other inflammatory cells, which would increase endogenous infiltration of the Matrigel and possibly allow for the MΦ-cTLR4 to shape the environment into an inflammatory state. This is just one inference from the observed results, however, more studies need to be performed to understand the interaction between the MΦ-cTLR4 cells and the endogenous innate immune system.

The FBR to implanted materials is characterized by a distinct avascular fibrous capsule made of collagen surrounding the implanted device. Thus, it is important to note the differences in collagen deposition for both untreated and CID-treated mice. It was observed that untreated mice had a greater amount of dense collagen formation surrounding the outside of the plug, as opposed CID-treated mice, which had a less and more interspersed collagen deposition that infiltrated the plug.

This could be potentially significant, as during the innate inflammatory response, M2 MΦs have been associated with the later stages of the inflammation response and are correlated with increased angiogenesis and fibrosis, (67) whereas M1 MΦs have been associated with the early stages of the inflammation response as well as inhibition of angiogenesis. These results suggest that CID-treated MΦ-cTLR4 cells might act to decrease the fibrosis response in the normal healing process, as these cells are producing competing signals to that of the collagen promoting M2 MΦs. Therefore, it would be interesting to know whether there are more M2 endogenous MΦs present in the plugs from untreated mice, when compared to CID-treated mice.

Co-localization experiments showed that MΦ-cTLR4 cells could survive for at least 14 days in an *in vivo* environment and remain in a pro-inflammatory functionally active state. Only $0.5x10^6$ cells were injected with the 400 uL Matrigel plug, which might be too low of a number to observe abundant GFP positive cells following the 7 and 14 day timepoints. In fact, there were very few instances where co-localization was observed even in CID-treated Matrigel plugs. A potential explanation for this might be that the MΦ-cTLR4 cells could be dispersed in and around the Matrigel plug, making it difficult to see the individual single engineered cells. In comparison, the cells that were found to exhibit co-localization of GFP and iNOS were contained with many other MΦ-cTLR4 cells in the pockets of the Matrigel plug, which gave a brighter signal. Thus, in order to see a more robust pro-inflammatory response, the number of injected MΦ-cTLR4 cells might need to be increased in future experiments.

While similarities exist between acute inflammation progression and the FBR process, one major difference includes the observation that the MΦ phenotypes in the FBR have been shown to

express a combination of both M1 and M2 MΦ markers (49, 107). This observation may indicate a dysregulation of the inflammatory response in the FBR. Thus, it could potentially be beneficial to control the FBR inflammation response to exhibit a distinct M1 MΦ response followed by a distinct M2 MΦ response (108). This may decrease fibrous capsule formation and integrate the implant better with the surrounding tissue by promoting more angiogenesis and less fibrosis. To this end, Spiller et al. created a scaffold that sequentially released a M1-promoting cytokine (IFN-γ) followed by a M2-promoting cytokine (IL-4) in an attempt to increase vascularization of scaffolds for bone regeneration. When implanted, the IFN-γ-loaded scaffolds induced a vascular network, however, the IL4- and sequential IFN-γ/IL4-loaded scaffolds did not promote further vascularization. In addition, at the two week timepoint there was no difference in the composition of M1 vs M2 MΦs between the groups (85). These findings suggest that the two distinct and sequential M1 and M2 MΦ phases need to be elicited in a specific temporal manner to promote persistent angiogenesis, inhibit fibrosis, and resolve the FBR. The engineered pro-inflammatory MΦs in this study may be the proper tool, to at least elicit a robust early M1 MΦ phase. Since the engineered MΦ-TLR4 cells are activated by the CID drug, they can be: 1) activated independently of the endogenous microenvironment, and 2) can be turned on early in the FBR but turned off at a later time to allow M2 MΦ processes to occur.

5.6 CONCLUSIONS

In this chapter, I investigated the influence of the MΦ-cTLR4 cells in an *in vivo* mouse model. I found that cell survival was evident in 7 day plugs, as well as 14 day CID-treated plugs. However, 14 day untreated plugs had very few, if any, alive cells in Matrigel pockets. Cell survival in 14 day CID-treated plugs indicate that activated MΦs might be able to survive longer than non-activated MΦs. Endogenous cell infiltration was also much less for 14 day untreated plugs, when compared

to 14 day CID-treated plugs. This suggests MΦ-cTLR4 cells within 14 day CID-treated plugs might have been able to influence the local environment to a greater degree and the recruitment of endogenous cells into the Matrigel plug is evidence for local environmental stimulus. Furthermore, an increase in collagen formation was observed for 14 day untreated plugs, when compared to 14 day CID-treated plugs. A greater amount of collagen formation in untreated plugs might indicate a fibrosis response around the plug, as the plug was not actively influencing the environment, due to the lack of live cells. Lastly, co-localization of GFP positive cells and iNOS regions were observed in both 7 day and 14 day CID-treated plugs, but not apparent in 14 day untreated plugs. This suggests that MΦ-cTLR4 cells were still functional and influencing the local environment to be that of an inflammatory state in CID-treated Matrigel plugs.

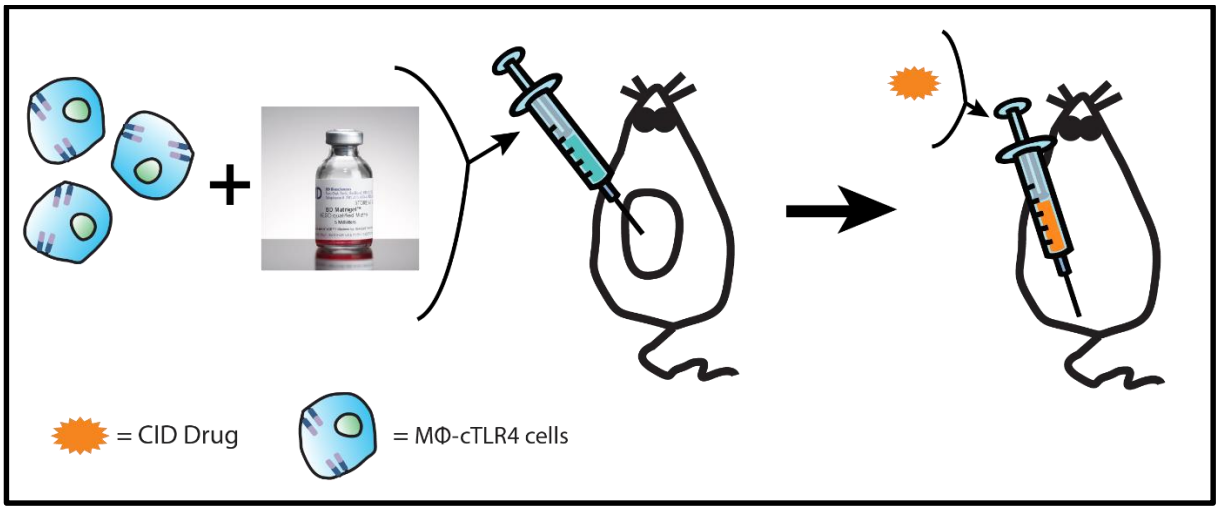

Figure 5.1: Chapter 5 Summary Diagram. MΦ-cTLR4 cells were tested *in vivo* using a Matrigel plug. Liquid Matrigel with MΦ-cTLR4 cells were s.c. injected into a mouse and left to solidify. Mice were injected with CID drug every other day with 2 mg/kg mouse weight. Matrigel plugs were then removed following 7 or 14 days and analyzed.

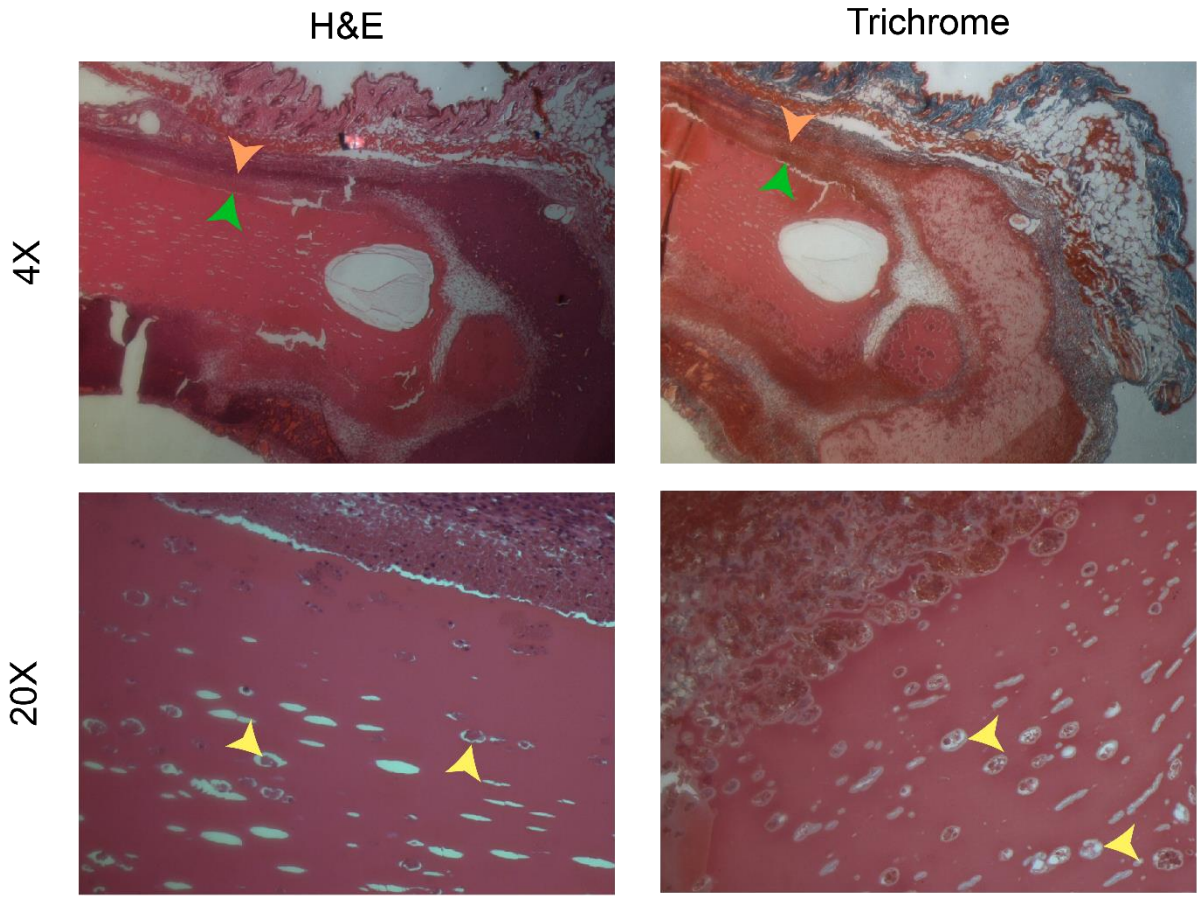

Figure 5.2: 14 Day Untreated Mice Matrigel Plug. Top right panel shows cell infiltration in H&E stained section. Top right panel shows cell infiltration in trichrome stained section. Orange arrow indicates outside border of Matrigel plug, while green arrow indicates the inside border of cell infiltration. Bottom left panel shows dead cells with no nuclei staining in Matrigel pockets in H&E stained section. Bottom right panel shows dead cells with no nuclei staining in Matrigel pockets in trichrome stained section. Yellow arrows indicate two separate pockets of dead cells.

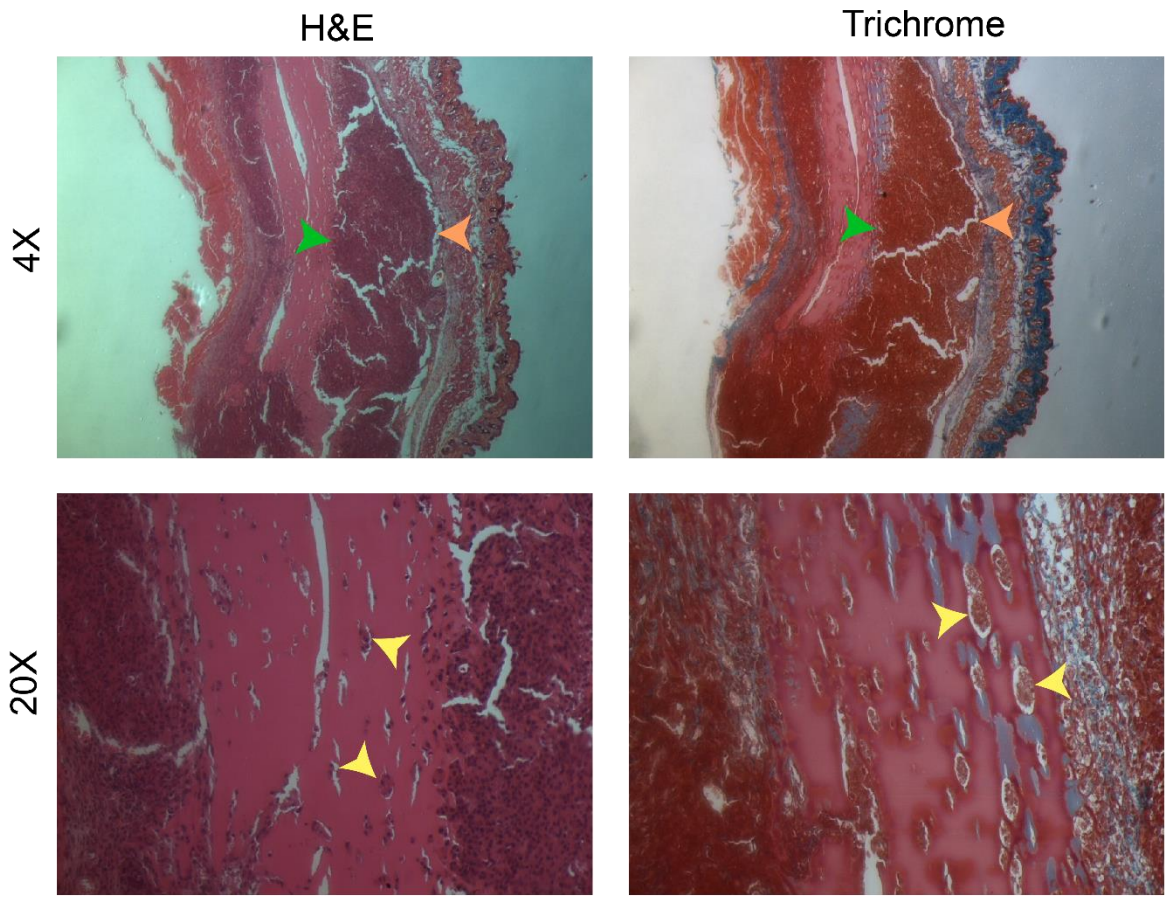

Figure 5.3: 14 Day CID-treated Mice Matrigel Plug. Top right panel shows cell infiltration in H&E stained section. Top right panel shows cell infiltration in trichrome stained section. Orange arrow indicates outside border of Matrigel plug, while green arrow indicates the inside border of cell infiltration. Bottom left panel shows alive cells with nuclei staining in Matrigel pockets in H&E stained section. Bottom right panel shows alive cells with faint nuclei staining in Matrigel pockets in trichrome stained section. Yellow arrows indicate two separate pockets of alive cells.

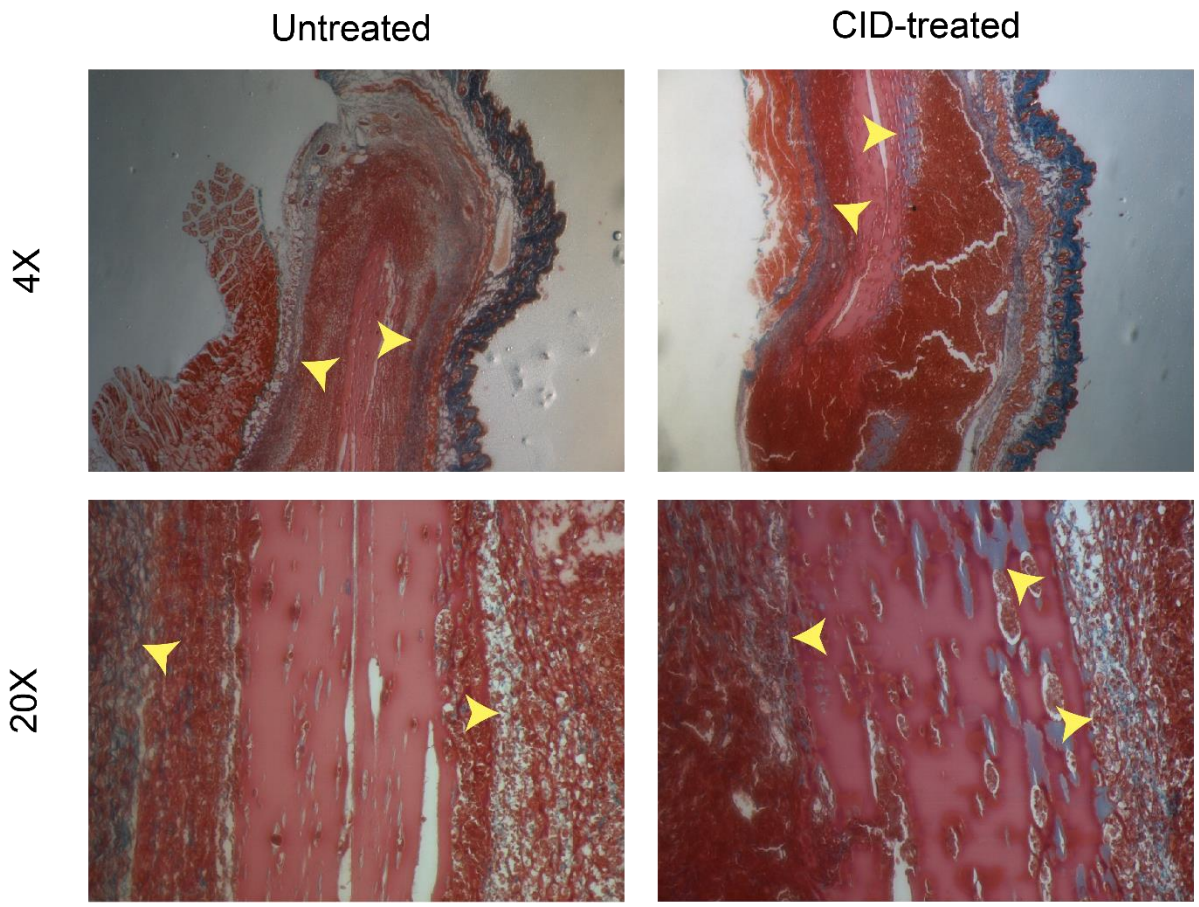

Figure 5.4: Collagen Deposition in Untreated and CID-treated Mice. Top left panel shows collagen surrounding outside of Matrigel plug of untreated mouse H&E stained section. Top right panel shows collagen interspersed throughout plug of H&E stained section. Yellow arrows on top panels indicate high density regions of collagen staining (blue). Bottom left panel shows detailed dense collagen fibril formation surrounding the outside of the untreated mouse plug. Bottom right panel shows loose fibril formation of collagen fibrils interspersed throughout CID-treated Matrigel plug. Yellow arrows on bottom panels indicate regions of collagen staining (blue).

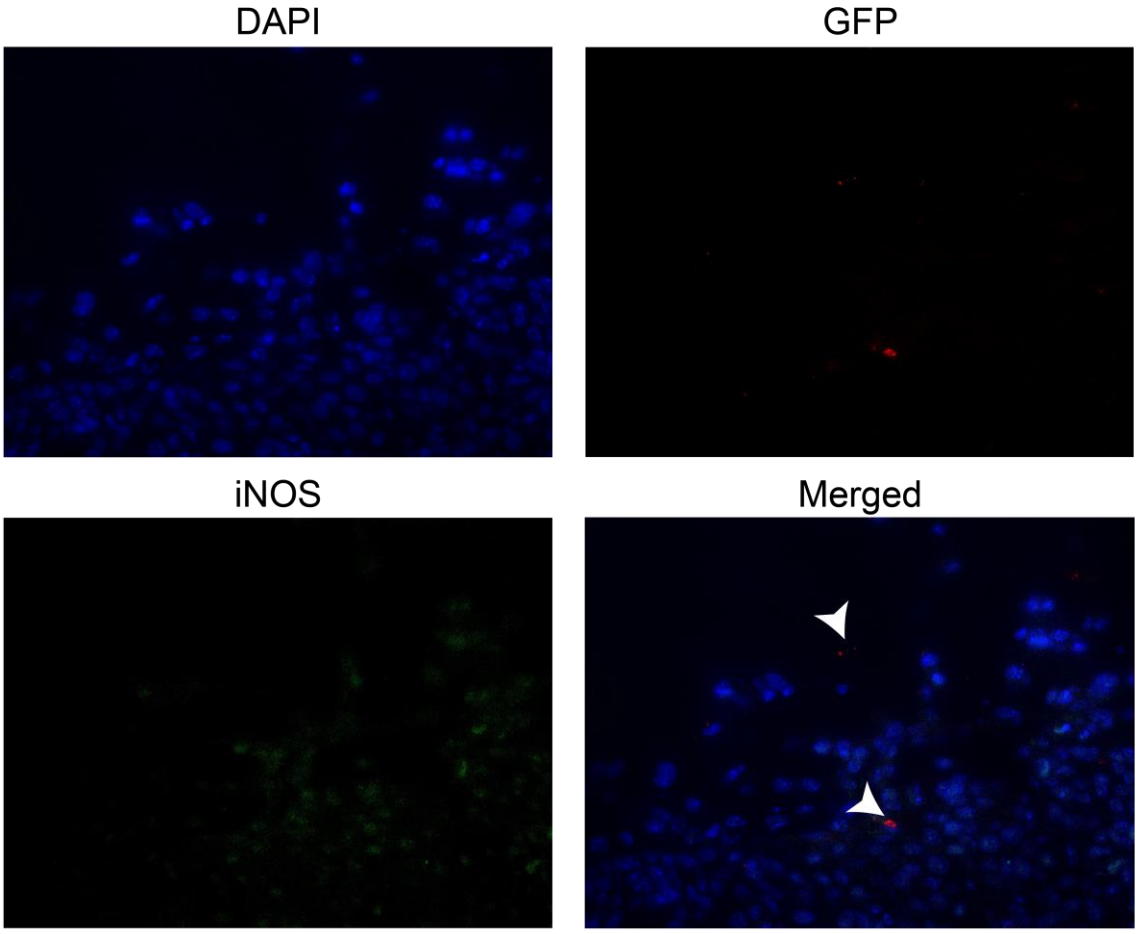

Figure 5.5: 14 Day Untreated Plugs with No GFP and iNOS Co-localization. Images taken at 40X. Top left panel shows dapi nuclei immunofluorescent staining, top right panel shows GFP immunofluorescent staining in MΦ-cTLR4 cells, bottom left shows iNOS immunofluorescent staining, and the bottom right panel shows the merged image. The merged image confirms absence of MΦ-cTLR4 cells being present in Matrigel plug pockets. White arrows indicate two instances of false GFP positive cells.

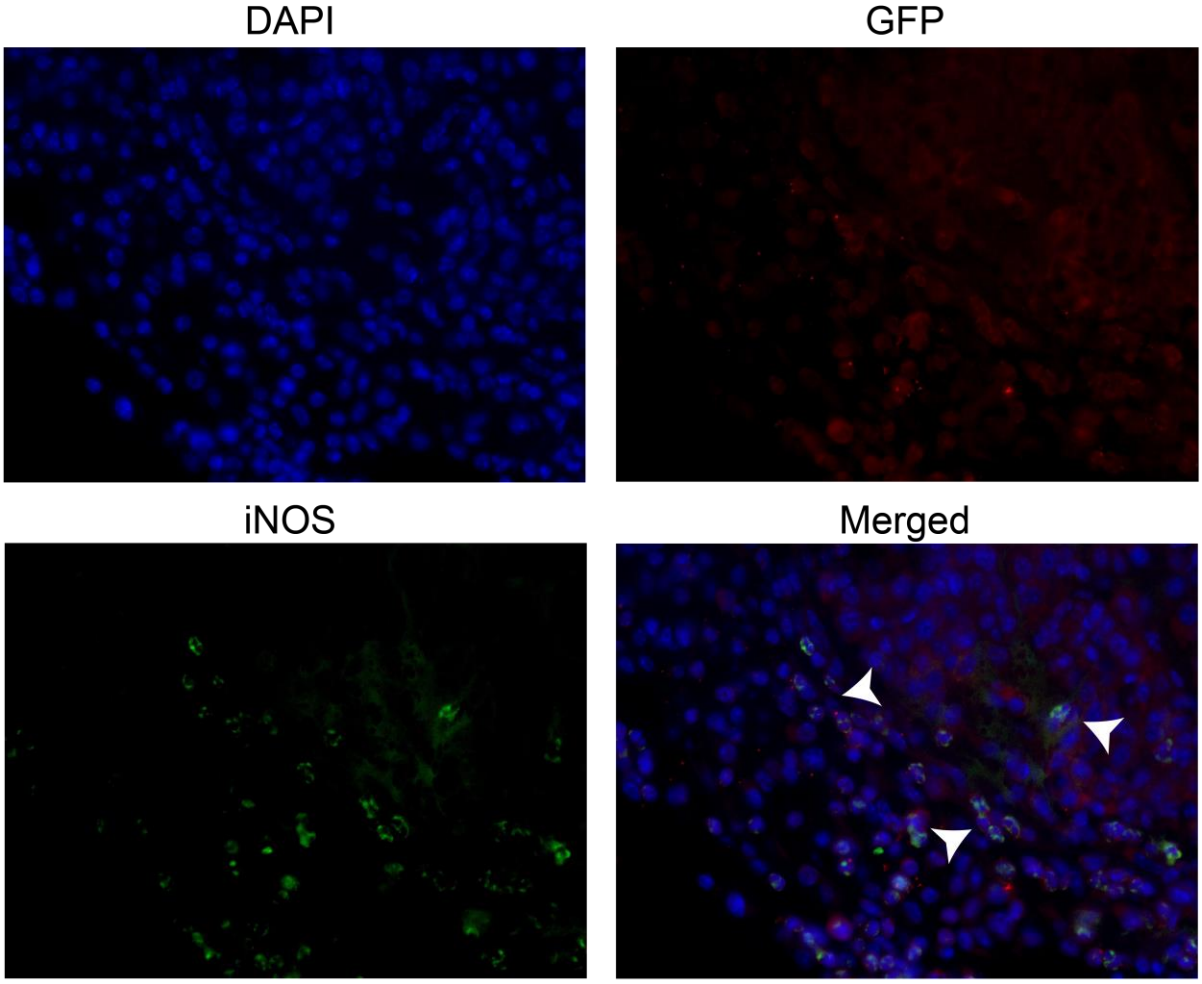

Figure 5.6: 7 Day CID-treated Plugs with GFP and iNOS Positive Cells with Co-localization. Images taken at 40X. Top left panel shows dapi nuclei immunofluorescent staining, top right panel shows GFP immunofluorescent staining in MΦ-cTLR4 cells, bottom left shows iNOS immunofluorescent staining, and the bottom right panel shows the merged image. The merged image confirms presence of MΦ-cTLR4 cells still being present and functionally active in Matrigel plug pockets. White arrows indicate three instances of cells that were positive for both iNOS and GFP.

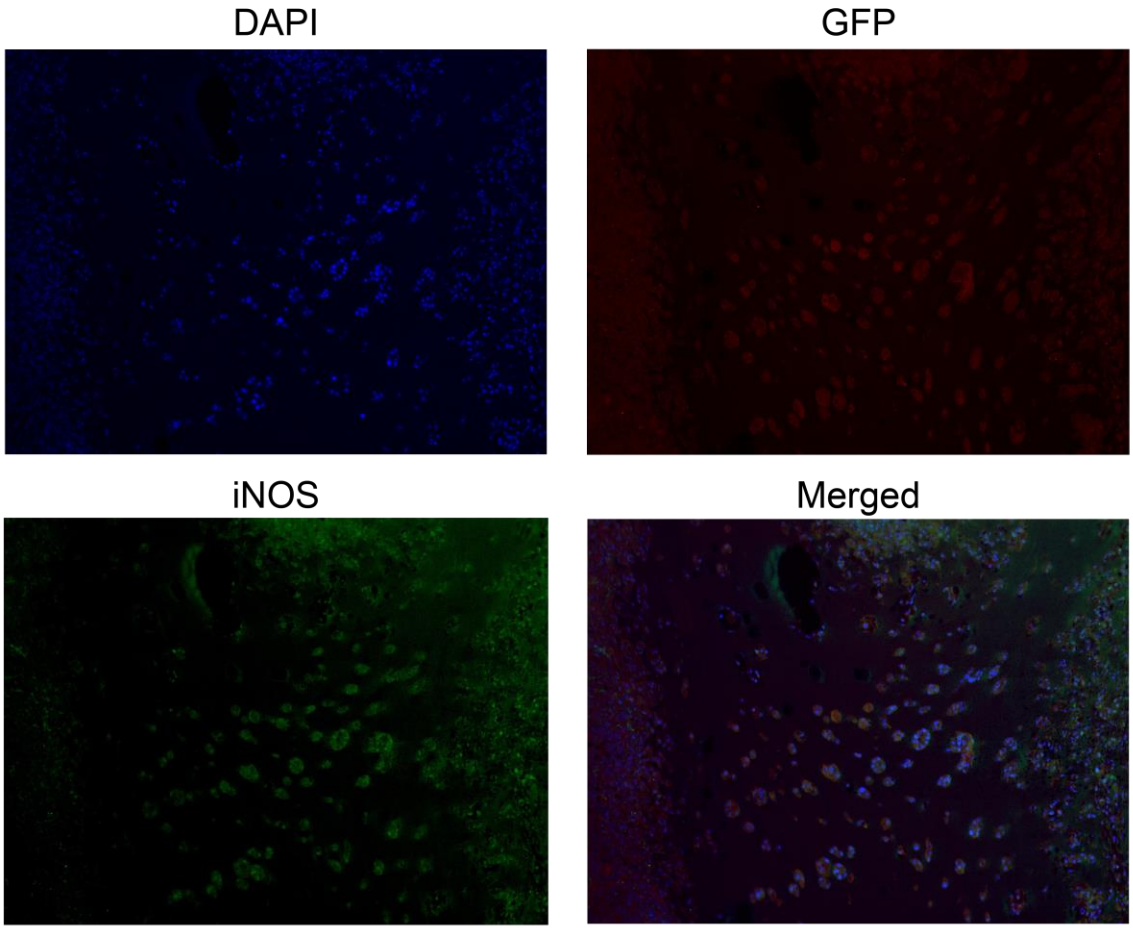

Figure 5.7: Co-localization of GFP and iNOS in 14 day CID-treated Matrigel plugs. Image taken at 10X magnification. Top left panel shows Dapi staining of nuclei, top right panel shows GFP positive cells, bottom left panel shows iNOS positive cells, and bottom right panel shows the merged image.

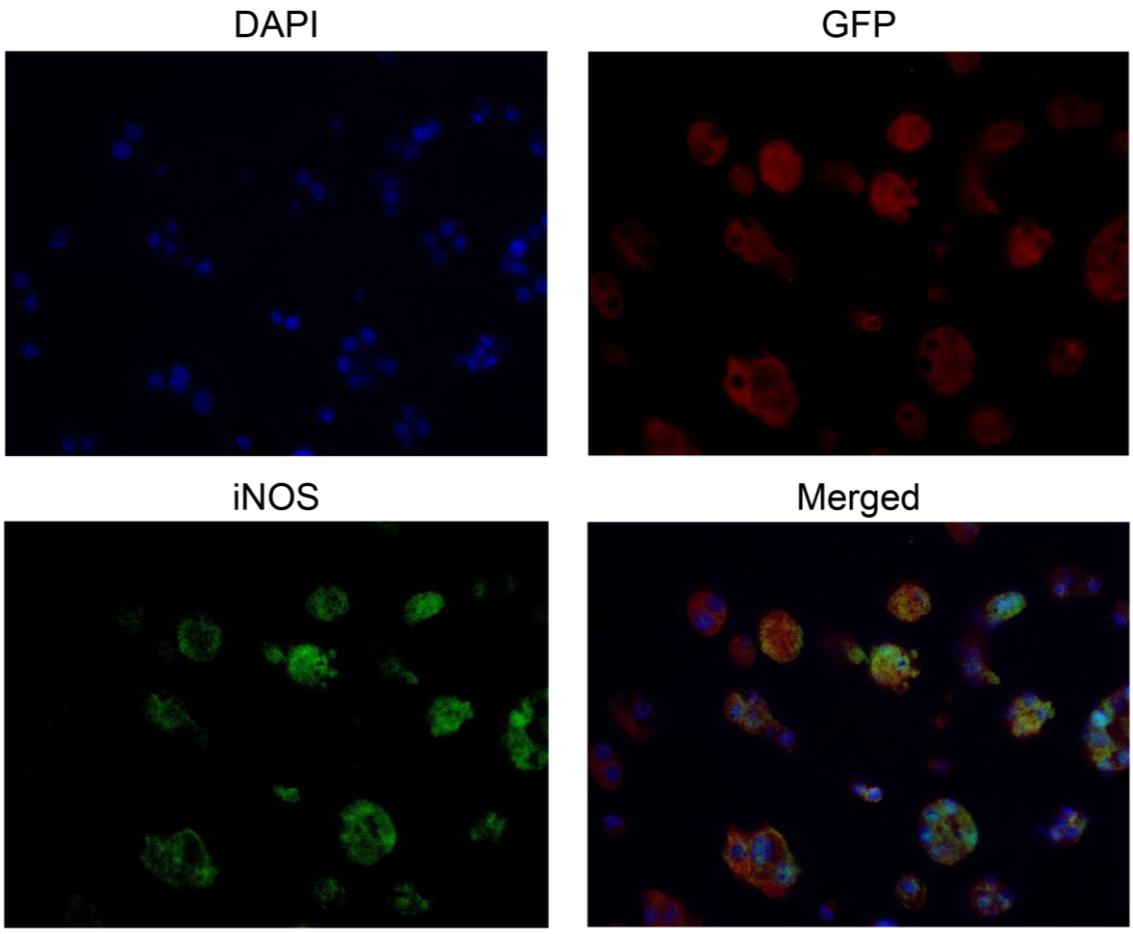

Figure 5.8: 14 Day CID-treated Plugs with GFP and iNOS Positive Cells with Co-localization. Image taken at 40X magnification. Top left panel shows Dapi staining of nuclei, top right panel shows GFP positive cells, bottom left panel shows iNOS positive cells, and bottom right panel shows the merged image.

Chapter 6. CONCLUSION AND FUTURE STUDIES

It has been shown previously that MΦs drive the wound healing response (86, 109, 110). In this dissertation, I have engineered tunable pro-inflammatory MΦs that could possibly be used to better regulate inflammation. By utilizing these MΦ-cTLR4 cells to control the host response, it might be possible to increase angiogenesis and decrease fibrosis for better integration of medical device implants. Additionally, these engineered cells could be used as a tool to better understand and better regulate M1 MΦ-like dynamics. While RAW264.7 cells are suitable to use during *in vitro* inflammation studies, future investigations will focus on using a more physiological engineered primary cell type, such as bone marrow derived MΦs (54). While ongoing studies continue to unravel MΦ-cTLR4 cell possibilities in both *in vitro* and *in vivo* settings, currently these engineered cells serve as a platform technology that could be applied to various inflammatory diseases including the FBR, fibrosis, atherosclerosis, and cancer.

Further *in vivo* testing is necessary for MΦ-cTLR4 cells, as the *in vivo* results in this dissertation represent a pilot study. Not only should the inflammatory state be further investigated in the Matrigel plugs, but the angiogenesis and fibrosis state should also be explored to a greater extent. For instance, the plugs could be analyzed for VEGF-A and TSP-1 expressing cells and compared to controls, as these are pro- and anti-angiogenic markers, respectively (111). Alternatively, quantitative PCR could be used for VEGF-A, and TSP-1, as well as fibroblast markers (*TE-7, HA-BP* and *COLLAGEN V*) (112). Angiogenesis should also be analyzed by counting CD31 positive lumen structures, in which CD31 is a classical endothelial cell marker. Once it has been established how the engineered cells influence these specific processes, the next step would entail testing the cells directly with a foreign implanted material, such as PET disks (113).

Even with the above suggestions and the progress made in this dissertation, there will still be a great amount of work that needs to be performed in order to get the proposed engineered MΦ-cTLR4 cells to a cell therapy stage. First and foremost, a M2 MΦ version of these engineered cells would be necessary to completely manipulate the host inflammatory response. To this end, I have currently created a cIL4R heterodimer construct that can be theoretically activated with a different CID drug, however, I have yet to characterize the M2 MΦ-cIL4R engineered cells or optimize the cell line. If these cells are functional, it could then be possible to modulate the inflammation in both directions, as well as finely tune the temporal activation of both M1 and M2 engineered cells. To simplify the system, both cTLR4 and cIL4R constructs could be transduced into the same cell, to create cells that could respond to both CID drugs. In this scenario, the same monocyte could be polarized back and forth with the different CID drugs and overall, less cells would be necessary for *in vivo* applications.

More testing of inflammation would need to be completed once the MΦ-cIL4R cells are validated. Modulation of inflammation toward either a pro-inflammatory or a pro-healing environment as well as degree of device integration could initially be tested. However, temporal modulation, in which MΦ-cTLR4 and MΦ-cIL4R cells are switched "on" and "off" at key timepoints could also elucidate key findings about the FBR. Another possible future study could entail location experiments for MΦc-TLR4 cells and MΦ-cIL4R cells following i.v. injection into the blood stream. Since monocytes have the natural tendency to home to sites of inflammation, it would be interesting to observe where the engineered cells locate in a mouse model that has an inflicted inflammatory event present, depending on polarization state. Lastly, pending successful *in vivo* experimentation of these engineered MΦs, clinical trials could potentially follow. Possible pro-

healing MΦ applications include better biomedical device implant integration, ischemia, and chronic inflammatory diseases, while possible pro-inflammatory applications include fibrotic diseases and inhibition of angiogenesis for cancer.

In conjunction with this dissertation, another MΦ cell tool is also in progress. In collaboration with Bryers lab, a MΦ reporter cell line has been designed that will express GFP when M2 processes are occurring in the cell, but express RFP when M1 processes are occurring in the cell. The GFP is driven by an Arginase 1 promoter (M2 marker) and the RFP is driven by an iNOS promoter (M1 marker). This reporter cell line would allow one to distinguish if cells are expressing M1 markers, M2 markers, or mixed M1/M2 markers and can help with tracking the polarization state of MΦs *in vivo*. A potential application of this reporter cell line, is the injection of these cells around an implanted foreign material. These cells would be able to confirm or refute current studies that claim certain MΦs are present in distinct zones around the implanted material in the FBR. These cells could also be used to investigate the polarization properties of sphere-templated pHEMA scaffolds (50).

In conclusion, there are an increasing amount of diseases as well as conditions, in which a key dysregulated inflammation role is being implicated. MΦ dynamics are an important part of many processes that involve innate functions and interactions. Thus, it is necessary to understand complete MΦ function and polarization, before any of these diseases or conditions can be cured. This dissertation provides a tool to allow these processes to be investigated in a more controlled and specific manner.

REFERENCES

1. Rich S. Better health care with quality medical devices: FDA on the cutting edge of device technology. International Journal of Trauma Nursing. 2002;8(3):89-90.

2. Brandt EN, editor. Improving medical implant performance through retrieval information: Challenges and opportunities. NIH Technology Assessment Conference Summary, Kensington, MD; 2000.

3. Morais JM, Papadimitrakopoulos F, Burgess DJ. Biomaterials/tissue interactions: possible solutions to overcome foreign body response. The AAPS journal. 2010;12(2):188-96.

4. Anderson JM. Biological responses to materials. Annual Review of Materials Research. 2001;31(1):81-110.

5. Vercruysse KP, Prestwich GD. Hyaluronate derivatives in drug delivery. Critical reviews in therapeutic drug carrier systems. 1998;15(5):513.

6. Uchegbu IF, SchÄTzlein AG, Tetley L, Gray AI, Sludden J, Siddique S, Mosha E. Polymeric Chitosan-based Vesicles for Drug Delivery. Journal of pharmacy and pharmacology. 1998;50(5):453-8.

7. Bhardwaj U, Sura R, Papadimitrakopoulos F, Burgess DJ. PLGA/PVA hydrogel composites for long-term inflammation control following sc implantation. International journal of pharmaceutics. 2010;384(1):78-86.

8. Patil SD, Papadmitrakopoulos F, Burgess DJ. Concurrent delivery of dexamethasone and VEGF for localized inflammation control and angiogenesis. Journal of controlled release. 2007;117(1):68-79.

9. Griffith LG, Naughton G. Tissue engineering--current challenges and expanding opportunities. Science. 2002;295(5557):1009-14.

10. Larsen GL, Henson PM. Mediators of inflammation. Annual review of immunology. 1983;1(1):335-59.

11. Rock KL, Latz E, Ontiveros F, Kono H. The sterile inflammatory response. Annual review of immunology. 2009;28:321-42.

12. Billadeau DD. PTEN gives neutrophils direction. Nature Immunology. 2008;9(7):716-8.

13. McDonald B, Pittman K, Menezes GB, Hirota SA, Slaba I, Waterhouse C, Beck PL, Muruve DA, Kubes P. Intravascular danger signals guide neutrophils to sites of sterile inflammation. Science. 2010;330(6002):362.

14. Korns DR, Frasch SC, Fernandez-Boyanapalli R, Henson PM, Bratton DL. Modulation of Macrophage Efferocytosis in Inflammation. Frontiers in Immunology. 2011;2. doi: 10.3389/fimmu.2011.00057.

15. Serhan CN, Brain SD, Buckley CD, Gilroy DW, Haslett C, O'Neill LAJ, Perretti M, Rossi AG, Wallace JL. Resolution of inflammation: state of the art, definitions and terms. The FASEB journal. 2007;21(2):325.

16. Lawrence T, Gilroy DW. Chronic inflammation: a failure of resolution? International journal of experimental pathology. 2007;88(2):85-94.

17. Gordon S, Martinez FO. Alternative Activation of Macrophages: Mechanism and Functions. Immunity. 2010;32(5):593-604. doi: 10.1016/j.immuni.2010.05.007. PubMed PMID: WOS:000278280500006.

18. Ward C, Dransfield I, Chilvers ER, Haslett C, Rossi AG. Pharmacological manipulation of granulocyte apoptosis: potential therapeutic targets. Trends in pharmacological sciences. 1999;20(12):503-9.

19. Murray LA, Chen Q, Kramer MS, Hesson DP, Argentieri RL, Peng X, Gulati M, Homer RJ, Russell T, van Rooijen N. TGF-beta driven lung fibrosis is macrophage dependent and blocked by serum amyloid P. The International Journal of Biochemistry & Cell Biology. 2010.

20. Anderson JM. Biological responses to materials. Annual Review of Materials Research. 2001;31:81-110. PubMed PMID: ISI:000171808700005.

21. Ratner BD, Bryant SJ. Biomaterials: Where we have been and where we are going. Annual Review of Biomedical Engineering. 2004;6:41-75. PubMed PMID: ISI:000223795500003.

22. Bryers JD, Giachelli CM, Ratner BD. Engineering biomaterials to integrate and heal: The biocompatibility paradigm shifts. Biotechnology and bioengineering. 2012;109(8):1898-911.

23. Prichard HL, Reichert WM, Klitzman B. Adult adipose-derived stem cell attachment to biomaterials. Biomaterials. 2007;28(6):936-46.

24. Brodbeck WG, MacEwan M, Colton E, Meyerson H, Anderson JM. Lymphocytes and the foreign body response: lymphocyte enhancement of macrophage adhesion and fusion. Journal of Biomedical Materials Research Part A. 2005;74(2):222-9.

25. Griffioen AW, Molema G. Angiogenesis: potentials for pharmacologic intervention in the treatment of cancer, cardiovascular diseases, and chronic inflammation. Pharmacological reviews. 2000;52(2):237-68.

26. Sunderkötter C, Steinbrink K, Goebeler M, Bhardwaj R, Sorg C. Macrophages and angiogenesis. Journal of Leukocyte Biology. 1994;55(3):410-22.

27. Frantz S, Vincent KA, Feron O, Kelly RA. Innate immunity and angiogenesis. Circulation research. 2005;96(1):15-26.

28. Jetten N, Verbruggen S, Gijbels MJ, Post MJ, De Winther MP, Donners MM. Anti-inflammatory M2, but not pro-inflammatory M1 macrophages promote angiogenesis in vivo. Angiogenesis. 2013:1-10.

29. Yamamoto M, Sato S, Hemmi H, Hoshino K, Kaisho T, Sanjo H, Takeuchi O, Sugiyama M, Okabe M, Takeda K. Role of adaptor TRIF in the MyD88-independent toll-like receptor signaling pathway. Science. 2003;301(5633):640-3.

30. Kawai T, Takeuchi O, Fujita T, Inoue J-i, Mühlradt PF, Sato S, Hoshino K, Akira S. Lipopolysaccharide stimulates the MyD88-independent pathway and results in activation of IFN-regulatory factor 3 and the expression of a subset of lipopolysaccharide-inducible genes. The Journal of Immunology. 2001;167(10):5887-94.

31. Doyle SE, Vaidya SA, O'Connell R, Dadgostar H, Dempsey PW, Wu T-T, Rao G, Sun R, Haberland ME, Modlin RL. IRF3 mediates a TLR3/TLR4-specific antiviral gene program. Immunity. 2002;17(3):251-63.

32. Hoebe K, Du X, Georgel P, Janssen E, Tabeta K, Kim S, Goode J, Lin P, Mann N, Mudd S. Identification of Lps2 as a key transducer of MyD88-independent TIR signalling. Nature. 2003;424(6950):743-8.

33. Wieland CW, Florquin S, Maris NA, Hoebe K, Beutler B, Takeda K, Akira S, van der Poll T. The MyD88-dependent, but not the MyD88-independent, pathway of TLR4 signaling is important in clearing nontypeable haemophilus influenzae from the mouse lung. The journal of immunology. 2005;175(9):6042-9.

34. Mantovani A, Sica A, Sozzani S, Allavena P, Vecchi A, Locati M. The chemokine system in diverse forms of macrophage activation and polarization. Trends in immunology. 2004;25(12):677-86.

35. Hoshino K, Takeuchi O, Kawai T, Sanjo H, Ogawa T, Takeda Y, Takeda K, Akira S. Cutting edge: Toll-like receptor 4 (TLR4)-deficient mice are hyporesponsive to lipopolysaccharide: evidence for TLR4 as the Lps gene product. The Journal of Immunology. 1999;162(7):3749-52.

36. Clackson T, Yang W, Rozamus LW, Hatada M, Amara JF, Rollins CT, Stevenson LF, Magari SR, Wood SA, Courage NL. Redesigning an FKBP–ligand interface to generate chemical dimerizers with novel specificity. Proceedings of the National Academy of Sciences. 1998;95(18):10437.

37. Chen M, Orozco A, Spencer DM, Wang J. Activation of initiator caspases through a stable dimeric intermediate. Journal of Biological Chemistry. 2002;277(52):50761-7.

38. Miller C, Blau C. Using gene transfer to circumvent off-target effects. Gene therapy. 2008;15(10):759-64.

39. Pajonk F, Weil A, Sommer A, Suwinski R, Henke M. The erythropoietin-receptor pathway modulates survival of cancer cells. Oncogene. 2004;23(55):8987-91.

40. Blau CA, Peterson KR, Drachman JG, Spencer DM. A proliferation switch for genetically modified cells. Proceedings of the National Academy of Sciences. 1997;94(7):3076.

41. Jin L, Siritanaratkul N, Emery DW, Richard RE, Kaushansky K, Papayannopoulou T, Blau CA. Targeted expansion of genetically modified bone marrow cells. Proceedings of the National Academy of Sciences. 1998;95(14):8093.

42. Jin L, Asano H, Blau CA. Stimulating cell proliferation through the pharmacologic activation of c-kit. Blood. 1998;91(3):890-7.

43. Zeng H, Masuko M, Jin L, Neff T, Otto KG, Blau CA. Receptor specificity in the self-renewal and differentiation of primary multipotential hemopoietic cells. Blood. 2001;98(2):328-34.

44. Zhao S, Zoller K, Masuko M, Rojnuckarin P, Yang XO, Parganas E, Kaushansky K, Ihle JN, Papayannopoulou T, Willerford DM. JAK2, complemented by a second signal from c-kit or flt-3, triggers extensive self-renewal of primary multipotential hemopoietic cells. The EMBO journal. 2002;21(9):2159-67.

45. Stokes KB. Preliminary studies on a new steroid eluting epicardial electrode. Pacing and Clinical Electrophysiology. 1988;11(11):1797-803.

46. Geelhood SJ, Horbett TA, Ward WK, Wood MD, Quinn MJ. Passivating protein coatings for implantable glucose sensors: Evaluation of protein retention. Journal of Biomedical Materials Research Part B: Applied Biomaterials. 2007;81(1):251-60.

47. Kyriakides TR, Hartzel T, Huynh G, Bornstein P. Regulation of angiogenesis and matrix remodeling by localized, matrix-mediated antisense gene delivery. Molecular Therapy. 2001;3(6):842-9.

48. Jay SM, Skokos E, Laiwalla F, Krady M-M, Kyriakides TR. Foreign body giant cell formation is preceded by lamellipodia formation and can be attenuated by inhibition of Rac1 activation. The American journal of pathology. 2007;171(2):632-40.

49. Madden LR, Mortisen DJ, Sussman EM, Dupras SK, Fugate JA, Cuy JL, Hauch KD, Laflamme MA, Murry CE, Ratner BD. Proangiogenic scaffolds as functional templates for cardiac tissue engineering. Proceedings of the National Academy of Sciences. 2010;107(34):15211-6.

50. Sussman EM, Halpin MC, Muster J, Moon RT, Ratner BD. Porous implants modulate healing and induce shifts in local macrophage polarization in the foreign body reaction. Annals of biomedical engineering. 2013:1-9.

51. Szabo G, Mandrekar P. Focus on: alcohol and the liver. Alcohol Research & Health. 2010;33(1-2):87.

52. Gay NJ, Gangloff M. Structure and function of Toll receptors and their ligands. Annu Rev Biochem. 2007;76:141-65.

53. Buchanan SGSC, Gay NJ. Structural and functional diversity in the leucine-rich repeat family of proteins. Progress in biophysics and molecular biology. 1996;65(1):1-44.

54. Chamberlain LM, Godek ML, Gonzalez-Juarrero M, Grainger DW. Phenotypic non-equivalence of murine (monocyte-) macrophage cells in biomaterial and inflammatory models. Journal

of Biomedical Materials Research Part A. 2009;88A(4):858-71. doi: 10.1002/jbm.a.31930. PubMed PMID: WOS:000263383700003.

55. Liou H-C, Sha WC, Scott ML, Baltimore D. Sequential induction of NF-kappa B/Rel family proteins during B-cell terminal differentiation. Molecular and cellular biology. 1994;14(8):5349-59.

56. García-Sastre A, Biron CA. Type 1 interferons and the virus-host relationship: a lesson in detente. Science. 2006;312(5775):879-82.

57. Sun M, Ames KT, Suzuki I, Fink PJ. The cytoplasmic domain of Fas ligand costimulates TCR signals. The Journal of Immunology. 2006;177(3):1481-91.

58. Kuenzel S, Till A, Winkler M, Häsler R, Lipinski S, Jung S, Grötzinger J, Fickenscher H, Schreiber S, Rosenstiel P. The nucleotide-binding oligomerization domain-like receptor NLRC5 is involved in IFN-dependent antiviral immune responses. The journal of immunology. 2010;184(4):1990-2000.

59. Fooksman DR, Grönvall GK, Tang Q, Edidin M. Clustering class I MHC modulates sensitivity of T cell recognition. The Journal of Immunology. 2006;176(11):6673-80.

60. Rementer CW, Wu M, Buranaphatthana W, Yang H-YL, Scatena M, Giachelli CM. An Inducible, Ligand-Independent Receptor Activator of NF-κB Gene to Control Osteoclast Differentiation from Monocytic Precursors. PloS one. 2013;8(12):e84465.

61. Wu M, Hussain S, He Y-H, Pasula R, Smith PA, Martin WJ. Genetically engineered macrophages expressing IFN-γ restore alveolar immune function in scid mice. Proceedings of the National Academy of Sciences. 2001;98(25):14589-94.

62. Griffiths L, Binley K, Iqball S, Kan O, Maxwell P, Ratcliffe P, Lewis C, Harris A, Kingsman S, Naylor S. The macrophage-a novel system to deliver gene therapy to pathological hypoxia. Gene therapy. 2000;7(3):255-62.

63. Martinez FO, Sica A, Mantovani A, Locati M. Macrophage activation and polarization. Frontiers in bioscience: a journal and virtual library. 2008;13:453.

64. Brown BN, Ratner BD, Goodman SB, Amar S, Badylak SF. Macrophage polarization: an opportunity for improved outcomes in biomaterials and regenerative medicine. Biomaterials. 2012;33(15):3792-802.

65. Knight JA. Review: Free radicals, antioxidants, and the immune system. Annals of Clinical & Laboratory Science. 2000;30(2):145-58.

66. Bouhlel M, Derudas B, Rigamonti E, Dièvart R, Brozek J, Haulon S, Zawadzki C, Jude B, Torpier G, Marx N. PPARγ activation primes human monocytes into alternative M2 macrophages with anti-inflammatory properties. Cell metabolism. 2007;6(2):137-43.

67. Sica A, Mantovani A. Macrophage plasticity and polarization: in vivo veritas. The Journal of clinical investigation. 2012;122(122 (3)):787-95.

68. Guiducci C, Vicari AP, Sangaletti S, Trinchieri G, Colombo MP. Redirecting in vivo elicited tumor infiltrating macrophages and dendritic cells towards tumor rejection. Cancer research. 2005;65(8):3437-46.

69. Saccani A, Schioppa T, Porta C, Biswas SK, Nebuloni M, Vago L, Bottazzi B, Colombo MP, Mantovani A, Sica A. p50 nuclear factor-κB overexpression in tumor-associated macrophages inhibits M1 inflammatory responses and antitumor resistance. Cancer research. 2006;66(23):11432-40.

70. Boehler R, Kuo R, Shin S, Goodman A, Pilecki M, Leonard J, Shea L. Lentivirus delivery of IL-10 to promote and sustain macrophage polarization towards an anti-inflammatory phenotype. Biotechnology and bioengineering. 2014;111(6):1210-21.

71. Zuo G-Q, Gong J-P, Liuo C, Li S-W, Wu C, Yang K, Li Y. Expression of lipopolysaccharide binding protein and its receptor CD14 in experimental alcoholic liver disease. WORLD JOURNAL OF GASTROENTEROLOGY. 2001;7(6):836-40.

72. Nomura F, Akashi S, Sakao Y, Sato S, Kawai T, Matsumoto M, Nakanishi K, Kimoto M, Miyake K, Takeda K. Cutting edge: endotoxin tolerance in mouse peritoneal macrophages correlates with down-regulation of surface toll-like receptor 4 expression. The Journal of Immunology. 2000;164(7):3476-9.

73. Lee S, Huen S, Nishio H, Nishio S, Lee HK, Choi B-S, Ruhrberg C, Cantley LG. Distinct macrophage phenotypes contribute to kidney injury and repair. Journal of the American Society of Nephrology. 2011;22(2):317-26.

74. Tabas I. Macrophage death and defective inflammation resolution in atherosclerosis. Nature Reviews Immunology. 2009;10(1):36-46.

75. Tonnesen MG, Feng X, Clark RA, editors. Angiogenesis in wound healing. Journal of Investigative Dermatology Symposium Proceedings; 2000: Nature Publishing Group.

76. Leibovich S, Ross R. The role of the macrophage in wound repair. A study with hydrocortisone and antimacrophage serum. The American journal of pathology. 1975;78(1):71.

77. Clark R, Stone R, Leung D, Silver I, Hohn D, Hunt T, editors. Role of macrophages in would healing. Surgical forum; 1976.

78. Thakral KK, Goodson WH, Hunt TK. Stimulation of wound blood vessel growth by wound macrophages. Journal of Surgical Research. 1979;26(4):430-6.

79. Polverini PJ, Cotran RS, Gimbrone MA, Unanue ER. Activated macrophages induce vascular proliferation1977.

80. Kobayashi S, Nagaura T, Kimura I, Kimura M. Interferon-γ-activated macrophages enhance angiogenesis from endothelial cells of rat aorta. Immunopharmacology. 1994;27(1):23-30.

81. Fantin A, Vieira JM, Gestri G, Denti L, Schwarz Q, Prykhozhij S, Peri F, Wilson SW, Ruhrberg C. Tissue macrophages act as cellular chaperones for vascular anastomosis downstream of VEGF-mediated endothelial tip cell induction. Blood. 2010;116(5):829-40.

82. Baer C, Squadrito ML, Iruela-Arispe ML, De Palma M. Reciprocal interactions between endothelial cells and macrophages in angiogenic vascular niches. Experimental cell research. 2013;319(11):1626-34.

83. Holt DJ, Chamberlain LM, Grainger DW. Cell–cell signaling in co-cultures of macrophages and fibroblasts. Biomaterials. 2010;31(36):9382-94.

84. Wottrich R, Diabaté S, Krug HF. Biological effects of ultrafine model particles in human macrophages and epithelial cells in mono-and co-culture. International journal of hygiene and environmental health. 2004;207(4):353-61.

85. Spiller KL, Nassiri S, Witherel CE, Anfang RR, Ng J, Nakazawa KR, Yu T, Vunjak-Novakovic G. Sequential delivery of immunomodulatory cytokines to facilitate the M1-to-M2 transition of macrophages and enhance vascularization of bone scaffolds. Biomaterials. 2015;37:194-207.

86. Koh TJ, DiPietro LA. Inflammation and wound healing: the role of the macrophage. Expert reviews in molecular medicine. 2011;13:e23.

87. Hansen-Algenstaedt N, Fukumura D, Stoll B, Hicklin D, Jain R, editors. Second wave of angiogenesis during KDR/Flk-1 antibody therapy. Proc Am Assoc Canc Res; 1999.

88. Guo S, DiPietro LA. Factors affecting wound healing. Journal of dental research. 2010;89(3):219-29.

89. Sainson RC, Johnston DA, Chu HC, Holderfield MT, Nakatsu MN, Crampton SP, Davis J, Conn E, Hughes CC. TNF primes endothelial cells for angiogenic sprouting by inducing a tip cell phenotype. Blood. 2008;111(10):4997-5007.

90. Urata Y, Yamaguchi M, Higashiyama Y, Ihara Y, Goto S, Kuwano M, Horiuchi S, Sumikawa K, Kondo T. Reactive oxygen species accelerate production of vascular endothelial growth factor by

advanced glycation end products in RAW264. 7 mouse macrophages. Free Radical Biology and Medicine. 2002;32(8):688-701.

91. Klug F, Prakash H, Huber PE, Seibel T, Bender N, Halama N, Pfirschke C, Voss RH, Timke C, Umansky L. Low-dose irradiation programs macrophage differentiation to an iNOS+/M1 phenotype that orchestrates effective T cell immunotherapy. Cancer cell. 2013;24(5):589-602.

92. Schmidt T, Carmeliet P. Blood-vessel formation: Bridges that guide and unite. Nature. 2010;465(7299):697-9.

93. Motro B, Itin A, Sachs L, Keshet E. Pattern of interleukin 6 gene expression in vivo suggests a role for this cytokine in angiogenesis. Proceedings of the National Academy of Sciences. 1990;87(8):3092-6.

94. Fee D, Grzybicki D, Dobbs M, Ihyer S, Clotfelter J, Macvilay S, Hart MN, Sandor M, Fabry Z. Interleukin 6 promotes vasculogenesis of murine brain microvessel endothelial cells. Cytokine. 2000;12(6):655-65.

95. Lin Z-Q, Kondo T, Ishida Y, Takayasu T, Mukaida N. Essential involvement of IL-6 in the skin wound-healing process as evidenced by delayed wound healing in IL-6-deficient mice. Journal of leukocyte biology. 2003;73(6):713-21.

96. Stempien-Otero A, Plawman A, Meznarich J, Dyamenahalli T, Otsuka G, Dichek DA. Mechanisms of cardiac fibrosis induced by urokinase plasminogen activator. J Biol Chem. 2006;281(22):15345-51. doi: 10.1074/jbc.M512818200. PubMed PMID: 16554301.

97. Meneghin A, Hogaboam CM. Infectious disease, the innate immune response, and fibrosis. Journal of Clinical Investigation. 2007;117(3):530.

98. Anders H-J, Ryu M. Renal microenvironments and macrophage phenotypes determine progression or resolution of renal inflammation and fibrosis. Kidney international. 2011;80(9):915-25.

99. Allavena P, Sica A, Solinas G, Porta C, Mantovani A. The inflammatory micro-environment in tumor progression: the role of tumor-associated macrophages. Critical reviews in oncology/hematology. 2008;66(1):1-9.

100. Wu Y, Ip JE, Huang J, Zhang L, Matsushita K, Liew C-C, Pratt RE, Dzau VJ. Essential role of ICAM-1/CD18 in mediating EPC recruitment, angiogenesis, and repair to the infarcted myocardium. Circulation Research. 2006;99(3):315-22.

101. Koch AE, Halloran MM, Haskell CJ, Shah MR, Polverini PJ. Angiogenesis mediated by soluble forms of E-selectin and vascular cell-adhesion molecule-11995.

102. Umemura N, Saio M, Suwa T, Kitoh Y, Bai J, Nonaka K, Ouyang G-F, Okada M, Balazs M, Adany R. Tumor-infiltrating myeloid-derived suppressor cells are pleiotropic-inflamed monocytes/macrophages that bear M1-and M2-type characteristics. Journal of leukocyte biology. 2008;83(5):1136-44.

103. Hoeksema MA, Stöger JL, de Winther MP. Molecular pathways regulating macrophage polarization: implications for atherosclerosis. Current atherosclerosis reports. 2012;14(3):254-63.

104. van Putten SM, Ploeger DT, Popa ER, Bank RA. Macrophage phenotypes in the collagen-induced foreign body reaction in rats. Acta biomaterialia. 2013;9(5):6502-10.

105. Garg K, Pullen NA, Oskeritzian CA, Ryan JJ, Bowlin GL. Macrophage functional polarization (M1/M2) in response to varying fiber and pore dimensions of electrospun scaffolds. Biomaterials. 2013;34(18):4439-51.

106. Lee K-H, Choi H-R, Kim C-H. Anti-angiogenic effect of the seed extract of< i> Benincasa hispida</i> Cogniaux. Journal of ethnopharmacology. 2005;97(3):509-13.

107. Badylak SF, Valentin JE, Ravindra AK, McCabe GP, Stewart-Akers AM. Macrophage phenotype as a determinant of biologic scaffold remodeling. Tissue Engineering Part A. 2008;14(11):1835-42.

108. Spiller KL, Anfang RR, Spiller KJ, Ng J, Nakazawa KR, Daulton JW, Vunjak-Novakovic G. The role of macrophage phenotype in vascularization of tissue engineering scaffolds. Biomaterials. 2014;35(15):4477-88.

109. Behm B, Babilas P, Landthaler M, Schreml S. Cytokines, chemokines and growth factors in wound healing. Journal of the European Academy of Dermatology and Venereology. 2012;26(7):812-20.

110. Hunt T, Knighton D, Thakral K, Goodson 3rd W, Andrews W. Studies on inflammation and wound healing: angiogenesis and collagen synthesis stimulated in vivo by resident and activated wound macrophages. Surgery. 1984;96(1):48-54.

111. Izumi Y, Xu L, Di Tomaso E, Fukumura D, Jain RK. Tumour biology: herceptin acts as an anti-angiogenic cocktail. Nature. 2002;416(6878):279-80.

112. Riddell M, Winkler-Lowen B, Chakrabarti S, Dunk C, Davidge S, Guilbert L. The characterization of fibrocyte-like cells: A novel fibroblastic cell of the placenta. Placenta. 2012.

113. Zaveri T. Modulating macrophage response to biomaterials: University of Florida; 2011.

VITA

EDUCATION *ACADEMIC BACKGROUND*

Doctorate of Philosophy in Bioengineering ***2010 -2015***
University of Washington, Seattle, WA
Thesis topic: Engineering macrophage polarization to control angiogenesis during the inflammatory response.

MBA Entrepreneurship Certificate ***2015***
University of Washington, Seattle, WA
Business topic: Biotechnology entrepreneurship.

Master of Science in Biochemistry & Molecular Biophysics ***2010***
University of Arizona, Tucson, AZ
Thesis topic: Chimeric Variants of two Cro proteins with 40% sequence identity but different folds.

Bachelor of Science in Biochemistry & Molecular Biophysics/ Molecular & Cellular Biology/ Mathematics ***2009***
University of Arizona, Tucson, AZ- Magna Cum Laude graduate

Thesis topic: Investigation of structural evolution in Cro proteins through hybrid sequence construction.

AWARDS *SCHOLARSHIPS AND FELLOWSHIPS*

College of Engineering Fellowship ***2013-2014***
- Applicant and recipient of the Kaiser Engineering Fellowship

Bioengineering Cardiovascular Training Grant (BCTG) ***2011-2013***
- Applicant and recipient of the NIH T32 Institutional Training Grant - Completed clinical imaging preceptorships and summer Biomedical Research Integrity courses

PUBLICATIONS *SELECTED PATENTS, PUBLICATIONS, ABSTRACTS, POSTERS AND TALKS*

Eaton KV, Yang HYL, Giachelli CM, Scatena M. "Engineering Macrophages to Control the Inflammatory Response and Angiogenesis." *Experimental Cell Research.* [Epub ahead of print].

Eaton KV, Scatena M, Giachelli CM. "A Method to Promote Pro-inflammatory Macrophages with a Small Molecule." US Provisional Patent 62/195725, July 22, 2015.

Eaton KV, Anderson WJ, Dubrava MS, Kumirov VK, Dykstra EM, Cordes MHJ. "Studying Protein Fold Evolution with Hybrids of Differently Folded Homologs." *Protein Engineering Design & Selection*. 2015; 28(8): 241-50.

Stewart KL, Nelson MR, **Eaton KV**, Anderson WJ, Cordes MHJ. "A Role for Indels in the Evolution of Cro Proteins." *Proteins: Structure, Function, and Bioinformatics.* 2013; 81(11): 1988-96.

Eaton KV, Ramanathan R, Au N, Gerig C, "Contact Lens With Activated Drug Delivery," US Provisional Patent 61/825732, May 21, 2013.

Eaton KV, Wu M, Yang HYL, Giachelli CM, Scatena M. "Engineered Macrophages for the Application of a Healing Cardiovascular Tissue Engineering Scaffold"- *National Institute of Biomedical Imaging & Bioengineering (NIBIB) 2012 Training Grantees Meeting and Society of Advancement of Chicanos & Native Americans in Science (SACNAS) 2012 National Conference.*

Eaton KV, Dubrava MS, Anderson WJ, Nguyen V and Cordes MHJ. “Chimeric and hybrid variants of two Cro proteins with 40% sequence identity but different folds”– *23rd Symposium of the Protein Society 2009.*

Eaton KV and Cordes MHJ. “Investigation of structural evolution in Cro proteins through hybrid sequence construction”– *UBRP Annual Conference 2008.*

Eaton KV. “Left ventricular hypertrophy in heart transplant patients due to Cyclosporin”– *Oral presentation at the Summer Institute on Medical Ignorance Annual Meeting 2003.*